USING GEL BASED PROTEOMICS TO STUDY SIGNALING, PHSYIOLOGY, AND BEHAVIOR IN *DROSOPHILA MELANOGASTER*

by

Malachi Andrew Blundon

A dissertation submitted in partial fulfillment
of the requirements for the degree of Doctor of Philosophy
Department of Biological Sciences
Carnegie Mellon University
Pittsburgh, PA

September 2017

_____
Dr. Brooke M. McCartney
Advisor
Department of Biological Sciences

_____
Dr. Jonathan S. Minden
Advisor
Department of Biological Sciences

_____
Dr. Aaron Mitchell
Department Head
Department of Biological Sciences

_____
Dr. Rebecca Doerge
Dean of Mellon College of Science

ACKNOWLEDGEMENTS

I would like to thank both my advisors, Dr. Brooke McCartney and Dr. Jonathan Minden, for your guidance, encouragement, and friendship. Thank you for everything. The opportunity I was given at Carnegie Mellon would not have been possible without you two helping me make it a reality.

To Brooke:

Thank you for your dedication and support. It was your drive that inspired me time and time again to keep pushing on during the multiple times I felt like giving up. I hope one day I become as smart of a scientist as you.

To Jon:

Thank you for your guidance and understanding. You never had to say much, but you have given me the life skills necessary to continue to make me a better person and scientist. If I turn out half as successful as you, I will be fortunate.

I would also like to thank the many undergraduates that have worked me over the years. Thank you to Amrithan Parthasarathy, Danielle Schlesinger, David Vinson, Hannah Kolev, Samantha Smith, Azmal Thahireen, and Chris Yang for assisting me with the APC project. Thank you to Anna Pyzel, Tiffany Lau, and Jennifer Huang for assisting me with the microbiota project. Without your help and tireless efforts most of the data in this dissertation would not have existed.

I would like to extend my gratitude to both past and present members from both the McCartney and Minden labs for the many ideas, suggestions, and support and helping me further advance my science. Many of the ideas and hypotheses in this dissertation were influenced by you guys. Thank you to Ezgi Kunttas-Tatli, Stacy Oliver, Olivia Molinar, Scott Keith, and Ashley Leslie from the McCartney lab. Thank you to Emily Furbee, Phu Van, Vinitha Ganesean, Ardon Shorr, Brendan Redler, and Amber Lucas from the Minden Lab. I am very glad that I met you all. We definitely had some good times and made some bad decisions along the way, but it was all worth it. Good luck to you all with your future!

Last and most importantly, I would like to thank my family. Without their love and support, I would not have pursued a higher education. You guys were always the foundation to my success. Thanks to my mother, Denise Blundon, for all your support and love during the speed bumps in my life (and I am sure there will be plenty more). Thanks to my sister, Jerika, my brother, Jeremiah, and to my baby brother, Joshua, for visiting me Pittsburgh throughout the years and supporting me throughout my graduate career. And finally, I would like to thank my father, John Blundon, for always being an inspiration in my life. I miss you. May this dissertation also make you proud.

PREFACE

Many aspects of my graduate career have been unique when compared to the "typical graduate." To continue this theme, I have structured this dissertation a bit differently. The main motivation behind this decision was to unite two wildly different projects together in the same dissertation. This dissertation first introduces the proteomics research field and Two-Dimensional Difference Gel Electrophoresis (2D-DIGE); the major technique used in my projects. Following the introduction, are two major chapters that include published and continued unpublished work for each project. These two chapters include their own Introduction, Discussion, and Future Work sections.

Chapter Two explains my first proteome screen, in which I identified a number of proteins that respond to the loss of *APC*, a well-known Wnt signaling tumor suppressor, in fly embryos. This proteome screen identified a metalloaminopeptidase as a novel regulator of β-catenin, Aminopeptidase P (ApepP). This work also begins to explore the interaction between APC and ApepP proteins and discuss how this interaction is important for APC-dependent cellular processes.

Chapter Three explains my second proteome screen, where I identified a number of head proteins that respond to the loss of the microbiota in adult flies. I discovered that Alcohol Dehydrogenase (ADH) protein levels were elevated in fly heads from flies that contained no microbiota. This works further characterizes alcohol related phenotypes in sterile flies, and begins to uncover the mechanism by which the microbiota influences ADH protein abundance and alcohol induced physiology and behavior.

TABLE OF CONTENTS

LIST OF FIGURES

LIST OF TABLES

CHAPTER 1: INTRODUCTION TO PROTEOMICS

Human implication

In the last two decades, the fields of genomics and transcriptomics have dominated large-scale biological studies, both at the basic and translational research fronts (Hawkins, Hon, and Ren 2011; McGettigan 2013). These studies have provided transformative insight for many aspects of biological research that has ultimately led to a richer understanding of the molecular basis of diseases and therapeutic strategies. Some highlighted include a better understanding of human heterogeneity and its contribution to various diseases (Venter et al. 2001; Burrell et al. 2013; McClellan and King 2010), a better understanding of signaling pathway coordination in development (Davidson 2010; Ben-Tabou de-Leon and Davidson 2007; Sauka-Spengler and Bronner-Fraser 2008), as well as the discovery of non-coding gene elements important for biological function (Esteller 2011; Geisler and Coller 2013; Mercer, Dinger, and Mattick 2009). Despite these significant developments, understanding the genome and transcriptome is severely limited in predicting complex biological processes that are important for disease progression and effective therapeutic strategies. This is because proteins functionally govern cellular processes and execute the activities dictated by genes to determine such properties as disease progression and therapeutic targets.

The field of proteomics is the study of large-scale protein networks referred to as proteomes. The study of proteomes provides the missing information not observed in genomic or transcriptomic approaches (Pradet-Balade et al. 2001). First, the level of transcription from a gene does not always correlate with the level of translation into its respective protein and *vice-versa*, each protein have their own protein stability based on a number of factors. Two, many transcripts give rise to more than one protein, through mechanisms like alternate splicing. And

three, an individual protein may exist as multiple isoforms resulting from post-translational modifications that can significantly affect protein activity.

Some of the central goals of proteomics include identifying protein changes that differentiate normal and diseased states in cells, tissues or organisms. In the clinical setting, this is achieved by identifying protein signatures, such as protein abundance differences between cellular states, which better describe the molecular pathology of the disease of interest. These protein signatures are often referred to as biomarkers or protein targets. Protein targets are identifying drug targets use for intervention or treatment of a disease. Biomarkers are protein signatures used to predict or monitor a number of complications including but not limited to diabetes (Riaz et al. 2010; X. Liu et al. 2009), heart disease (Kiernan, Nedelkov, and Nelson 2006), infectious diseases (He et al. 2003), Parkinson's disease (van Dijk et al. 2010), Alzheimer's disease (Blennow et al. 2010), and various cancers (Minami et al. 2010; Ransohoff et al. 2008; Gemoll et al. 2010; Chong et al. 2010; Al-Ruwaili et al. 2010; Byrne et al. 2009). Additionally biomarkers are used clinically as a screening tool for diseases and drug therapies (Bhatt et al. 2010; Tavakoli, Hull, and Michael Okasinski 2011; Pierrakos and Vincent 2010; Frank and Hargreaves 2003; Belkowski, Polkovitch, and D'Andrea 2005; Blennow 2010; Sim and Ingelman-Sundberg 2011).

Now with the accreditation of clinical proteomics, the proteomics field has united with genomic and metabolomic research to create two emerging fields called proteogenomics and metaproteomics (not to be confused with the other metaproteomics definition – the analysis of a particular protein or set of proteins across many proteomics studies) (VerBerkmoes et al. 2009; Seifert et al. 2012; Hettich et al. 2013; Kolmeder and de Vos 2014; Kanazawa et al. 2005; Altelaar, Munoz, and Heck 2012). These collaborative fields provide supporting evidence to

drive each other's hypothesis to better understand a disease model or drug target. Proteogenomics' most significant human health contribution to this date has been to the cancer field, providing an improved understanding of cancers like acute myeloid leukemia (Hernandez-Valladares et al. 2017), specific lymphomas (Rolland et al. 2017), breast cancer (Mertins et al. 2016), and colon cancer (Woo et al. 2015), some studies leading to the discovery of new therapeutic options. Contrariwise, the emergence of metaproteomics is driven by the microbiome research field. This field is particularly interested in the scope of metabolites produced by the gut microbiota that influence disease states like obesity (Martinez, Leone, and Chang 2017; Kolmeder et al. 2015) and inflammatory bowel disease (X. Zhang et al. 2017; Martinez, Leone, and Chang 2017; Mayers et al. 2017), as well as normal physiology and health (X. Zhang et al. 2017; Zwittink et al. 2017). The collaborative efforts like the ones described above, will be vitally important for the comprehensive understanding of human health and disease in the future.

Top down vs. bottom up proteomic approaches

Similar to genomic and transcriptomic strategies, proteomics strategies consist of both top down and bottom up approaches for identifying proteins (Moradian et al. 2014; Wehr 2006; Lippolis and De Angelis 2016). The proper definitions of top down and bottom up proteomics are not well established, however. The first convention was described by the mass spectrometry field, where top down approaches focused on samples containing intact proteins, while bottom up approaches fragmented the proteins into peptides and analyzed those peptides to infer identity of the proteins (Wehr 2006). This definition has now been expanded to consider sample complexity due to the introduction of new technology (Wright et al. 2012; Mesri and Mehdi 2014). For the purposes of this dissertation, we will use the new convention, where bottom up

proteomics typically includes separation or simplification of protein mixtures, before enzymatic fragmentation and identification of the protein(s) via mass spectrometry (sometimes referred to as gel based proteomics). Top down approaches work with complex protein samples (< 5 proteins in a sample) and use statistical analyses to identify and quantify meaningful proteins (sometimes referred to as gel free proteomics; Fig. 1.1). Both strategies have their advantages and disadvantages in identifying proteins. Some are highlighted below.

Top down proteomics

Top down proteomics is the newer approach that identifies proteins by breaking intact protein through ionization and subsequent gas-phase fragmentation during the process of mass spectrometry. Because my work focuses on bottom up proteomics, I will not be covering these approaches in any detail. An advance review of the latest top down approaches is described by Toby et al. (Toby, Fornelli, and Kelleher 2016). A clear advantage of these strategies is the potential to scan the entire protein sequence to locate PTMs. Because top down proteomics strategies are relatively new, they suffer from several disadvantages. These approaches often require additional validation, as the intact protein samples produce more complex spectra that make protein identification difficult. As a consequence, these experiments require more powerful mass spectrometry equipment, such as a Fourier-transform ion cyclotron resonance (FT-ICR) mass spectrometer, that are often too expensive for a typical lab. Secondly, these approaches are limited to identifying proteins below 50 kDa, as the technology to analyze larger whole proteins is not yet available.

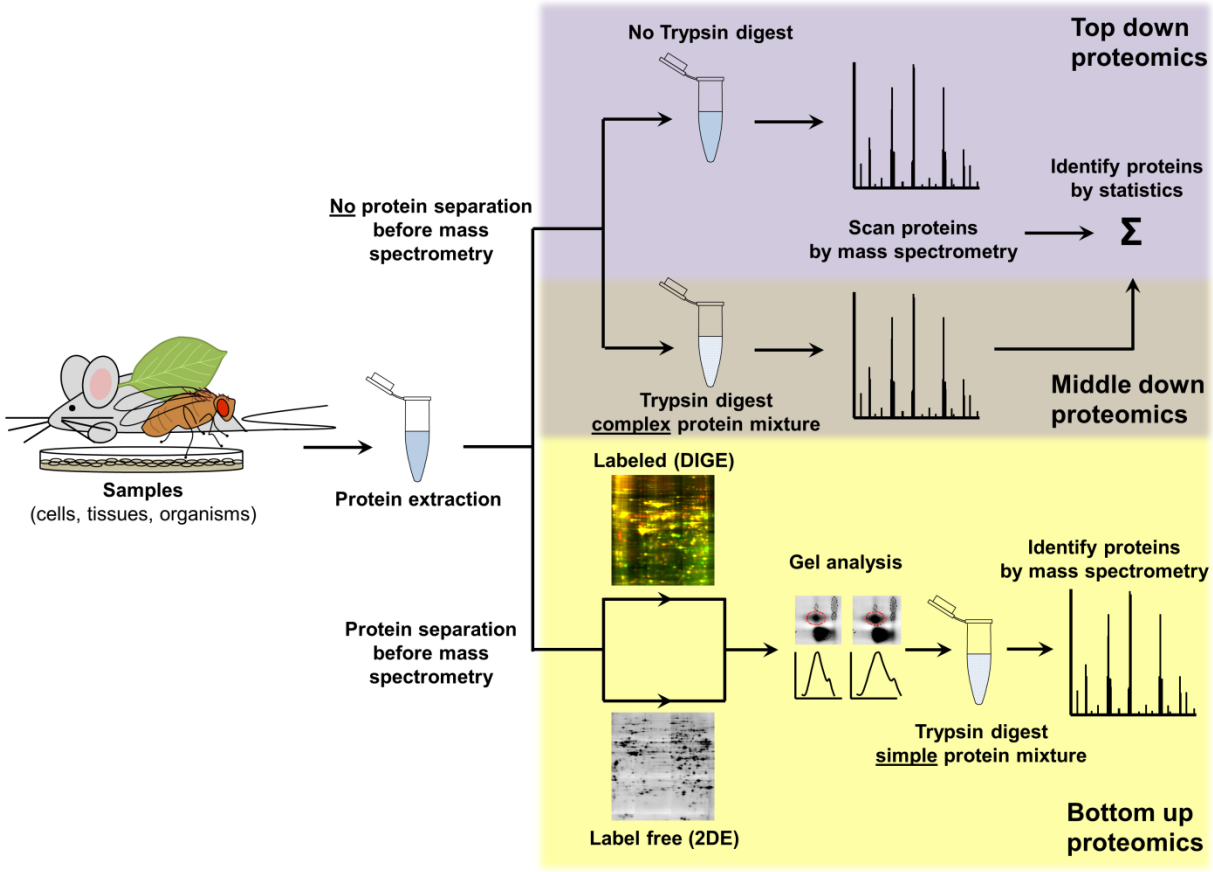

Figure 1.1. Comparing top down, middle down, and bottom up proteomics.

Principal differences between top down (purple), middle down (brown), and bottom up proteomics (yellow). Top down proteomics identifies proteins by analyzing complex protein samples containing whole intact protein. Fragmentation of whole proteins is performed inside the mass spectrometer. Middle down proteomics first fragments the complex sample, usually by Trypsin digest, before mass spectrometry analysis. This is often referred to as "shotgun proteomics". Bottom up proteomics first separates the complex protein sample by gel electrophoresis or column chromatography. Here we are showing two examples of two dimensional gel electrophoresis strategies, DIGE which uses fluorescent labeling to compare two samples on the game gel and 2DE, which uses silver stain or Coomassie blue for protein

comparison. After the protein sample has been simplified by gel separation, the samples are digested and the peptide fragments are analyzed to infer the protein present in the sample.

Bottom up proteomics

Bottom up investigations involve more mature proteomics approaches that first began by analyzing peptide fragments from simple protein mixtures that were first separated by gel electrophoresis or column chromatography. The identification of proteins in the sample was deduced by identifying peptides first using peptide mass fingerprinting and later by Tandem MS (MS-MS). Now, with the new development of high-resolution mass spectrometers (Williams et al. 2017; Xian, Hendrickson, and Marshall 2012), complex samples can be digested and analyzed without gel or column separation. This type of approach is a hybrid between top down and bottom up, and is sometimes referred to as a middle down approach or "shot gun" proteomics.

One obvious advantage of a bottom up approach is the ability to identify and quantify proteomic changes before mass spectrometry analysis with the invention of gel separation techniques, like Two Dimension Difference Gel Electrophoresis (2D-DIGE). By identifying proteome changes before mass spectrometry analysis, one can narrow the list of proteins of interest, saving on cost for mass spectrometry experiments. Additionally, there are now quantitative mass spectrometry techniques that use various labeling strategies to quantify peptides from both simple and complex protein samples (Bantscheff et al. 2007). Some of these mass spectrometry strategies, like iTRAQ or SILAC, have been more successful than others. One clear disadvantage of a bottom up strategy is relying on peptide analysis to infer protein identification and quantitative abundance. Typically, full protein sequence coverage is not represented in a peptide mixture and some peptide fragments are often enriched due to Trypsin cleavage bias. These problems make it challenging to accurately quantify differences in protein abundance between two samples and identify structural or regulatory details of the protein, such

as post-translational modifications (PTMs). However, some of these challenges, like the identification of PTMs, are solved by high resolution gel techniques like 2D-DIGE.

Two-Dimensional Difference Gel Electrophoresis (2D-DIGE)

Historically in the Minden lab, we have focused on two-dimensional electrophoresis (2DE) protein separation because of its accessibility to most laboratories. This approach was described simultaneously by several groups in 1975 (Klose 1975; O'Farrell 1975; Scheele 1975). Despite the substantial advances in the technology since its launch — the most notable of which was the introduction of immobilized pH gradients in the first dimension (Görg, Postel, and Günther 1988; Hamdan and Righetti 2005) — some of the more significant systemic shortcomings have remained unsolved. The most troublesome of these is the inherent lack of reproducibility between gels. Efforts to solve these limitations have mostly focused on developing computational methods for gel matching. These approaches have had limited success because the sources of gel-to-gel variation are numerous, complex and difficult to model (Miller et al. 1982; Dowsey et al. 2010; J. M. Park et al. 2014).

Difference gel electrophoresis (DIGE) was developed to overcome the irreproducibility problem in the 2DE methodology by labeling two samples each with a different fluorescent dye prior to running them on the same gel (Fig 1.2; Unlu, Morgan, and Minden 1997; Viswanathan, Unlu, and Minden 2006). The fluorescent dyes used in DIGE, Cy3-NHS and Cy5-NHS (Fig. 1.1), are cyanine based, molecular-weight matched, amine reactive and positively charged. These characteristics, coupled with sub-stoichiometric labeling, result in no electrophoretic mobility shifts arising between the two differentially labeled samples when they are co-electrophoresed. Therefore, in DIGE, every identical protein in one sample superimposes with its differentially

labeled counterpart in the other sample, allowing for more reproducible and facile detection of differences. Furthermore, DIGE is a sensitive technique, capable of detecting as little as 0.2 fmol of protein, and this detection system is linear over a ~10,000-fold concentration range (Unlu, Morgan, and Minden 1997; Gong et al. 2004; Lilley and Friedman 2004; Friedman and Lilley 2008).

The most important considerations in performing DIGE experiments are experimental design and sample preparation (M. M. Shaw and Riederer 2003). DIGE has been used to analyze proteome changes from a wide variety of cell types, tissue types, model organisms, and body fluids including serum (Marouga, David, and Hawkins 2005; H. Wang et al. 2005; Okano et al. 2006; Diez et al. 2010; Martyniuk, Alvarez, and Denslow 2012; Arentz et al. 2015). The sample-preparation protocol depends on the sample type. Most samples require mild homogenization in lysis buffer to extract protein. DIGE is an extremely sensitive method, in which a 15% change in protein abundance is more than two standard deviations (SDs) above the normal variation (Gong et al. 2004). Despite DIGE being sensitive and reproducible, two caveats need to be mentioned. First, 2DE does not efficiently resolve integral membrane proteins. This is due to their hydrophobic domains causing precipitation during isoelectric focusing (IEF). Second, labeling with the amine-reactive DIGE dyes limits one to sub-stoichiometric labeling (also known as minimal labeling), where less than 5% of all proteins carry a single bound dye molecule, and the rest have no bound dye. For proteins that are >25 kDa, there is no appreciable molecular-weight shift between labeled and unlabeled protein, while there is a slight but predictable shift for smaller proteins in which unlabeled proteins run about half a spot diameter faster than their labeled counterparts. This shift problem has been addressed with the development of cysteine-reactive dyes. These dyes allow one to saturation-label all available cysteines, which eliminates

the shift between labeled and unlabeled proteins, as all proteins are maximally labeled (Kondo et al. 2003; Sitek et al. 2006; J. Shaw et al. 2003). Regardless of these limitations, DIGE combined with MS is an economical, sensitive, and robust approach for comparative proteomics. This dissertation provides two examples of how powerful this gel based bottom up proteomics approach can be.

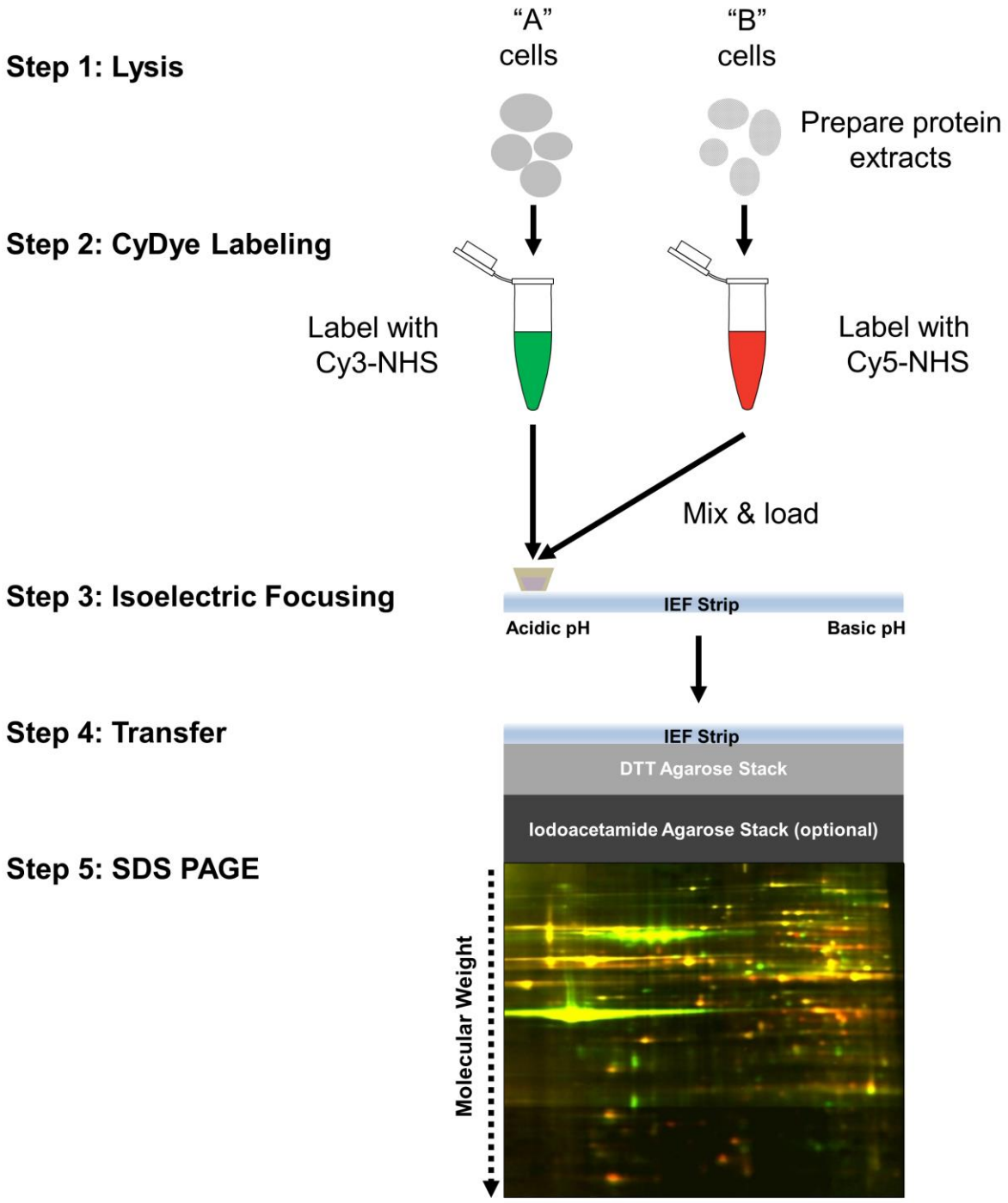

Figure 1.2. The Two Dimensional Difference Gel Electrophoresis (2D-DIGE) work flow.

A schematic of the 2D-DIGE analysis. Extracts are made of two cell samples, denoted 'A' and 'B'. These extracts are separately labeled with Cy3-NHS and Cy5-NHS, which covalently link to lysine residues. The labeled protein extracts are then combined and co-electrophoresed on an

isoelectric focusing strip gel. Following transfer of the IEF strip, proteins are separated based on their size in the 2nd dimension – SDS PAGE. The 2D gel is then imaged on a fluorescent gel imager at the Cy3 and Cy5 emission wavelengths. Shown here is a color overlay of Cy3 (green) and Cy5 (red) images of mitochondria extracts from mouse cell line. Regions of equal Cy3 and Cy5 signals appear yellow.

CHAPTER 2: PROTEOMIC ANALYSIS REVEALS APC-DEPENDENT POST TRANSLATIONAL MODIFICATIONS AND IDENTIFIES A NOVEL REGULATOR OF β-CATENIN

Summary

Wnt signaling generates patterns in all embryos, from flies to humans, and controls cell fate, proliferation, and metabolic homeostasis. Inappropriate Wnt pathway activation results in diseases, including colorectal cancer. The *Adenomatous polyposis coli* (*APC*) tumor suppressor gene encodes a multifunctional protein that is an essential regulator of Wnt signaling and cytoskeletal organization. While progress has been made in defining the role of APC in a normal cellular context, there are still significant gaps in our understanding of APC-dependent cellular function and dysfunction. We expanded the APC-associated protein network using a combination of genetics and a proteomic technique called Two-dimensional Difference Gel Electrophoresis (2D-DIGE). We show that loss of *APC2* causes protein isoform changes reflecting misregulation of post-translational modifications (PTMs), which are not dependent on β-cat transcriptional activity. Mass spectrometry revealed that proteins involved in metabolic and biosynthetic pathways, protein synthesis and degradation, and cell signaling are affected by the loss of *APC2*. We demonstrate that changes in phosphorylation partially account for the altered PTMs in *APC* mutants, suggesting that APC mutants affect other types of PTM. Finally, through this approach Aminopeptidase P was identified as a new regulator of β-catenin abundance in *Drosophila* embryos. This study provides new perspectives on APC's cellular effects that may lead to a richer understanding of APC's role in development.

Introduction

Cell growth, division, and survival are functions that exist in all living organisms. Proper regulation of these functions influences a number of organismal processes such as embryonic development, cellular expansion, and tissue maintenance. These processes require the careful coordination of many signaling pathways. Disruption of these pathways can lead to an array of pathological or disease states such as but not limited to cancer. For instance, it has been demonstrated that uncontrolled or inappropriate cell proliferation is strongly associated with defects in signal transduction proteins (Giancotti 2014). One set of well-studied signaling pathways is the Wnt signaling group. These signaling pathways influence patterns in all embryos, from flies to humans (Clevers and Nusse 2012; Bejsovec 2013). Extensive study of this pathway group has also revealed the importance of Wnt signaling in other cellular processes such as stem cell behavior and cell fate determination, metabolic homeostasis, as well as cytoskeletal dynamics in cell division, migration and adhesion (Holland et al. 2013; Polakis 2012). The clinical importance of this pathway group has been demonstrated by mutations that lead to a variety of cancers and type II diabetes (Welters and Kulkarni 2008).

The Wnt signaling group is comprised of three signal transduction pathways referred to as the canonical Wnt pathway, the non-canonical planar cell polarity pathway, and the non-canonical Wnt/calcium pathway. All three pathways are activated by the binding of a Wnt-protein ligand to a Frizzled family receptor protein on the surface of the cell (Rao and Kühl 2010). The general focus of this study is on the canonical Wnt pathway (Figure 2.1.). Normal canonical Wnt signaling regulates embryonic patterning as a result of controlling stem cell behavior and cell fate determination (Polakis 2012; Kozinski and Dobrzyn 2013). More recently, Wnt's signaling role in metabolic homeostasis has become appreciated (Ring, Kim, and Kahn

2014). The default state of the canonical Wnt signaling pathway is "off" when no Wnt-ligand is present. In this state, an important transcription factor, β-catenin (β-cat), is down regulated and destroyed by a protein complex called the destruction complex. This protein complex includes the following proteins: Axin (Axn), Adenomatous polyposis coli (APC), protein phosphatase 2A (PP2A), glycogen synthase kinase 3 (GSK3), and casein kinase 1α (CK1α). This complex of proteins binds and phosphorylates β-cat, targeting it for proteosomal degradation. As a result β-cat protein levels remain low in the cytoplasm, effectively keeping downstream Wnt target gene activation off. Activation of the canonical Wnt pathway through ligand/receptor binding removes the negative regulation of β-cat by deactivating the destruction complex and translocating components of the destruction complex to the cell membrane through interactions with scaffolding proteins, Disheveled (Dsh), and Axn. In turn, β-cat protein accumulates in the cytoplasm and translocates into the nucleus where it acts as a transcriptional co-activator with the TCF/LEF family of transcription factors. This results in gene transcription activation of Wnt target genes responsible for many of the aforementioned cellular processes above. The clinical importance of this pathway has been demonstrated primarily by its inappropriate activation, such as in colorectal cancer where mutations in the negative regulator and tumor suppressor *Adenomatous polyposis coli* (*APC*) initiate tumorigenesis in the majority of both sporadic and inherited cases (Logan and Nusse 2004; J Schneikert, Grohmann, and Behrens 2007).

The most common mutation in colorectal cancers occurs in APC (>80%), which disrupts APC's Wnt signaling function (Nieuwenhuis and Vasen 2007). A heritable form of colon cancer, Familial adenomatous polyposis (FAP), is caused by inheriting a mutation in the APC gene that usually results in a truncation of the APC protein. Eventually, the cells lose heterozygosity by

acquiring a second APC mutation spontaneously resulting in accelerated formation of polyps that continue to develop and become cancerous (H. Oshima et al. 1997; M. Oshima et al. 1995).

Ligand-independent activation of Wnt signaling due to loss of APC clearly contributes to colon cancer initiation, however, less is known about how disruption of APC's other cellular functions impacts cancer development. In addition to their role in Wnt signaling, APC proteins also function in actin assembly, cell-to-cell adhesion, and microtubule network formation through interactions with cytoskeletal proteins (I. Nathke 2006). Disruption of these functions has negative consequences including decreased cell migration and differentiation, chromosomal instability, and increased proliferation that may contribute to cancer initiation and progression (I. S. Nathke 2004; I. Nathke 2006). Furthermore, new APC protein domains are still being identified that in turn are uncovering new protein and pathway interactions (Z. Zhang et al. 2010; Ezgi Kunttas-Tatli, Roberts, and McCartney 2014). The most recently identified functional sequence is in APC's basic domain where an intrinsically disordered region allows APC to bind to RNA targets (Preitner et al. 2014). This discovery extends APC's interactome to the transcript level, vastly expanding APC's potential biological roles in the cell.

To better understand the cellular consequences of *APC* loss that may contribute to cancer initiation, we used *Drosophila melanogaster* embryogenesis as a model. First, APC proteins are well conserved between mammals and fruit flies, making *Drosophila* a tractable system to study APC-dependent protein networks. Both mammals and Drosophila have two APC proteins, APC and APCL in humans and APC1 and APC2 in Drosophila, respectively. The *Drosophila* APC proteins contain many of the same conserved domains as seen in human APC (Jean Schneikert et al. 2013). However, APC, APCL, and APC1 have additional C-terminal domains that APC2 lacks, suggesting both shared and divergent roles between APC proteins in the cell. Among the

shared domains, APC proteins have three important domain repeats required for destruction complex function and Wnt signaling regulation (reviewed in Barua and Hlavacek 2013). The C-terminal SAMP domains facilitate the necessary interaction between APC and Axn. In the center of the protein are the 15 and 20 amino acid repeats (15Rs and 20Rs respectively), which bind directly to β-cat and are thought to recruit β-cat to the destruction complex (Ezgi Kunttas-Tatli et al. 2012). In addition to regulating Wnt signaling, APC proteins regulate cytoskeletal functions through a series of interaction domains: the Armadillo (Arm) repeats, that are binding sites for many cytoskeletal regulators including IQGAP, Rho-GEF, and ASEF (Kawasaki et al. 2009; Kawasaki et al. 2000; Kawasaki, Sato, and Akiyama 2003; I. Nathke 2006; Tirnauer 2004), the basic region, and the EB1 domain. APC, APCL, and APC1 all have a basic domain, a binding site for microtubules and the formin Diaphanous (Wen et al. 2004; Webb, Zhou, and McCartney 2009). APC and APC1 have an EB1 domain that functions as a binding site for the microtubule protein, EB1 (Barth, Siemers, and Nelson 2002). The exception is that APCL can also bind to EB1, although the domain does not share primary sequence with APC (Nakagawa et al. 2000). Lastly, as in humans, the *Drosophila* genome contains two *APC* genes (Logan and Nusse 2004).

Our lab and others have demonstrated that *Drosophila* and vertebrate APC proteins are functionally conserved; both fly APC proteins negatively regulate Wnt signaling (Ahmed et al. 1998; B M McCartney et al. 1999), collaborate with the formin Diaphanous (Webb, Zhou, and McCartney 2009; R Jaiswal et al. 2013), and can localize to microtubules (B M McCartney et al. 2001; Akong et al. 2002). In addition, *Drosophila* APC1 binds actin monomers,

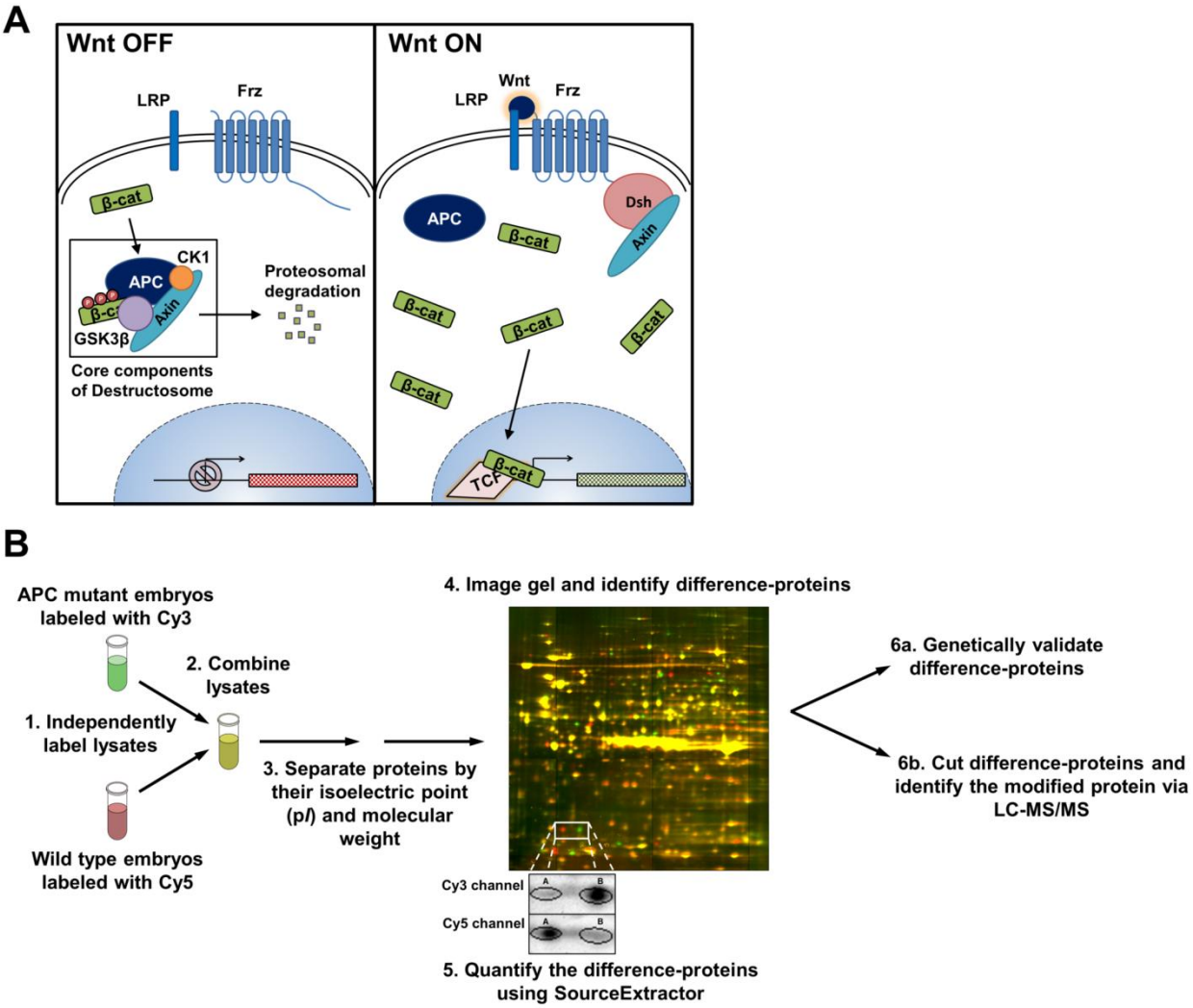

Figure 2.1. Summary of the Wnt signaling pathway and 2D-DIGE work flow.

(**A**) The Wnt signaling pathway. When no Wnt ligand is present (left) the destructosome promotes cytoplasmic β-cat degradation. With a Wnt ligand (right), the destructosome is deactivated and cytoplasmic β-cat accumulates, enters the nucleus and activates Wnt target genes. (**B**) Principal steps in the 2D-DIGE workflow: (1) covalent labeling of protein lysates with either propyl-Cy3 or methyl-Cy5, (2) combine labeled protein lysates, (3) co-electrophorese on a 2DE gel, (4) fluorescent gel imaging of Cy3 (green) and Cy5 (red) (common spots are shown as yellow spots, while difference-proteins appear as green or red), (5) selected spots

shown in the inset are quantified using Source Extractor and concurrently (6a.) genetically validate the difference-proteins and (6b.) identify the proteins by LC-MS/MS.

nucleates F-actin assembly (Richa Jaiswal et al. 2013), and binds the microtubule plus-tip protein EB1 (Brooke M McCartney et al. 2006). Previous studies have examined the global cellular consequence of *APC* disruption using RNA-seq and 2D-DIGE proteomics (Chafey et al. 2009; Wu et al. 2012). However, the results of these studies may have reflected chronic changes due to loss of APC's non-Wnt activities, as well as the primary and downstream effects of ligand-independent Wnt target gene activation. The RNA study examined biopsies from stage 3 colorectal cancer patients, where the proteome study examined mouse liver where *APC* loss was induced 7 days prior to proteomic analysis. We are using the early Drosophila embryo (0-2 hrs after egg laying) as our model system. At this time in development, zygotic transcription is largely silenced (ref). Thus, our model provides a unique opportunity to see proteome changes that could be masked by the ligand-independent hyperactivation or misregulation of β-cat transcription.

Using the early *Drosophila* embryo and 2D-DIGE, we show here the initial identification of 16 protein differences between wild-type and *APC2* mutant embryos. All of these difference-proteins were the result of isoform shifts, rather than changes in abundance, indicating these proteins are post-translationally regulated, not transcriptionally regulated. Additionally, we identified a number of overlapping changes in *APC1* null and *APC2 APC1* double null embryos. To demonstrate APC specificity, we screened these 16 difference-proteins for their ability to be reproduced in an independent *APC2* mutant background, and to be rescued by exogenous *APC2* expression. LC-MS/MS was used to identify the *APC2*-dependent changes, which include proteins involved in cellular processes such as metabolic and biosynthesis pathways, protein synthesis and degradation, cell signaling and cellular stress response. These results demonstrate that APC post-translationally influences an array of protein targets, revealing a novel mechanism

to regulate cellular processes at the proteome level. Loss of APC contributes to the acute misregulation of these proteins. This new insight contributes to a deeper understanding of the global cellular consequences of *APC* loss that may be factors in cancer development.

Methods

Fly work

Stocks: *APC2^{g10}/TM6, Tb* (Brooke M McCartney et al. 2006); *APC2^{33}/TM3, Sb* (Takacs et al. 2008); *FRT82B APC1^{Q8}/TM6, Tb* (Ahmed et al. 1998); *FRT82B APC2^{g10} APC1^{Q8}/TM6, Tb* (Ezgi Kunttas-Tatli et al. 2012); *P[endoP-EGFP-APC2-FL]; APC2^{g10}* (Ezgi Kunttas-Tatli et al. 2012), *P{EPgy2}ApepP^{EY02585}/CyO, Mi{MIC}ApepP^{MI01970}/SM6a, Twk^{1}* (*y, w, P{ey-FLP.N}2; tweek1 P{y+,ry+}25F, P{neoFRT}40A*) and *Twk^{2} (y, w, P{ey-FLP.N}2; tweek2 P{y+, ry+}25F, P{neoFRT}40A* (Verstreken et al. 2009). Homozygous *APC1^{Q8}* and *APC2^{g10} APC1^{Q8}* embryos were generated using the FRT/FLP/DFS technique (Chou and Perrimon 1996).

Single embryo work

Wild-type and homozygous mutant *ApepP* and *Twk* embryos were collected for 12 hours and incubated for 2 days at 29ºC to allow all embryos to fully develop. Cuticle preparations and hatch rate analysis were as described by (Wieschaus & Nusslein-Volhard, 1986). Stage 6-8 (4-6 hrs at 29ºC) wild-type and homozygous mutant *ApepP* embryos were collected, dechorinated, and fixed in a 1:1 heptane:37% formaldehyde solution (B M McCartney et al. 1999). Mouse anti-Armadillo (N27A1, 1:250) antibodies were obtained from the Developmental Studies Hybridoma Bank. Secondary antibodies were conjugated with various Alexa dyes (Invitrogen, 1:1000). Embryos were imaged with a spinning disc confocal microscope (Solamere Technology Group) with a QICAM-IR camera (Qimaging) on a Zeiss Axiovert 200M, using QED InVivo software. For Fig. 8, Arm image analysis was performed by 5 µm stack projections. Arm striped pattern was quantified using ImageJ (NIH) software.

Two-dimensional fluorescence difference gel electrophoresis (2D-DIGE)

Embryos for 2D-DIGE were collected for 2 hour intervals, following one hour pre-collection period. All samples were visually inspected to remove old (beyond 2 hours) and damaged embryos. Protein samples were prepared by pooling the embryos in standard embryo wash (120 mM NaCl, 0.04% Triton X-100) into one tube. Once sufficient embryos were amassed, they first were dechorionated and transferred to a 1.5 ml centrifuge tube that had a fitted plastic pestle. The standard embryo wash was removed and the embryos were washed three times with DIGE embryo wash (0.01% CHAPS and 5 mM HEPES pH 8.0). The DIGE embryo wash contains low salt and replaces the Triton from the standard embryo wash with CHAPS. High salt and strong detergents interfere with IEF. After the washes, lysis buffer (7 M urea, 2 M thiourea, 4% CHAPS, 10 mM DTT and 10 mM Na-Hepes pH 8.0) was added to 0.5 µl of lysis buffer per embryo, with a maximum of 200 µl per tube. The tube was then transferred to ice and the embryos were homogenized manually with the fitted pestle. Embryo lysates were adjusted to 2 mg/ml protein concentration with lysis buffer. Protein lysate solutions containing a total of 100 µg of protein were labeled with 2 µl of either 1mM propyl-Cy3-NHS or 0.83 mM methyl-Cy5-NHS – referred to as Cy3 and Cy5, respectively (CyDye DIGE Fluors; GE Healthcare) as described previously (Unlu, Morgan, and Minden 1997). We also performed reciprocal labeling experiments to control for dye-dependent changes and to have technical replicates of each sample. Two-dimensional electrophoresis (2DE) was performed. First, isoelectric focusing was carried out on 18 cm, pH 3-10 non-linear Immobiline DryStrip gels according to the manufacturer's protocol (GE Healthcare). The strips were electrophoresed on an IPGphor apparatus (GE Healthcare) for a total of 28-32 kVhrs. After isoelectric focusing, the strips were loaded onto the second dimension 12% SDS-polyacrylamide gel, overlayed with 1% agarose, 65

mM Tris pH 6.8, 0.1% SDS and 65 mM DTT (Van, Ganesan, et al. 2014). The strips were sealed onto the stacking gel using an agarose sealing gel containing 1% agarose, 65 mM Tris pH 6.8, 0.1% SDS, and 0.002% bromophenol blue. Second dimension electrophoresis was performed at 4 °C at 60 V until the dye front had passed through the stacking gel and 300 V for the remainder of the run.

2D-DIGE imaging analysis and protein quantification

After second dimension electrophoresis, the gels were removed from the glass plates and equilibrated in a solution of 40% methanol and 10% acetic acid for at least one hour. The gels were placed in a Structured Illumination Gel Imager (Van, Bass, et al. 2014) and imaged at two excitation wavelengths (545±10 nm for Cy3 and 635±15 nm for Cy5) using a cooled CCD camera with a 16-bit CCD chip (Roper Scientific). Two separate images for Cy3- and Cy5-labeled proteins were acquired and viewed as a two-frame movie played in a continuous loop. Image manipulation and viewing was done with ImageJ (NIH) software. Protein differences were detected visually by movies containing grey scale images of each channel, and confirmed with a two-color, red-green overly of the Cy3 and Cy5 channels, as shown in Fig. 2.

Protein spots were quantified using an astronomical image analysis software package, Source Extractor (Bertin and Arnouts 1996). To determine the fold-difference between mutant *APC* and wild-type expression of a protein, the image fragments were summed to generate a composite image. The summed image was submitted to SExtractor as previously described (Van, Bass, et al. 2014). To aid in calibrating protein quantification and for balancing the displayed contrast of the Cy3 and Cy5 images, we measured the intensity ratio for 6 known unchanged spots (referred to Appendix A, Table 1).

Protein identification

Spots of interest from the 2D-DIGE gels were picked robotically from gels containing both *APC* mutant and wild-type embryo samples (Van, Ganesan, et al. 2014). In-gel digestion of the protein spots was done with trypsin using a standard manual extraction protocol (Speicher et al. 2000). LC-MS/MS analysis was performed at the University of Pittsburgh Genomics and Proteomics Core Facility on a Thermo Scientific LTQ-XL instrument equipped with a Dionex Ultimate 300 HPLC. The detector m/z range was set to 85.00-2000.00 with 400-450 scans per spectrum. The resulting spectra were visually inspected for quality control using Xcalibur 2.2 (Thermo Scientific). Pre-acquisition calibration was performed using Picosure (New Objective) Test Standards (MH+ 985.4577±1, 988.4762±1, 987.5138±1, 1045.5345±1, 1182.5570±1, 986.5549±1, 985.5961±1, 1098.6801±1). MS/MS data were submitted to Mascot 2.4.1 for database searching. The search was performed to query the database (Taxonomy: *Drosophila*) downloaded from Uniprot (August 2013), allowing one missed cleavage site by trypsin. Carbamidomethyl modification of cysteine and methionine oxidation were set as variable modifications. All matches that occurred above a 95% confidence interval (CI), with significant scores for the peptides defined by Mascot probability analysis greater than "identity" were considered for protein identifications.

Additionally, each protein identified was scrutinized using five criteria: (1) each suspected protein isoform pair should contain peptides corresponding to the same *Drosophila melanogaster* protein(s), (2) the same set of spots in reciprocally-labeled gels from the same 2D-DIGE experiment should contain the same peptides corresponding to the protein(s) identified in criterion 1 (technical replicate), (3) each protein identified should be represented by more than 2 peptides from at least two independent mass spectrometry experiments (biological replicate), (4)

the observed molecular weight of the protein identified on a 2D-DIGE gel should approximately match the theoretical molecular weight of the identified protein and (5) the observed p*I* of the protein identified on a 2D-DIGE gel should approximately match the theoretical p*I* of the identified protein. Criteria 4 and 5 were only approximate because proteins often deviate from their predicted mass and p*I* on 2DE gels, which is particularly true for p*I* since the IEF pH gradients were non-linear.

Phosphatase treatment

Wild-type and *APC2*^{g10} embryo lysates (100 µl at 5 mg/ml) were made using 1X NEBuffer for PMP supplemented with 2mM $MnCl_2$ (50 mM HEPES, 100 mM NaCl, 2 mM DTT, 0.01% Brij 35, pH 7.5). Control samples were treated with 1% PhosSTOP Phosphatase Inhibitor Cocktail (Roche). Experimental samples were treated with 300 units of Lambda Protein Phosphatase (New England BioLabs) and incubated at 30°C for 4 hours. The phosphatase reaction was quenched using 50 mM Na_2EDTA at 65°C for 1 hour. Urea, thiourea, CHAPS, HEPES pH 8.0, and DTT were added to the lysates to yield 250 µl of a 2 mg/ml final lysate. The lysates were then analyzed by 2D-DIGE.

Immuno-blotting

Immuno-luminescence was detected using a LAS-300, Fujifilm Luminescent Image Analyzer (Formally Fuji, now GE).

For ApepP analysis: Wild-type , mutant *ApepP*, and mutant *APC2* embryo lysates were prepared in 2X Leammli sample buffer treated with 0.1% Protease Inhibitor Cocktail (Sigma) and separated by SDS-PAGE. Proteins were transferred to Protran nitrocellulose membranes

(Whatman) for 2 hours at constant 35 V and confirmed by Ponceau S stain. Membranes were immuno-blotted using mouse anti-*Drosophila* Armadillo antibody (1:250) and mouse anti-*Drosophila* tubulin loading control antibody was (1:100) provided by DSHB. Goat anti-mouse HRP[2] secondary antibody (Jackson Immunoresearch) was used at 1:2,000.

For CaBP1 analysis: Wild-type and mutant *APC2* embryo lysates were labeled in separate reactions with Cy3 dye and run on two independent 2DE gels, as described above. Transfer was confirmed by Cy3 imaging. Membranes were immuno-blotted using a Rat anti-*Drosophila* Calcium Binding Protein 1 antibody (1:500) generously provided by Dr. Yoshinobu Nakanishi (Okada et al. 2012). Goat anti-rat HRP[2] secondary antibody (Jackson Immunoresearch) was used at 1:10,000.

Aminopepidase P proteolytic assay

We performed the ApepP proteolytic assay as described in (Kulkarni and Deobagkar 2002). Single male or female adult flies were homogenized with a fitted plastic pestle in 50 µL of ice cold lysis buffer (1mM $MgCl_2$, 100mM HEPES at pH 8, 1mM PBS), in a 1.5 mL microcentrifudge tube, until no particulates were visible. The homogenates were centrifuged at 10,0000 G for 10 minutes. Five µL of the supernatant was taken and used for the reaction. Reactions were incubated with tri-peptide substrate for one hour at 37 °C, after the reaction was killed using 1mM HCl and the OTPA dye was added to the reaction. 1mM EDTA was used as an ApepP inhibitor. Absorbance measurements were taken at 455nm using a Tecan Safire 2 Plate Reader (Tecan Group Ltd., Männedorf, Zürich, Switzerland). Absorbance values were normalized to total protein concentrations for each sample. Background noise from the OPTA

dye was also subtracted from each sample. Absorbance values were compared to w^{1118} to calculate the relative activity.

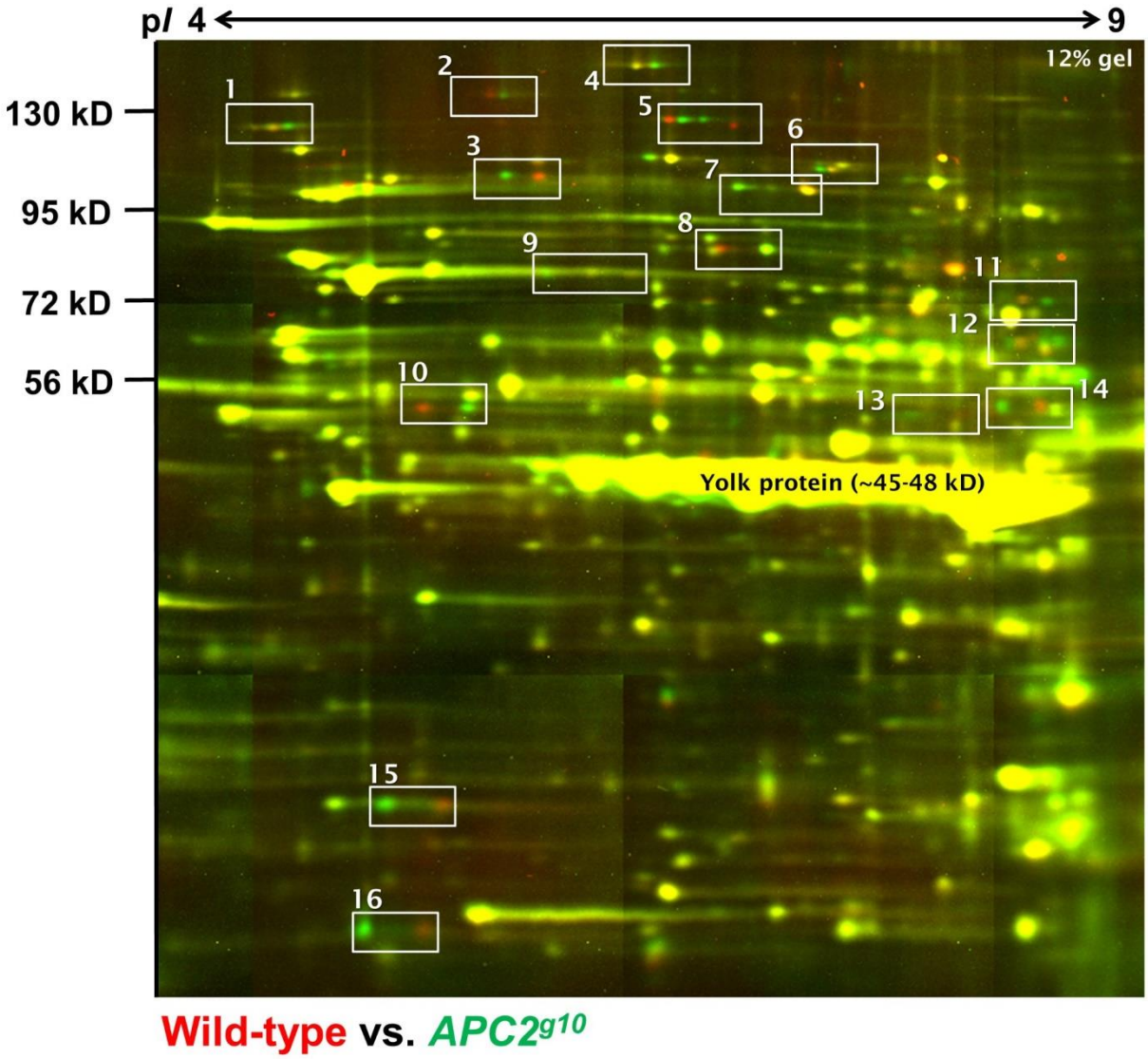

Figure 2.2. 2D-DIGE of *APC2* null versus wild-type *Drosophila* embryos.

A tiled array of a whole gel comparing of *APC2*^{g10} embryos (shown in green) and wild-type embryos (shown in red). The 16 *APC2*-dependent difference-protein pairs are demarcated with white boxes. Contrast and brightness were manipulated on the whole-gel images using ImageJ.

Results

Comparison of the *APC2* null and wild-type proteomes

To understand the proteome changes that occur when APC protein is absent from the early embryo, we compared lysates of *APC2* null and wild-type embryos (Fig. 2.1). Early embryos (0-2 hours AEL) were chosen to characterize the earliest detectable proteome changes associated with APC loss. At this stage, these embryos contain many syncytial nuclei within a single cell, where transcription is strongly inhibited with the exception of some patterning and housekeeping genes (Qin et al. 2007; Tadros and Lipshitz 2009). Thus, we predicted that the differences between the *APC2* and wild-type proteomes would mostly appear as post-translational changes, rather than protein abundance changes resulting from transcriptional activation of Wnt targets. Lysates from mutant and wild-type embryos were separately labeled with either Cy3 or Cy5 DIGE dyes, shown as green and red, respectively. The separately labeled lysates were combined and run on the same 2DE gel. Protein spots that are common to both lysates are yellow, while proteins that are enriched in one lysate will appear more red or more green. PTM differences appear as closely spaced reciprocally changing spots: one protein spot increases while its neighbor decreases (Fig. 2.1, step 4, white box).

APC2 is the most abundant of the two APC proteins during early embryogenesis and functions in Wnt signaling and cytoskeletal regulation (B M McCartney et al. 1999; B M McCartney et al. 2001; Webb, Zhou, and McCartney 2009; Zhou et al. 2011; Ezgi Kunttas-Tatli et al. 2012; Ezgi Kunttas-Tatli, Roberts, and McCartney 2014; E. Kunttas-Tatli et al. 2015). 2D-DIGE comparison of $APC2^{g10}$ (*APC2* null) and wild-type embryos revealed 16 prominent protein changes that were observed in 100% of the trials (n = 30), all of which appeared to be PTMs as evidenced by two or more protein spots horizontally arranged changing reciprocally (Fig. 2.2,

white boxes). Such horizontal shifts indicate a change in isoelectric point (p*I*) or net protein charge, but not protein mass. Ten of the 16 difference-proteins showed an increase in the acidic isoform in *APC2* mutants and the remainder showed a decrease in the acidic isoform. This set of protein changes was observed in 30 high-quality biological replicates and is composed of moderately to highly abundant proteins. Other lower abundance protein changes were observed, but not as consistently, likely due to gel-to-gel variation.

The 16 difference-protein pairs in the $APC2^{g10}$ embryos were quantified using an open-source astronomy software package, SourceExtractor, previously described (Bertin and Arnouts 1996; Gong et al. 2004; Van, Bass, et al. 2014, Appendix, Table 1). The typical variation in measured abundance of common protein spots is less than 4% for 2D-DIGE, thus the cutoff for significant total abundance change was set to > ±10%, which is 2.5 standard deviations from the typical variance (Gong et al. 2004). Just over half of the difference-protein pairs (9 of 16) were close to being perfectly reciprocal changes (< 10% total protein change) (Fig. 2.3A). The remaining 7 exhibited total abundance changes of >10% (Fig. 2.3B), where there was a reduction in the total abundance of each isoform pair, suggesting increased protein degradation in $APC2^{g10}$ embryos. None of the difference-protein pair regions showed a significant increase in total isoform abundance. Thus the loss of *APC2* in early embryos, where there is no Wnt pathway activation and very little transcription, leads to significant protein changes affecting PTMs that may decrease the stability of a subset of these proteins.

Identification of difference-proteins isoform pairs in *APC2* null and wild-type proteomes

The difference-protein pairs were analyzed by MS to identify the proteins and confirm that each pair of protein spots represented protein isoforms. Protein spots were cut out of the gels

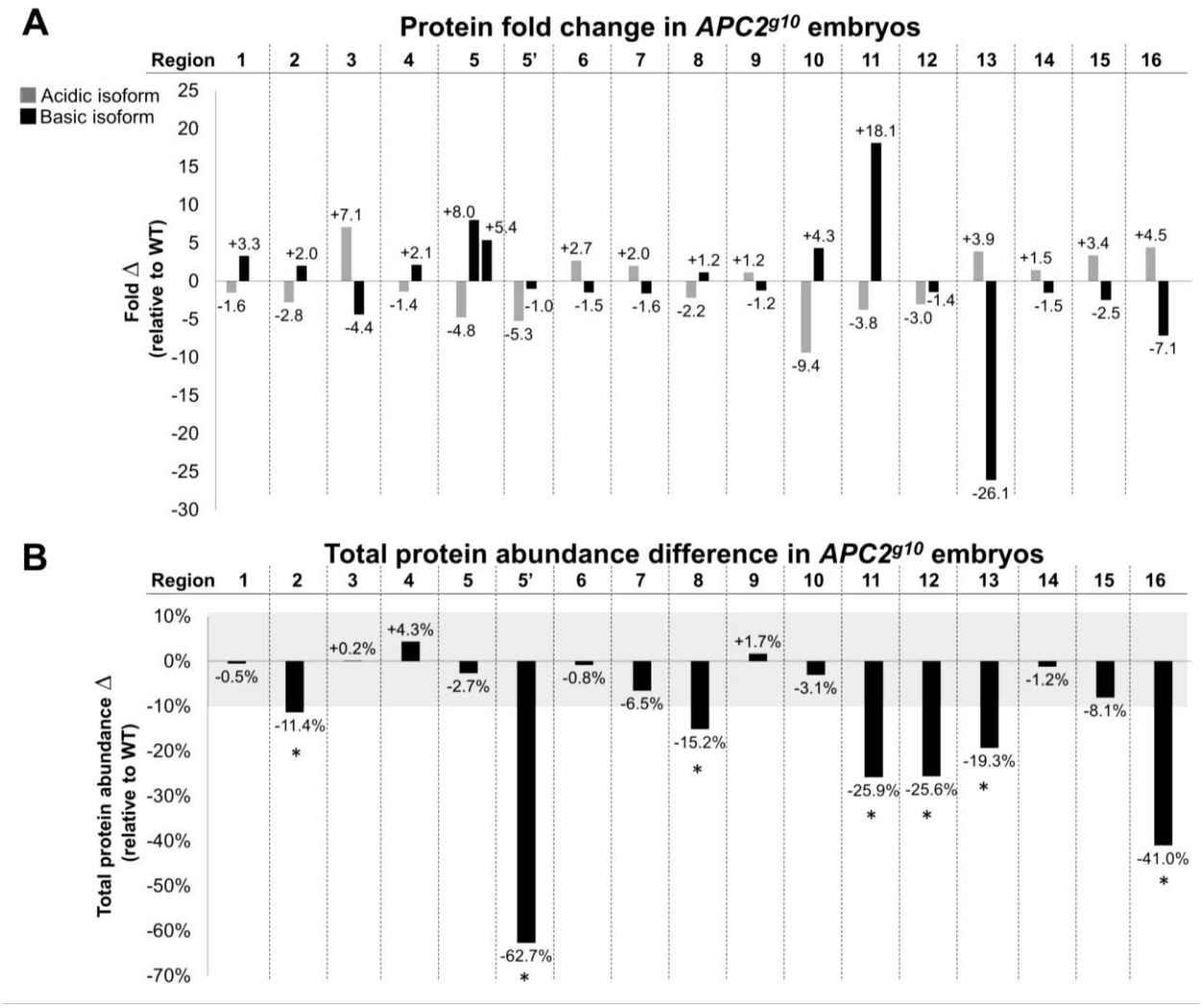

Figure 2.3. Quantification of the *APC2* difference-proteins.

(**A**) Plots the measured fold-change for each difference-protein pair that was calculated using the Cy3 and Cy5 raw fluorescence intensities as exemplified in panel A. Cy3/Cy5 ratios <1 were converted to negative fold-change. (**B**) The total protein abundance, defined as the sum of the fluorescent intensities of putative difference-protein isoforms, was calculated for each protein region in wild-type and *APC2*^{g10} embryos. The percent difference of the total protein isoform fluorescence was then calculated. Difference-proteins that displayed a > 10% change in total abundance were marked with an asterisks (*).

by a robotic cutting tool incorporated into the gel imager and in-gel trypsin digestion was performed on each gel fragment. The peptide fragments were recovered and analyzed by LC-MS/MS. MS analysis revealed that some difference-protein pairs contained more than one protein species. A list of protein identifications for the 16 difference-protein isoform pairs was generated from at least two biological replicates (Fig. 2.4A, Table 2). In addition, protein spots from gels containing reciprocally-labeled samples were analyzed to provide technical replicates, further validating the protein identifications. All identified proteins had predicted masses and isoelectric points that were relatively well matched to the observed difference-proteins on the 2DE gel. The combined MS data from the technical and biological replicates was used to generate a list of most-likely protein candidates for the 16 difference-protein pairs observed in the *APC2* null vs. wild-type comparison (Fig. 2.4A). The identified proteins span a range of cellular functions, from metabolic proteins being the most prominent difference-proteins to RNA binding proteins, proteases and chaperones (Fig. 2.4B).

We used immunoblot analysis to confirm the identity of one of the difference-proteins for which a Drosophila-specific antibody was available. Calcium Binding Protein 1 (CaBP1) shifts to a more basic isoform in *APC2* mutants (Fig. 2.2, Region 10; Fig. 2.5.1, Table 2C). Wild-type and $APC2^{g10}$ lysates were independently labeled with Cy3 dyes and electrophoresed on separate 2DE gels. Fluorescence images were captured of the proteins before being transferred to nitrocellulose membranes (Fig. 2.5.2). The fluorescence and immunoblot images (Fig. 2.5.3) were superimposed to show that the acidic isoform is in greater abundance in wild-type embryos, while the basic isoform is more abundant in $APC2^{g10}$ mutant embryos (Fig. 2.5.4), confirming our MS identification of CaBP1, and that its isoform distribution is altered in *APC2* null mutants.

Comparison of the *APC* null proteomes

Drosophila APC2 and APC1 proteins both function in the destructosome and exhibit redundancy in the regulation of Wnt signaling during embryogenesis (Akong et al. 2002; Ezgi Kunttas-Tatli et al. 2012). Thus, we predicted that at least some of the proteome changes seen in *APC2* null mutants would also be observed in *APC1* null embryos. To understand the interplay between APC2 and APC1 on a proteome-wide level, we compared lysates from $APC2^{g10}$ embryos to $APC1^{Q8}$ embryos (Appendix A, Table 3C), as well as *APC2 APC1* double null ($APC2^{g10}APC1^{Q8}$) embryos (Appendix A, Table 3C). Since *APC1* and *APC2 APC1* null females are not viable, germ line mosaics from heterozygous mutant $APC1^{Q8}$ or $APC2^{g10}APC1^{Q8}$ females were made using the FLP/FRT system (Chou and Perrimon 1996). A total of 14 changes in $APC1^{Q8}$ embryos and 23 changes in $APC2^{g10}APC1^{Q8}$ embryos were observed in comparison to wild-type embryos. We do not think that the increase or decrease in the total number of changes compared to $APC2^{g10}$ is significant, owing to the experimental variability. Comparing the difference-protein pairs between *APC2* null embryos versus wild-type and *APC1* null embryos versus wild-type showed that these two mutants shared eleven of APC's difference-proteins, five were unique to *APC2* null embryos (Appendix A, Table 3C). None of the difference-proteins were specific to *APC1* null embryos. Comparing the difference-protein pairs between *APC2* null embryos versus wild-type and *APC2 APC1* double null embryos versus wild-type showed that these two mutants shared ten of APC2's difference-protein pairs, six were unique to *APC2* null embryos and 11 were specific to *APC2 APC1* double null embryos.

Of the eleven common difference-protein pairs between *APC2* and *APC1* mutants and the ten common difference-protein pairs between *APC2* and *APC2 APC1*mutants, six were shared by all three mutant-types being compared. Five additional difference-proteins were common only to

APC1 and *APC2*-these were not observed in the *APC2 APC1* mutants; while four difference-proteins were common only to *APC2* and *APC2 APC1* mutants, not observed in *APC1* null versus wild-type alone. Overall, there was one difference-protein that was unique to *APC2* mutants, none were unique to *APC1* mutants, and ten were unique to the *APC2 APC1* double mutants. These data suggest that there is a complex interplay between *APC1*, *APC2*, and the *APC2 APC1* double mutants that is neither purely additive, nor synergistic, indicating the APC1 and APC2 proteins serve both individual and shared functions. An alternative explanation for some of these results is that some of these unique changes may be independent of the *APC* genes, and instead be due to differences in genetic background. This may explain why the six *APC2* null unique changes were not observed in the *APC2 APC1* double mutant embryos.

The difference-proteins isoform pairs are due to multiple types of PTMs

Because phosphorylation is the most common post-translational modification (Khoury, Baliban, and Floudas 2011), and the APC-containing destructosome possesses two kinases, GSK3β and CK1α, we tested the hypothesis that many of the observed difference-proteins were due to phosphorylation changes by treating wild-type and *APC2*^{g10} embryo lysates with a broad spectrum phosphatase, Lambda Protein Phosphatase (λPP). 2D-DIGE was used to compare λPP-treated wild-type or *APC2* mutant embryo lysates versus untreated lysates. Dephosphorylated proteins shift to the right (more basic) relative to untreated lysates, while non-phosphorylated (or λPP refractory) protein will be unaffected. The efficacy of phosphatase treatment was confirmed by observing the entire yolk protein population shifting to the right (data not shown). Unfortunately, the λPP reaction conditions interfered with isoelectric focusing in the basic region of the 2DE gels preventing analysis of 7/16 of the difference-proteins isoform pairs. The acidic

half of the gels was well resolved, and we were able to assess 9/16 of the difference-proteins isoform pairs. Surprisingly, phosphorylation was found to play a minor role in generating the isoform changes. Below are two examples of what we observed.

Dp1 difference-protein isoforms displayed phosphatase sensitivity (Fig. 2.6A). Dp1 has two isoforms on 2DE gels: the acidic L isoform, which is elevated in wild-type embryos (Fig. 2.6A', left panel) and the basic R isoform that is elevated in *APC2* mutant embryos (Fig. 2.6A", left panel). The L isoform shifted to the right upon λPP treatment, indicating that this isoform is phosphorylated (Fig. 2.6A', right panel). The R isoform did not shift due to λPP treatment, indicating that it is not phosphorylated (Fig. 2.6A", right panel). Interestingly, in both wild-type and *APC2* mutant embryos conversion of the L isoform to the R is incomplete, suggesting that Dp1 may be partially refractory to λPP or that some fraction of the L protein spot bears a different PTM.

ApepP appears to be insensitive to phosphatase treatment (Fig. 2.6B). ApepP has three isoforms on 2DE gels. In wild-type embryos the more basic, R, isoform is elevated (Fig. 2.6B', left panel), while in *APC2* mutant embryos it is the acidic L isoform that is elevated (Fig. 2.6B", left panel). The middle isoform does not significantly change in *APC2* mutant embryos compared to wild-type (Fig. 2.6B, ApepP). Surprisingly, none of the isoforms shifted upon λPP treatment, suggesting that none of the ApepP isoforms are phosphorylated, or ApepP is completely resistant to λPP. We observed this to be true for the majority of the resolved difference-proteins isoforms (8 of 9) suggesting that phosphorylation is not the major post-translational modification altered in *APC2* null embryos.

A Identified proteins for *APC2* null protein-differences

Region	Gene	Protein name	Isoform in $APC2^{g10}$	Mol. mass (kDa)	pI*	Molecular Function
1	*CG2918*	N/A	Basic	103	5.1	Protein chaperone
2	*ade2*	Phosphoribosylformylglycinamidine synthase	Basic	148	6.6	Metabolic protein
3	*Irp-1B*	Iron binding protein 1	Acidic	99	5.7	RNA-binding
4	*Dp1*	Dodeca-satellite-binding protein 1	Basic	144	5.9	DNA-binding
5	*CG1516*	Pyruvate carboxylase	Basic Acidic	133	6.2	Metabolic protein
6	*CG14476*	N/A	Acidic	106	6.1	Metabolic protein
7	*GlyP*	Glycogen phosphorylase	Acidic	97	6.1	Metabolic protein
8	*Aats-gly*	Glycyl-tRNA synthetase	Basic	76	6.0	Metabolic protein
9	*ApepP*	Aminopeptidase P	Acidic	63	5.6	Protease
10	*CaBP1*	Calcium binding protein 1	Basic	47	5.5	Signaling
11	*mRpS30*	Mitochondrial ribosomal protein S30	Basic	65	8.5	RNA-binding
12-1	*Cbs*	Cystathionine beta-synthase	Basic	57	6.6	Metabolic protein
12-2	*CG8231*	TCP-1zeta	Acidic	58	6.2	Protein chaperone
13	*La*	La autoantigen-like protein	Acidic	45	7.7	RNA-binding
14	*blw*	Bellwether, ATP synthase subunit	Acidic	59	9.1	Metabolic protein
15	*Uch*	Ubiquitin carboxy-terminal hydrolase	Acidic	26	5.3	Protease
16	*CG1633*	Jafrac 1	Acidic	22	5.5	Metabolic protein

B Overall protein identification synopsis

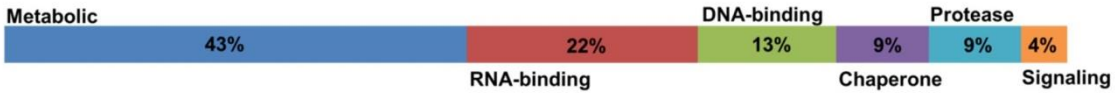

Figure 2.4. MS Identification of the *APC2*-dependent difference-proteins.

(**A**) A list of the most likely protein identifications for the 16 difference-proteins observed in $APC2^{g10}$ versus wild-type embryos comparisons. (**B**) Graphical representation of the molecular functions performed by the identified difference-proteins (see Appendix for full details).

Controlling for genetic background effects

Controlling for genetic variability has always been a concern when determining differential expression of proteins in proteomic comparisons between two conditions. We asked if any of the 16 difference-protein isoforms were variably expressed across multiple wild-type strains, by comparing the proteome of our lab's w^{1118} wild-type strain (w^{Mc}) to two other closely related, yet independently segregated w^{1118} lines: w^{D} and w^{P} (Fig. 2.7A, Table S3A). The w^{P} wild-type strain is originally from the Peifer lab (University of North Carolina at Chapel Hill), from which the McCartney w^{1118} line was derived and used for outcrossing of the $APC2^{g10}$ stock. The w^{D} strain was obtained from the Duke University Model Systems Genomics Facility where our *APC2-FL* transgenic line was generated in this genetic background (Brooke M McCartney et al. 2006), and subsequently crossed into the $APC2^{g10}$ background for genetic rescue experiments. Thus these two independent wild-type w^{1118} strains were the most relevant wild-type genotypes to determine if the protein changes that are found in our original w^{Mc} vs. $APC2^{g10}$ comparison are variable. From this analysis, we found that w^{D} shares 3 difference proteins with $APC2^{g10}$ and w^{P} shares an additional 6 difference proteins with $APC2^{g10}$ (Appendix A, Table 3A). Because of the possibility that the changes to these 9 difference-proteins are not specific to $APC2^{g10}$ and instead result from common background effects, we chose to continue our analysis with the remaining wild-type independent (WTI) difference-proteins (1, 4, 7, 9, 11, 12, and 16) that did not appear as changes in any of our three wild type w^{1118} strains.

Validating the APC-dependent difference-protein isoform pairs

We next asked if exogenous expression of full-length APC2 protein was able to rescue the remaining seven WTI difference-proteins in *APC2* null embryos (1, 4, 7, 9, 11, 12, and 16)

(Appendix A, Table 3A). First, the proteome of *APC2*^{g10} embryos was compared to *APC2*^{g10} embryos carrying two copies of a full length *APC2* transgene (*FL-GFP-APC2;APC2*^{g10}). This *APC2* transgene, which is driven by the native *APC2* promoter, is expressed at endogenous levels (Brooke M McCartney et al. 2006) and it rescues both the cytoskeletal defects seen in the early embryo and Wnt signaling defects observed later in embryogenesis (Zhou et al. 2011; Ezgi Kunttas-Tatli et al. 2012). Surprisingly, only five of the seven WTI difference-proteins – CG2918, Dp1, GlyP, ApepP, and Cbs/TCP were reverted by ectopic expression of APC2 (e.g. Fig. 2.7B, ApepP, left panel vs. middle panel). Further evidence for the effect of ectopic APC2 expression in *FL-GFP-APC2* embryos was confirmed by the presence of these five difference-protein changes when compared to *APC2* null embryo lysates (Fig. 2.7B, ApepP, left panel vs. right panel). The remaining two WTI difference-protein pairs, mRpS30 and Jafrac1, were not reversed by ectopic APC2 expression (e.g. Fig. 2.7B, Irp-1B).

There are two possible explanations for why *FL-GFP-APC2* failed to rescue two of the WTI difference-protein pairs in *APC2*^{g10}: (1) these protein differences are due to genetic background differences in *APC2*^{g10} that were not present in the other wild-type *w*^{1118} lines, or (2) the FL-GFP-APC2 protein has reduced function compared to wild type APC2, and that the proteomic changes are highly sensitive to APC2 activity. To distinguish between these two possibilities, an independent *APC2* null allele, *APC2*^{33}, was analyzed. *APC2*^{33} was created by imprecise excision of a P-element within *APC2*, deleting a large portion of the 5' end of the gene, spanning from the promoter to the fifth Armadillo repeat (Takacs et al. 2008). All WTI difference-proteins, except #16-Jafrac1, were observed in the *APC2*^{33} versus wild-type comparison, suggesting that they are *bona fide APC2*-dependent protein changes. Thus, the failure of *FL-GFP-APC2* to compensate for some of the WTI difference-proteins is likely due to

insufficient activity (Appendix, Table 3B). To further support that these changes are APC-dependent, a variety of these changes can be reproduced in various *APC* knockdown situations (Fig. 2.7C; Appendix A, Table S3). Isoform differences in proteins Dp1, GlyP, ApepP, and mRpS30 recapitulated by knocking down *APC2* with a dsRNA driven by a strong maternal driver (MTD) as compared to w^{Mc}. CG2918, Dp1, GlyP, and ApepP displayed isoform differences when comparing $APC1^{Q8}$ null germ line clone embryos to w^{Mc} embryos. Isoform changes in CG2918, ApepP, and mRpS30 were observed when comparing $APC2^{g10}APC1^{Q8}$ null germ line clone embryos. Together, these data strongly support that six of the seven WTI difference-protein isoform pairs are indeed *APC*-dependent changes and not due to genetic background mutations.

The APC-dependent difference-proteins isoform pairs do not require β-cat transcription

Previously published proteome studies of APC mutant tissue identified a number of proteins with elevated levels, presumably resulting from the transcriptional activation of Wnt target genes via β-cat (Chafey et al. 2009). In our analysis, only two of the APC-dependent difference-proteins displayed a total abundance change and in both cases it was a decrease in protein abundance in the *APC2* mutant, likely associated with decreased protein stability (mRpS30 and Cbs/TCP; Fig. 2.3B). This observation, coupled with the strong suppression of zygotic transcription in 0-2 hr embryos, suggested that the APC-dependent protein isoform differences were not a result of β-cat dependent transcriptional activation. To test this hypothesis directly, we asked if the APC-dependent isoform differences required the activation of Wnt target genes by expressing a dominant negative form of TCF (TCFΔN), a transcription factor essential for β-cat mediated transcription, in embryos reduced for *APC2*. The complexity of the

genetics prevented us from performing this experiment in the *APC2* null background, and instead we reduced *APC2* activity using dsRNA. Embryos derived from *MTD-GAL4>UAS-APC2*^{dsRNA} females exhibited the same protein isoforms differences for Dp1, GlyP, ApepP, and mRpS30 as *APC2* null embryos do (Fig. 2.7C). It is likely that CG2918 and Cbs/TCP are unchanged due to insufficient knockdown of *APC2* with the dsRNA. Next, we generated embryos derived from *MTD-GAL4>UAS-TCFΔN; UAS-APC2*^{dsRNA} females to simultaneously knock down *APC2* and block Wnt dependent transcription from the start of oogenesis. When we compared the proteome of *TCFΔN;APC2*^{dsRNA} embryos to *APC2*^{dsRNA} embryos, we found that the four *APC2*-dependent protein changes we observed in both *APC2* null and *APC2*^{dsRNA} embryos are unaffected by the blockade of Wnt dependent transcription (Fig. 2.7C). Importantly, if we crossed the *MTD-GAL4>UAS-TCFΔN; UAS-APC2*^{dsRNA} females to males carrying a *tubulin-GAL4* to drive ubiquitous expression of both *TCF*Δ*N* and *APC2*^{dsRNA} zygotically past 2 hours of development, we find that a portion of these embryos die with a cuticle phenotype consistent with the TCFΔN block of Wnt dependent transcription (a lawn of denticles, data not shown; Parker, Jemison, and Cadigan 2002). Although we cannot rule out the possibility that CG2918 and Cbs/TCP may behave differently, these results strongly support the hypothesis that the APC-dependent difference-protein isoform pairs are not a consequence of transcriptional activation through β-cat and TCF. Interestingly, GlyP, ApepP, mRpS30, and Cbs/TCP exhibit APC-dependent protein isoform changes in embryos knocked down for GSK3β (Sgg in Drosophila), or expressing a stabilized form of β-cat (*arm*^{s10}), two APC independent ways to accumulate stabilized β-cat (Fig. 2.7C; Pai et al. 1997). This suggests that the accumulation of stabilized β-cat, but not β-cat dependent transcriptional activation, is required for these protein isoform changes.

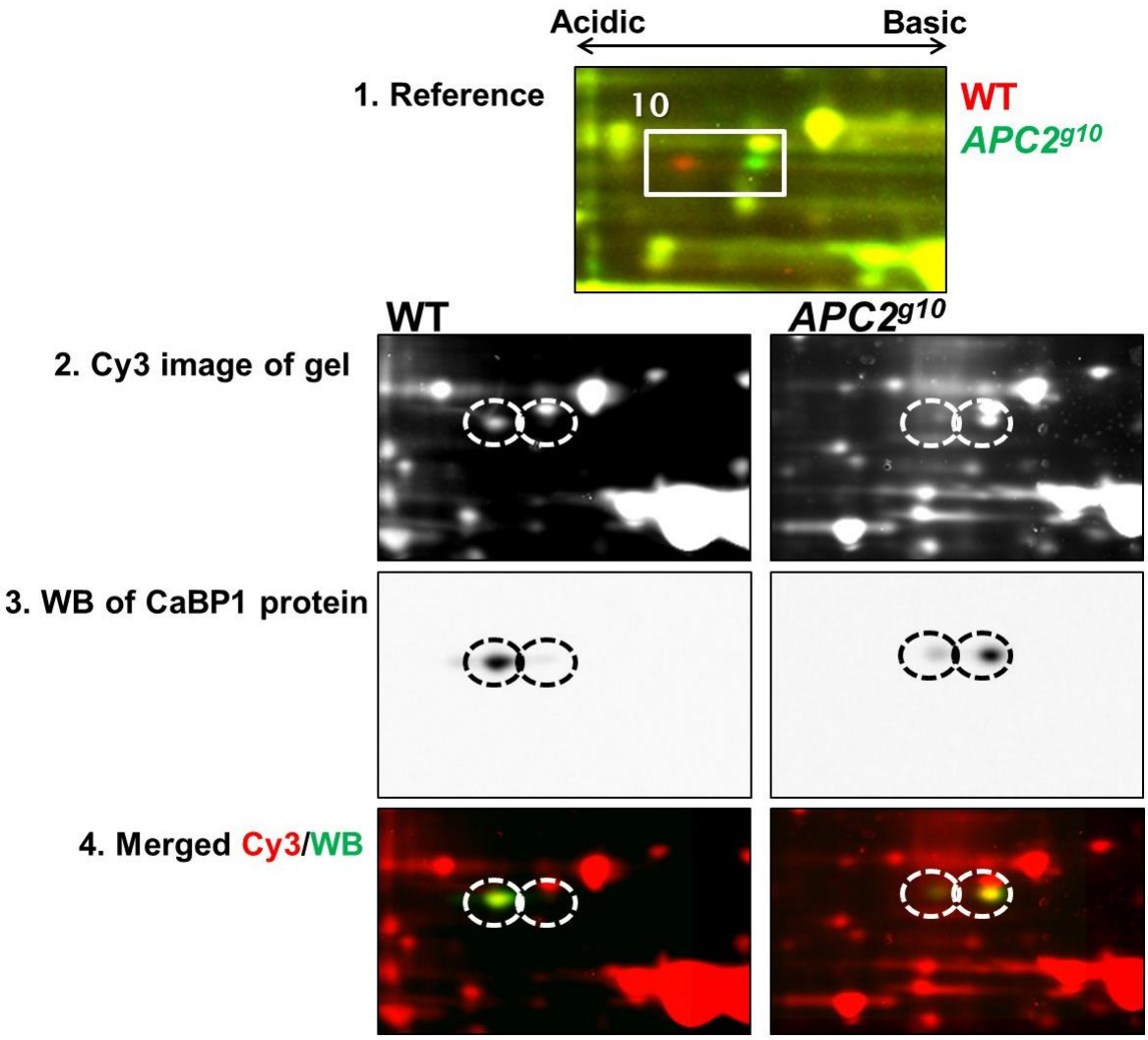

Figure 2.5. Immuno-blot confirmation that Calcium-Binding Protein 1 isoform distribution is an APC2-dependent difference-protein.

(1) 2D-DIGE image of the region containing Calcium-Binding Protein 1 isoforms. (**2**) Fluorescent images of wild-type and *APC2*^{g10} embryo lysates that were separately labeled with Cy3 DIGE dye, resolved on different 2DE gels and transferred to nitrocellulose. (**3**) Immuno-blot images of proteins stained with anti-DmCaBP1 antibody. (**4**) Superimposed images of total, Cy3-labeled protein (red) and the CaBP1 2D-immuno-blot (green) confirm protein identification by LC-MS/MS. The predominant isoform found in wild-type lysate is the left isoform, while is right isoform is the predominant isoform seen in *APC2* null embryos.

Aminopeptidase P is a novel regulator of β-cat levels during embryogenesis

To investigate the functional relationship between APC2 and our APC-dependent difference-proteins, we asked if mutants in any of the WTI difference-proteins could affect APC-dependent processes, such as regulating the stability of β-cat (Armadillo (Arm) in Drosophila). Because ApepP was affected in all backgrounds where components of the Wnt pathway were manipulated, we predicted that ApepP might be responding to changes in the destructosome or to the accumulation of stabilized Arm, and consequently, ApepP itself may play a role in the Wnt pathway. To test this hypothesis, we examined the effect of two P-element insertions into *ApepP*, $ApepP^{EY02585}$ ($ApepP^{EY}$) and $ApepP^{MI01970}$ ($ApepP^{MI}$), on Wnt dependent patterning and morphogenesis in the embryo. $ApepP^{EY}$ is a maternal effect embryonic semi-lethal allele (Appendix A, SFig. 2.1F, 54% of progeny die as embryos) bearing a P-element insertion in the gene's 5'-UTR that reduces ApepP protein abundance and alters its isoform distribution (Fig. 2.8G). The cuticles of these maternally and zygotically $ApepP^{EY}$ dead embryos resembled those of embryos with mild hyper-activation of the Wnt pathway (Brooke M McCartney et al. 2006; Swarup and Verheyen 2012). These phenotypes include a reduction in body length, defects in head morphogenesis and head holes, and loss of denticles (Fig. 2.8B). In addition, fusion of the first and second denticle rows was frequently observed (Fig. 2.8B', yellow arrow), and is known to result from the expression of stabilized Arm in these rows of cells (Pai et al. 1997), although we do not see this in *APC2* mutants (Brooke M McCartney et al. 2006). $ApepP^{EY}$ cuticles also exhibited large body holes that we do not find in *APC2* mutants (Fig. 2.8C & C', yellow circle). All of these defects were also visible in $ApepP^{MI}$ embryos carrying an independent P-element insertion in the 5'-end of the *ApepP* coding region and in $ApepP^{EY}/ApepP^{MI}$ transheterozygotes, suggesting that these defects are due to *ApepP* disruption (Appendix A, SFig. 1B-D).

The *ApepP* gene lies within an intron of the gene *tweek (twk)* that plays critical roles in synaptic vesicle recycling in larval to adult stages (Verstreken et al. 2009). The *EY02585* insertion fails to complement point mutants specifically affecting *twk* (*twk*^{1} and *twk*^{2}*;* Verstreken et al. 2009), suggesting that *EY02585* disrupts both *ApepP* and *twk*. This work on *twk* showed that the primary lethal phase is larval through pharate adult. Because rescuing transgenes do not exist to separate *ApepP* and *twk* function, we asked whether the embryonic lethal phenotypes we observed in *EY02585* embryos could be the result of *twk* disruption. We assessed embryonic lethality in the progeny of *twk*^{1}/+ or *twk*^{2}/+ parents (Appendix A, SFig. 2B). While there was some embryonic lethality (*twk*^{1} = 4% and *twk*^{2} = 16%), the cuticle phenotypes do not resemble those of *EY02585* embryos (Appendix A, SFig. 3B). Therefore, our data strongly suggest that the embryonic lethality and cuticle phenotypes associated with *EY02585* are the result of disrupting *ApepP*, and not *twk*, during embryogenesis.

Because defects in *ApepP* resembled the effects of mild inappropriate Wnt pathway activation, we predicted that reduction of *APC2* in *ApepP*^{EY} homozygous embryos might enhance the *ApepP*^{EY} phenotypes. To test this, we first assessed the cuticle phenotypes of the progeny of *ApepP*^{EY}/*ApepP*^{EY}; *APC2*^{g10}/+ parents. Because the progeny of *APC2*^{g10}/+ parents are 97% embryonic viable with no visible cuticle defects in the few embryos that fail to hatch (data not shown), any phenotypes that we see in embryos from *ApepP*^{EY}/*ApepP*^{EY}; *APC2*^{g10}/+ parents will be due to the *ApepP*^{EY}/*ApepP*^{EY} genotype or its genetic interaction with *APC2*^{g10}. Dose reduction of *APC2* did not enhance the embryonic lethality of *ApepP*^{EY} homozygous embryos (Appendix A, SFig. 1F, 48% progeny die), but the *ApepP*^{EY} homozygous cuticle defects were modified. The large *ApepP*^{EY}/*ApepP*^{EY} body holes were almost completely absent, denticle row fusion was strongly reduced, but defects in head morphogenesis, like those in *APC2* mutants, were more

prevalent (Fig. 2.8D). While the resulting phenotype is complex, and does not precisely resemble either the *ApepP* or the *APC2* phenotype, it is consistent with a genetic interaction as $APC2^{g10}$ appears to modify the effects of $ApepP^{EY}$. We found a more clear and striking example of genetic interaction between *ApepP* and *APC2* in adults; while both $ApepP^{EY}/ApepP^{EY}$ and $APC2^{g10}/APC2^{g10}$ are separately adult viable (although not at the expected Mendelian ratios, Table 2.1; this work and Brooke M McCartney et al. 2006; Ezgi Kunttas-Tatli et al. 2012) neither $ApepP^{EY}/ApepP^{EY}$; $APC2^{g10}$ nor $ApepP^{EY}/CyO$; $APC2^{g10}$ are adult viable or even survive to pupal stages (n = 151; Table 2.1). This suggests that any disruption of *ApepP* drives *APC2* null homozygotes to complete zygotic lethality, and that a simple dose reduction of *APC2* significantly suppresses the adult viability of $ApepP^{EY}/ApepP^{EY}$ (Table 2.1). Together, these data suggest that *ApepP* and *APC2* interact genetically and that their functional relationship may be in the negative regulation of Wnt signaling.

Consistent with this hypothesis, $ApepP^{EY}$ mutants exhibited dramatically elevated levels of Arm similar to *APC2* mutants (Fig. 2.8H). At 0-2 hours AEL, *ApepP* mutants exhibited a ~6-fold increase in Arm protein relative to wild-type (Fig. 2.8I). *APC2* null mutants exhibited a ~15-fold Arm increase (Fig. 2.8J). Wild-type embryos at 4-6 hours AEL accumulate Arm in ectodermal stripes due to Wnt signaling that leads to destructosome deactivation. In strong *APC2* hypomorphs, this pattern of Arm accumulation is lost and all cells appear to accumulate uniform levels of Arm (Brooke M McCartney et al. 2006). Similarly, 92% of $ApepP^{EY}/ApepP^{EY}$ embryos (n=51) show a visible disruption in the pattern of Arm accumulation, with a decrease in stripe (peak)/inter-stripe (valley) ratio (Fig. 2.8E vs. F plot profiles) consistent with a more uniform pattern of Arm accumulation. Surprisingly, both *ApepP* mutants and *APC2* null mutants show a decrease in overall Arm protein levels at this time compared to wild-type (~2 and ~ 4-fold

respectively; Fig. 8J,K). Overall, these data strongly support the hypothesis that like APC2, ApepP plays an important role in regulating β-cat protein levels to prevent ligand-independent activation of Wnt signaling during embryogenesis.

APC2 regulates ApepP proteolytic activity

To begin to understand the connection between ApepP and APC2, we asked if APC2 influences ApepP proteolytic activity. Because *APC2* and *ApepP* genetically interact (Table 2.2), $ApepP^{EY}$ mutants resemble embryonic defects of mild inappropriate Wnt pathway activation (Fig. 2.8A-C), and APC2 regulates ApepP PTM-isforms (Fig. 2.8G), we predicted that APC2 protein regulates proteolytic activity by modifying PTM-isoforms of ApepP. To test this, we used a well-established ApepP proteolytic assay first developed by Simmons and Orawski for bovine work, and later adapted by Kulkarni and Deobagkar for *Drosophila* (Fig. 2.9A; Kulkarni and Deobagkar 2002; Simmons and Orawski 1992). This assay measures endogenous ApepP proteolytic activity by adding a saturating amount of cleavable Arg-Pro-Pro tri-peptide substrate. ApepP recognizes the Pro-Pro motif and cleaves off the Arg residue, which has a high affinity for a specific fluorescent dye (OPTA), producing a fluorescent signal proportional to the amount of ApepP activity present. We tested both male and female adults (Fig. 2.9B,C). Relative to wild-type activity (100%), we observed a significant decrease in ApepP activity in $APC2^{g10}$ mutant lysates (~23%; Fig. 2.9B,C). The activity was restored by reintroducing the *FL-APC2* gene in the *APC2* null background. ApepP activity was also present, but lower in *APC2* heterozygous mutant embryos (50-60%), suggesting ApepP function is sensitive to the amount of APC2 protein present. Interestingly, we did observe 30-40% ApepP proteolytic activity in $ApepP^{EY}$ mutants, confirming that the P-element insertion does not completely abolish ApepP protein activity. This observation is consistent with our 2D-DIGE results showing that ApepP protein

was still present in *ApepP*^{EY} mutant embryos with a different isoform distribution. (Fig. 2.8G). Overall, these data support that APC2 protein function can influence ApepP's proteolytic activity.

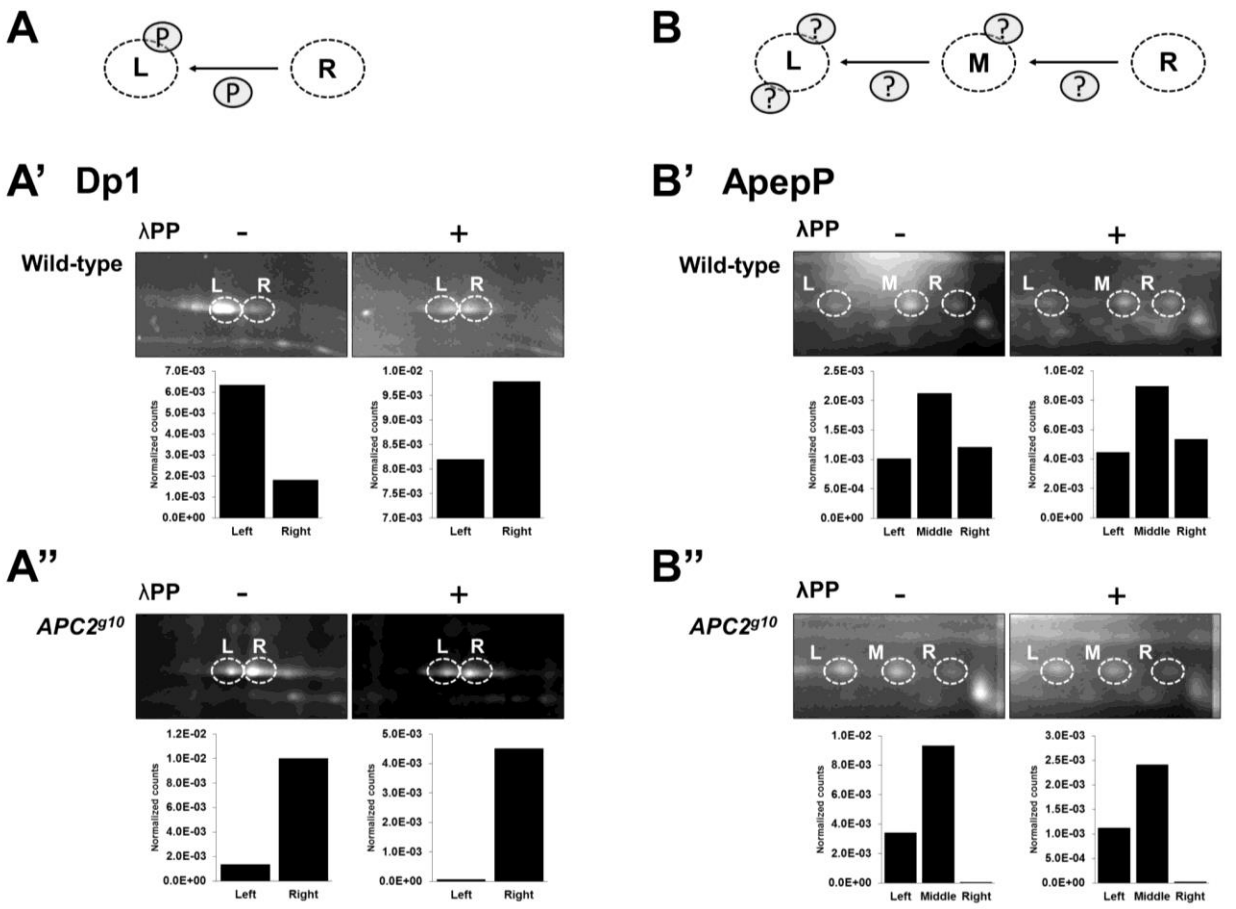

Figure 2.6. APC2-dependent isoform changes are due to phosphorylation and other PTMs. (**A**) A model for the PTM responsible for Dodeca-satellite-binding protein 1 (Dp1) isoforms. **(A')** Dp1 isoforms are affected by phosphorylation, as the left isoforms collapses to the right isoform after λPP treatment for both wild-type and *APC2*^{g10} embryo lysates. (**B**) A model for the PTM(s) responsible for Aminopeptidase P (ApepP) isoforms. **(B')** ApepP isoforms were not affected by λPP treatment, as there were no isoform shifts observed after phosphatase treatment. White dashed circles indicate the difference-protein isoforms.

Discussion

APC proteins exhibit remarkable functional breadth, playing key roles in such diverse areas of cell biology as Wnt signaling, microtubule stability, and actin assembly (Brooke M. McCartney and Näthke 2008; Cadigan and Peifer 2009; Ring, Kim, and Kahn 2014). Surprisingly, new roles for APC proteins are still being discovered (Preitner et al. 2014). This functional complexity makes it challenging to develop a comprehensive understanding of the cellular consequences of *APC* mutations, and how these changes affect cancer initiation and progression. To address these gaps, we conducted a comparative proteomic analysis using 2D-DIGE in *Drosophila* embryos null for APC proteins and discovered a set of APC-dependent protein isoform changes due to PTMs. 2D-DIGE comparisons of livers isolated from wild-type and *APC* knockout mice 7 days post-knockout revealed significant protein abundance changes (Chafey et al. 2009). Many of these changes likely result from transcriptional activation by β-cat. In 0-2 hour *Drosophila* embryos, transcription is largely silent, and more acute difference-protein isoforms were revealed as a result of changes in PTMs. We genetically validated that a subset of these difference-protein isoforms were due to the loss of APC activity. Remarkably, we also demonstrated that the validated APC-dependent difference-protein isoform pairs are very likely not the direct or indirect result of β-cat transcriptional activation. First, none of the difference-protein isoform pairs had elevated total protein abundance. Secondly, of the APC-dependent difference-protein isoforms we reproduced four out of six of the protein isoform changes (GlyP, ApepP, mRpS30, and Cbs/TCP) when also expressing a dominant negative form of the TCF protein in an *APC2* reduced background (the remaining 2 could not be assessed; Fig. 2.7C). This fact suggested to us that the APC dependent protein isoform changes were likely the result of disrupting APC's non-destructosome functions. However, when we examined proteomic changes

in embryos reduced for GSK3ß activity, or expressing a stabilized form of Arm we were surprised to find that GlyP, ApepP, mRpS30, and Cbs/TCP exhibit an APC mutant isoform profile. These data suggest that the modifications of these four difference-proteins may be a result of merely elevating β-cat in the cytoplasm. If this is the case, it suggests that during normal development in cells where the Wnt pathway is activated, the destructosome deactivated, and Arm is stabilized, GlyP, ApepP, mRpS30, and Cbs/TCP will undergo the same protein isoform changes that we are observing here during ligand-independent stabilization of β-cat. This raises the intriguing possibility that these protein isoform changes play a role in the cellular response to Wnt pathway activation via a non-transcriptional mechanism. The remaining two APC-dependent difference-protein isoforms, CG2918 and Dp1, did not respond to either β-cat manipulation, suggesting that these may result from disruption of APC's other activities such as their cytoskeletal functions.

Loss of APC proteins impacts phosphorylation and other post-translational modifications

Phosphorylation is the predominant PTM in eukaryotic cells (Khoury, Baliban, and Floudas 2011). Because APC proteins are complexed with kinases GSK3β and CK1 in the destructosome, and APC enhances GSK3β activity *in vitro* (Zumbrunn, Kinoshita et al. 2001, Ha, Tonozuka et al. 2004, Rao, Makhijani et al. 2008, Valvezan, Zhang et al. 2012), we predicted that the difference-protein isoforms were primarily due to changes in phosphorylation. Thus, we were surprised to find that this does not appear be the case for the majority of isoform changes: of the 9 difference-proteins (1, 2, 3, 4, 8, 9, 10, 15, 16) that we could assess under the conditions of λPP treatment, only one of the difference-protein isoform changes (#4-Dp1) appears to be due to phosphorylation differences, while the remaining difference-proteins are

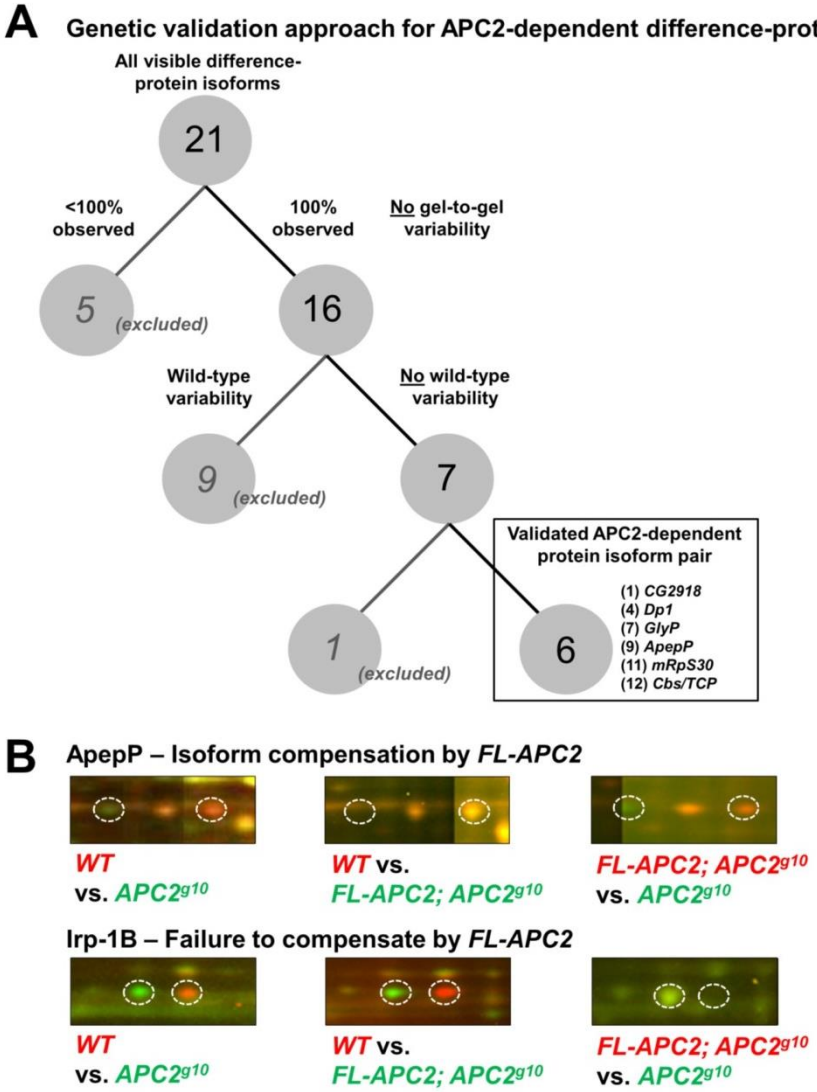

Figure 2.7. Validating the APC-dependent difference-proteins in *APC2* null embryos.

(A) A decision tree showing the genetic approach taken to validate the APC-dependent difference-proteins. Seven of the 16 difference-proteins were concluded to be APC-dependent and independent of wild-type variation. **(B)** 2D-DIGE comparisons of *FL-GFP-APC2;APC2*^{g10} vs. *APC2*^{g10} and *FL-GFP-APC2;APC2*^{g10} vs. *wild type* embryo lysates were performed to test if ectopic APC2 was sufficient to reverse the observed *APC2*^{g10} vs. *wild type* proteome changes. Shown here are difference-proteins, ApepP and Irp-1B, that exemplify reversal and failure to compensate, respectively.

thus predicted to be modified by alternative PTMs. As the second most prominent reversible PTM, acetylation may contribute to some of the difference-protein isoform changes. Interestingly, acetylation plays a role in β-cat signaling at the level of the TCF complex (Lévy et al. 2004), and appears to play a role in Wnt-mediated breast cancer proliferation (S. H. Wang et al. 2014). Finally, ApepP-dependent cleavage of short N-terminal peptides may alter a protein's p*I*, but not its apparent molecular weight on 2DE gels, which would appear as a horizontal shift, reminiscent of common PTMs. A subset of the APC dependent protein isoform changes also appear in *ApepP* mutants, suggesting that these changes could result from changes to ApepP activity (data not shown). Identifying the mechanisms by which APC regulates these PTMs is vital to understanding the non-transcriptional effects of APC loss in normal development, as well as in the onset of cancer.

ApepP regulates β-catenin abundance

ApepP is a metalloaminopeptidase that removes amino acids adjacent to the amino termini of peptides with a prolyl residue in the second position (Yaron 1987; Yaron and Naider 1993). ApepP is ubiquitous and conserved from bacteria to vertebrates (Kulkarni and Deobagkar 2002; Ersahin, Szpaderska, and Simmons 2003; Ersahin et al. 2005). Mammalian ApepP exists in two forms, cytosolic and membrane bound, and functions in the maturation of active peptides, including hormones (Bradykinin), neuropeptides (Substance P), and neurotransmitters (Medeiros and Turner 1994; Yoshimoto, Orawski, and Simmons 1994; Kim et al. 2000). The cytosolic form of Drosophila ApepP is functionally conserved with human ApepP, and can hydrolyze both Bradykinin and Substance P (Kulkarni and Deobagkar 2002). Our results suggest that ApepP is necessary for β-cat regulation as *ApepP* mutants display an array of Wnt activation phenotypes,

Table 2.1: APC-dependent differences in APC mutant embryos, APC knockdown (dsRNA) embryos, and APC-independent β-cat stabilized embryos

	FL-GFP-APC2; APC2^{g10}	***APC1^{Q8}***	***APC2^{g10}APC1^{Q8}***	***APC2^{33}***	***APC2 dsRNA***	***TCFΔN; APC2 dsRNA***	***arm^{s10}***	***sgg dsRNA***
(1) *CG2918*	nc (compensated)	✓	✓	✓	nc	nc	nc	nc
(4) *Dp1*	nc (compensated)	✓	nc	✓	✓	✓	nc	nc
(7) *GlyP*	nc (compensated)	✓	nc	✓	✓	✓	nc	✓
(9) *ApepP*	nc (compensated)	✓	✓	✓	✓	✓	✓	✓
(11) *mRpS30*	✓	nc	✓	✓	✓	✓	✓	✓
(12) *Cbs/TCP*	nc (compensated)	nc	nc	nc	nc	nc	✓	nc

nc, no change.

accumulate Arm in the early embryo like *APC2* mutants, and genetically interact with *APC2*^{g10} (Fig. 2.8). Of ApepP's three isoforms seen in our DIGE analysis comparing wild-type embryos to *APC* mutant embryos, the right and left isoforms change while the middle isoform does not (Fig. 2.2A, Region 9). These isoform differences in ApepP were also observed with Sgg knockdown and the expression of stabilized Arm (Fig. 2.7C). From these observations, we propose a model where ApepP protein isoforms, presumably a reflection of ApepP's enzymatic activity, are regulated in part by the stabilization of β-cat. To support this, we show that APC2 influences ApepP function promoting ApepP proteolytic function via PTM modification (Fig. 2.9B,C). However, the fact that disruption of ApepP activity in the P-element insertion mutants appears to stabilize Arm and activate Wnt signaling suggests that this is a complex feed-back driven pathway, and that the proper regulation of ApepP activity is required to prevent the inappropriate stabilization of β-cat and downstream Wnt pathway activation (Fig. 2.10). To further test this model we next we need to identify the APC-dependent PTM modification that regulates ApepP's proteolytic activity.

Wild-type variable difference-protein isoform pairs are APC-like difference-protein isoforms

We were surprised to find that over half of the difference-protein isoforms identified in *APC2* mutant embryos were also variable in different *w*^{1118} strains (Appendix A, Table 3A). Because all of the original 16 difference-proteins were observed in some form of APC knockdown in multiple genetic backgrounds (Appendix A, Table 3C), we further characterized a subset of variable difference-proteins, Aats-gly, CaBP1, and UCH, by comparing isoform ratios and total abundance within like *APC2*^{g10} vs. *wild type* (ApepP, right panel), while the control *FL*-

GFP-APC2;APC2^{g10} vs. *wild type* compensates for the isoform shift (ApepP, middle panel). The converse effect was seen for failed compensations, such as in Irp-1B. the different w^{1118} strains and between *APC2* null embryos (data not shown). Interestingly, the wild-type variable difference-protein isoforms displayed different types of total abundance and isoform changes relative to *APC2* null embryos. This distinction suggests that these variable difference-proteins may be particularly sensitive to developmental perturbations. Further investigation of wild-type to wild-type proteomic variability is required to elucidate this intriguing observation.

Conclusion

Taken together, our results suggest that loss of *APC* has diverse post-translational consequences to the proteome. The most notable observation from these studies is that even in the absence of a Wnt signal and with limited transcription, the loss of APC2 causes many significant PTM changes, affecting a wide variety of proteins over a relatively short period of development. Identification of these changes provides unique insight into the proteomic and cellular responses to the loss of a single protein. The discovery of these APC-dependent PTM changes was made possible by 2D-DIGE, which maintains proteins in their intact state throughout the separation and detection process. It is very unlikely that this array of PTM-dependent changes would have been detected by bottom-up, MS-based proteomics because proteins are fragmented prior to analysis. A single PTM that alters the charge of a protein will be readily detectable by 2D-DIGE, while this PTM change translates into one modified peptide out of all the peptides generated by trypsin digestion of a whole proteome. The likelihood of detecting a peptide carrying an unknown PTM change is exceptionally low (1 out of tens of thousands of peptides per PTM). Thus, combining 2D-DIGE and MS is the best route to

identifying such PTM changes. This type of analysis may prove useful for dissecting the global cellular consequences of genetic mutations in other oncogenes, tumor suppressors, and disease genes with implications for understanding the etiology of normal and cancer development.

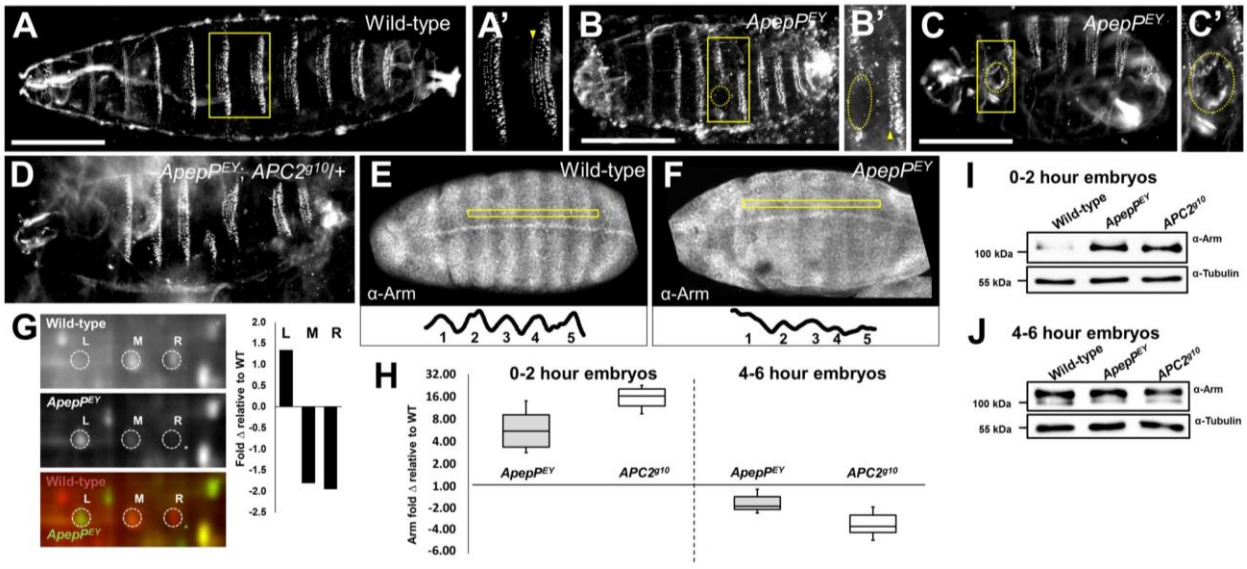

Figure. 2.8. *ApepP^{EY}* embryos display Wnt activation phenotypes similar to *APC2* mutant embryos.

Cuticle analysis of: (**A**) Wild-type, (**B**) *ApepP^{EY}* head, and cuticle defects. *ApepP^{EY}* mutant embryos exhibit fusion of the first and second denticle rows (compare **A'** to **B'**, yellow arrow) as well as denticle loss (**B'**, yellow circle). (**C**) *ApepP^{EY}* body defects. (**C'**) *ApepP^{EY}* mutant embryos exhibit body holes not associated with *APC2^{g10}* mutant embryos. (**D**) A homozygous *ApepP^{EY}* mutant embryo with reduced APC2 protein expression. (**E**) β-cat protein localization and accumulation in a wild-type embryo shows a pronounced striping pattern, while (**F**) shows that *ApepP^{EY}* mutant embryos exhibit a more uniform distribution of β-cat protein. (**G**) 2D-DIGE comparison of wild-type versus *ApepP^{EY}* embryos showing that total ApepP protein is decreased in mutant embryos and that there is a shift in isoform distribution toward the left isoform in *ApepP^{EY}* mutant embryos. (**H**) Displays the quantification of three replicates of the experiments shown in panels H and I. (**I**) Shows anti-Arm immuno-blots of 0-2 hour AEL wild-type, *APC* and *ApepP* mutant embryos, where β-cat levels increase in the mutants. (**J**) Shows anti-Arm

immuno-blots of 4-6 hour AEL wild-type, *APC* and *ApepP* mutant embryos, where β-cat levels slightly decrease in the mutants relative to wild-type.

Table 2.2: Genetic interaction between *ApepP* and *APC2* is reflected in adult viability

Parental genotype	Genotype of adult progeny	n	Mendelian Expected	Adjusted Expected*	Observed	Chi-square
ApepP^{EY}/CyO	*ApepP^{EY}/CyO*	100	66%	N/A	78%	X^2=5.47 Df=1 p<0.05
	ApepP^{EY}/ApepP^{EY}		33%	N/A	22%	
APC2^{g10}/TM6 Tb	*APC2^{g10}/TM6, Tb*	100	66%	N/A	88%	X^2=19.94 Df=1 p<0.001
	APC2^{g10}/APC2^{g10}		33%	N/A	12%	
ApepP^{EY}/CyO; APC2^{g10}/TM6 Tb	*ApepP^{EY}/CyO; APC2^{g10}/TM6, Tb*	151	44%	67.50%	87%	X^2=29.01 Df=3 p<0.001
	ApepP^{EY}/ApepP^{EY}; APC2^{g10}/TM6, Tb		22%	22.50%	13%	
	ApepP^{EY}/CyO; APC2^{g10}/APC2^{g10}		22%	7.50%	0%	
	ApepP^{EY}/ApepP^{EY}; APC2^{g10}/APC2^{g10}		11%	2.50%	0%	

*The observed frequencies of homozygotes in the progeny of *ApepP^{EY}/CyO* and *APC2^{g10}/Tb* parents were used to adjust the expected values of homozygotes in the progeny of *ApepP^{EY}/CyO;APC2^{g10}/TM6, Tb* parents.

N/A, not applicable.

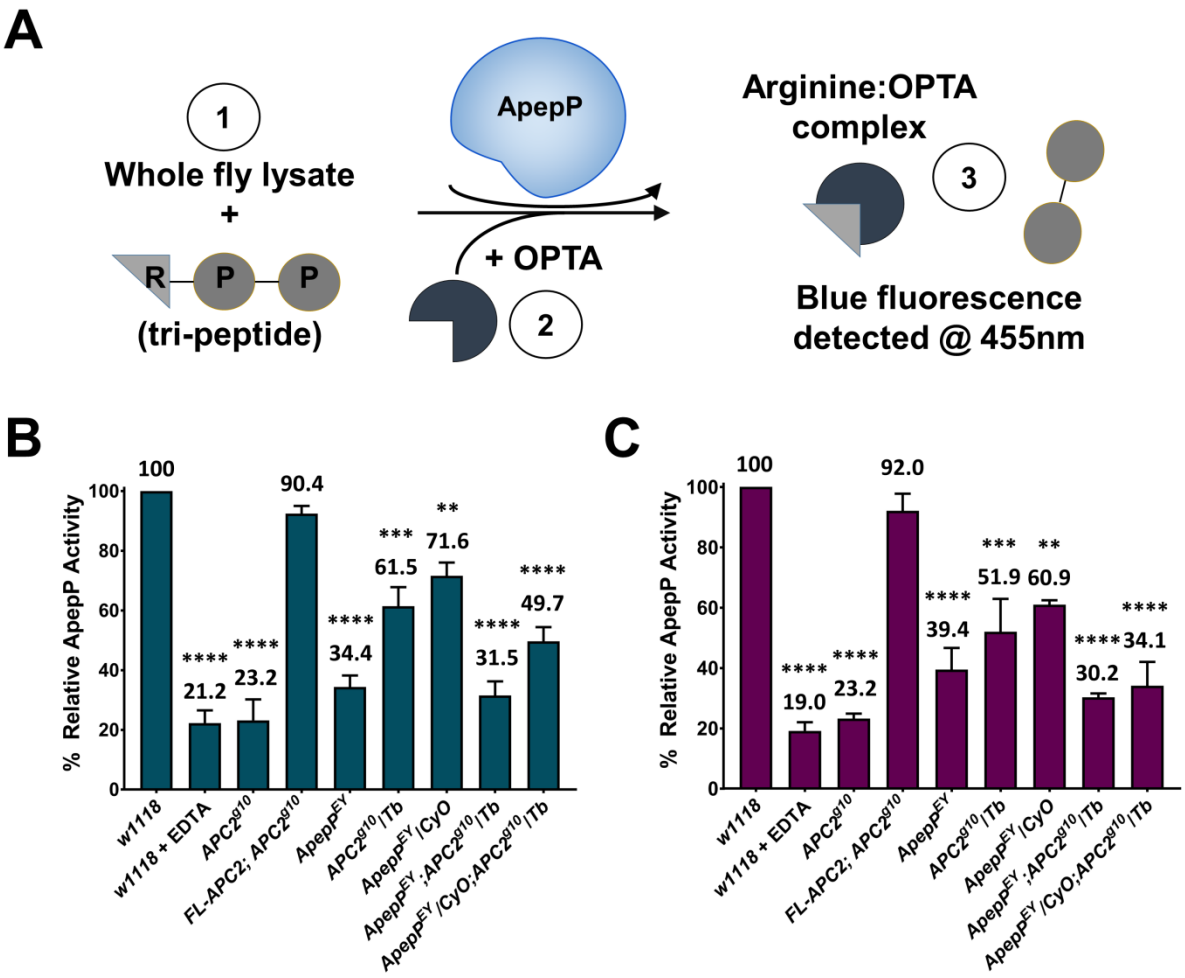

Figure 2.9. APC2 regulates ApepP's proteolytic activity.

(**A**)The ApepP proteolytic function assay. (**B**) Endogenous ApepP proteolytic activity levels in male flies and (**C**) female flies. The n tested for both males and females is three flies, each bar represents the average of 3 flies. Bars indicate standard error of the mean. Statistical significance was assigned by a One-way ANOVA (Turkey's multiple comparisons post hoc test) comparing experimental values to wild-type (w^{1118}). * < 0.05, ** < 0.005, *** < 0.0005, **** < 0.0001

Future directions

The published work identified a number of APC-dependent difference-proteins by rigorous validation and discovered that ApepP is a regulator of β-cat protein abundance necessary to prevent ligand-independent activation of Wnt signaling during embryogenesis. We have since further characterized ApepP's relationship with APC2 by demonstrating that APC2 promotes ApepP's proteolytic activity. Although great progress has been made, a few important questions remain to be answered to fully understand the relationship between APC2 and ApepP in Wnt signaling.

Is ApepP part of the destruction complex?

Because ApepP's activity is regulated by APC2, and ApepP is required for normal ß-catenin degradation, we predicted that ApepP might be a component of the cytoplasmic destruction complex. We started to investigate this by co-expressing ApepP with various components of the destruction complex in S2 cells, a *Drosophila* derived cell line (Fig. 2.11A), that we have previously shown is a good model system for assessing destruction complex localization and dissecting destruction complex structure (Zhou et al. 2011; Ezgi Kunttas-Tatli, Roberts, and McCartney 2014). Specifically, we over-expressed ApepP protein with APC2, Axin, the scaffolding proteins of the destruction complex, or Arm (β-cat), the main target of the destruction complex. We then asked if ApepP co-localized with any of the three proteins. Preliminarily, ApepP does not co-localize with APC2 or Axin puncta by themselves (Fig. 2.11C). While ApepP and Arm are both cytoplasmic in the absence of excess APC2 or Axin (Fig. 2.11A), there is no evidence of specific colocalization. However, more investigation is required to fully establish Apep's role in the destruction complex. For example, both scaffolding

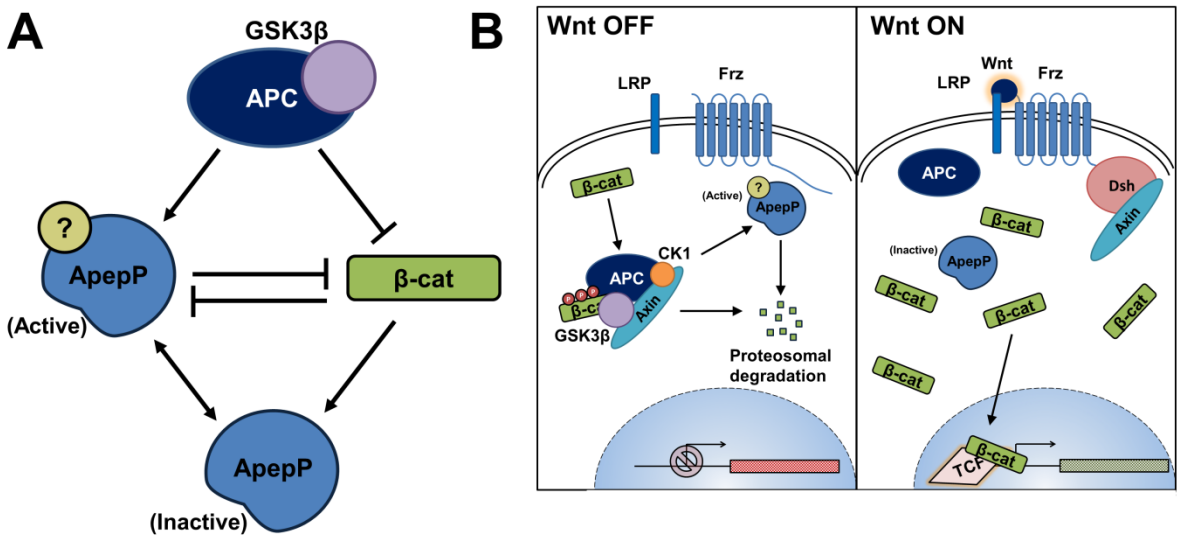

Figure. 2.10. A proposed model for APC2 and ApepP β-cat regulation in Wnt signaling.

(**A**) APC promotes ApepP proteolytic function to regulate β-cat protein abundance in a complex feed-back driven pathway. (**B**) The Wnt signaling pathway. When no Wnt ligand is present (left) the destructosome promotes cytoplasmic β-cat degradation by promoting ApepP proteolytic activity via unidentified PTM modification. With a Wnt ligand (right), the destructosome is deactivated, ApepP proteolytic activity is inhibited by loss of PTM modification, and cytoplasmic β-cat accumulates, enters the nucleus and activates Wnt target genes.

proteins may be required to integrate ApepP into the destruction complex. We are investigating this possibility by performing a triple transfection experiment using ApepP, APC2, and Axin.

Identify the APC-dependent PTM modification(s) for ApepP

Our 2D-DIGE analysis revealed that the ApepP protein isoform distribution was modified in *APC2* null mutant embryos (Fig 2.7B). We ruled out the possibility that this difference in isoform distribution is a result of aberrant phosphorylation modification (Fig. 2.6B-B"). We have attempted to identify the PTM modification(s) by directed mass spectrometry using ApepP protein isolated from embryo lysate separated by 2DE electrophoresis. So far this effort has been unsuccessful in identifying any PTMs. The suspected reason for unsuccessful PTM identification is low protein yield in our mass spectrometry samples, resulting in low coverage of the protein sequence. To this date, our best attempt covered 30% of the ApepP protein sequence. We believe more protein material is necessary in order to achieve the coverage and depth for PTM identification. To do this, we will purify ApepP protein from bacteria, incubate the purified protein with wild-type or *APC2* null mutant embryo lysate, and then use directed mass spectrometry to identify the differences in ApepP PTM isoforms.

Creation of an ApepP null fly line

The $ApepP^{EY}$ mutation was identified as partial loss of function allele (Fig. 2.9B,C). Although this hypomorphic allele helped us uncover a functional link between APC2 and ApepP, elucidating the precise mechanism by which ApepP regulates β-cat and Wnt signaling is still challenging. As a result, we have made efforts to generate a complete loss of function *ApepP*

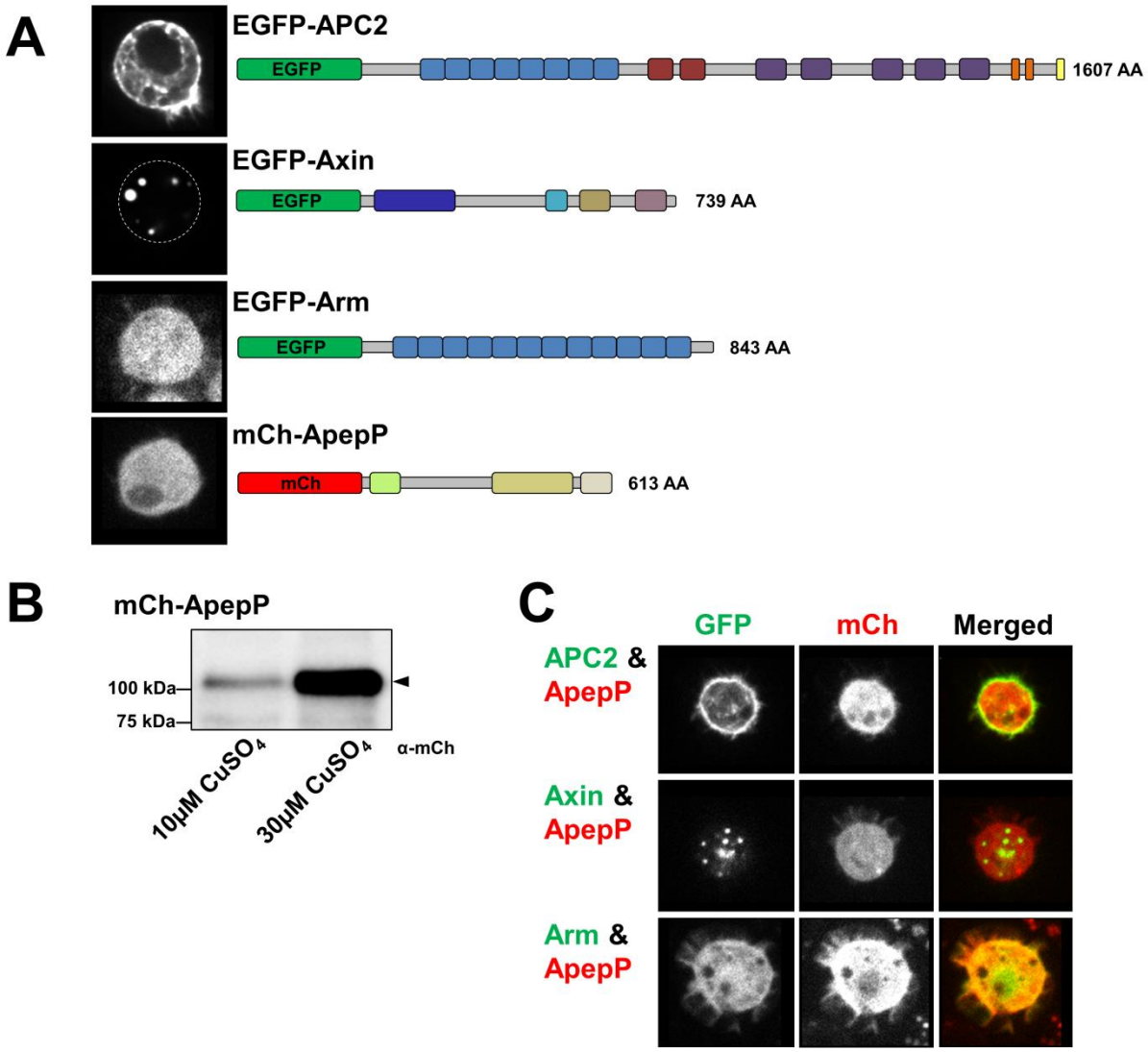

Figure 2.11. ApepP targets Arm (β-cat) independently of the destruction complex.

(**A**) A schematic representation of *Drosophila* APC2, Axin, Arm, and ApepP. APC2, Axin, and Arm were tagged with an enhanced GFP moiety at the N-terminal end, while ApepP was tagged with a mCherry moiety. Over-expressed APC2 localized to the cortex and small puncta in the cytoplasm, Axin creates cytoplasmic puncta, while Arm and ApepP is cytoplasmic. (**B**) Anti-mCh immunoblot of S2 cell lysate. Expression of the ApepP fusion protein was expressed using two different $CuSO_4$ induction concentrations. (**C**) ApepP protein (red) does not co-localize with

APC2 or Axin (green) (top and middle rows), while possible co-localization with Arm protein (bottom row) may be observed.

allele using CRISPR technology (Port et al. 2014). We designed a mutagenesis strategy that targeted the *ApepP* start codon in two different locations (Fig. 2.12A). Putative mutant fly lines were generated by injecting Cas9 embryos with plasmids carrying the guide RNA for target site 1, or target site 2, or a combination of target site 1 and 2. This process created roughly 50 putative *ApepP* mutant lines. We are actively screening these fly lines by assessing adult stock ratios, embryonic lethality, cuticle phenotypes, and ApepP proteolytic activity. So far we have screened the stocks produced from the target 1 mutagenesis and identified two fly lines that produce nearly no homozygous adults (Table 2.3), and share similar hyperactive Wnt embryonic phenotypes (Fig. 2.12 C,D). However, these fly lines still have very low ApepP proteolytic activity (Fig. 2.12E), similar to $ApepP^{EY}$ mutants. Interestingly, additional target 1 cohort fly lines that have skewed adult viability ratios also have reduced ApepP proteolytic function (Fig. 2.12E). This trend may suggest that target 1 mutagenesis was not effective. Luckily, we still have two cohorts of putative mutant fly lines to screen through (target 2 mutagenesis, mixed target 1 and target 2 mutagenesis).

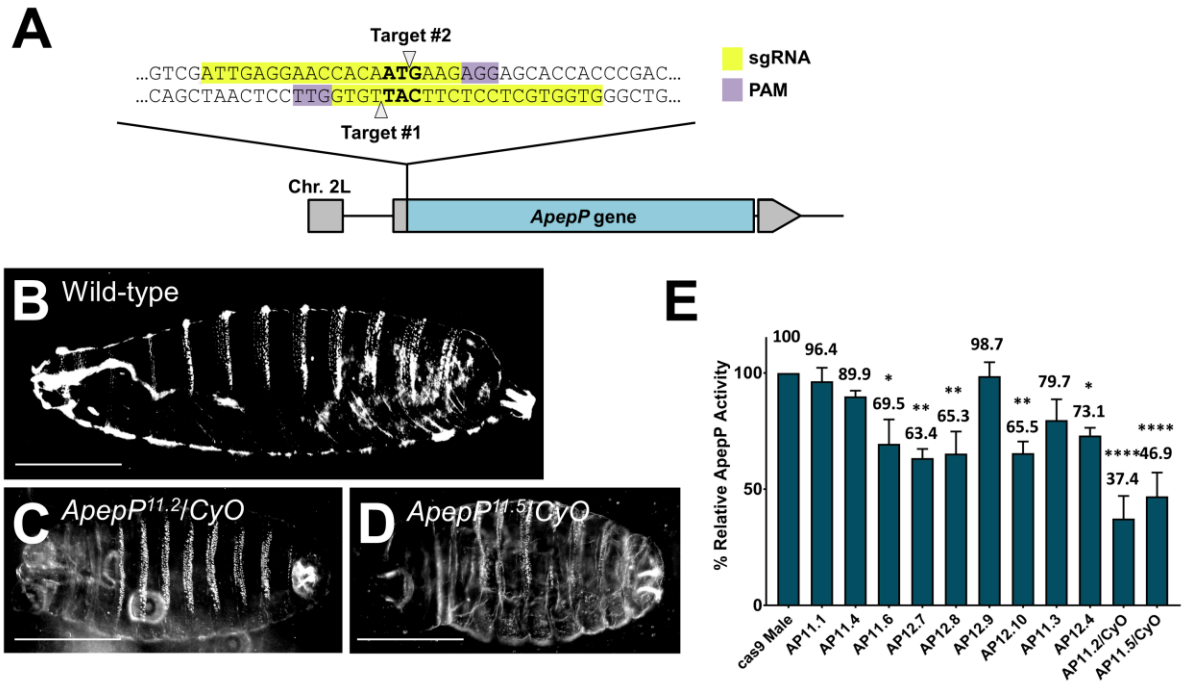

Figure 2.12. Screening the *ApepP* CRISPR mutant fly stocks.

(**A**) A schematic showing the CRISPR target site for *ApepP* mutagenesis. We targeted the start codon with two different oligos. (**B-D**) Cuticle analysis showed that *ApepP*$^{11.2}$*/CyO* (**C**), and *ApepP*$^{11.5}$*/CyO* (**D**) mutant embryos exhibit denticle row defects compared to wild type cuticles (B), similar to what we observed in *ApepP*^{EY} mutant embryos (Fig. 2.8B). (**E**) Endogenous ApepP proteolytic activity levels in male flies of the genotypes indicated. n = 3. Bars indicate standard error of the mean. Statistical significance was assigned by a One-way ANOVA (Turkey's multiple comparisons post hoc test) comparing experimental values to wild-type (w^{1118}). * < 0.05, ** < 0.005, *** < 0.0005, **** < 0.0001

Table 2.3 Adult viability ratios for two putative *ApepP* null fly lines

Parental genotype	Genotype of adult progeny	n	Mendelian Expected	Observed
ApepP$^{11.2}$/CyO	*ApepP$^{11.2}$/CyO*	154	66%	98%
	ApepP$^{11.2}$/ ApepP$^{11.2}$		33%	2%
ApepP$^{11.5}$/CyO	*ApepP$^{11.5}$/CyO*	132	66%	99%
	ApepP$^{11.5}$/ ApepP$^{11.5}$		33%	1%

CHAPTER 3: MICROBIOTA-DEPENDENT DYSREGULATION OF ALCOHOL DEHYDROGENASE IN DROSOPHILA IS ASSOCIATED WITH CHANGES IN ALCOHOL-INDUCED HYPERACTIVITY AND ALCOHOL PREFERENCE

Summary

While we are gaining appreciation for the many roles that the gut microbiota plays in diverse aspects of host biology including metabolism, immunity, and behavior, the scope of those effects and their underlying molecular mechanisms are poorly understood. To address these gaps, we used Two-dimensional Difference Gel Electrophoresis (2D-DIGE) to identify proteomic differences between male and female Drosophila raised with a conventional microbiota (CV) and those raised in a sterile environment (axenic, AX). We discovered 16 microbiota-dependent protein differences in the Drosophila head, and identified a male-specific elevation in Alcohol Dehydrogenase (ADH) in AX animals. Because ADH is a key enzyme in alcohol metabolism, we asked whether physiological and behavioral responses to alcohol were altered in AX males. Here we show that alcohol-induced hyperactivity, the first response to alcohol exposure, is significantly increased in AX males, requires ADH activity, and is modified by genetic background. While ADH activity is required, we did not detect significant microbe-dependent differences in systemic ADH activity or ethanol level. Like other animals, Drosophila can exhibit a preference for ethanol consumption, and here we show significant microbiota-dependent differences in ethanol preference in males. This work is the first to demonstrate that host-microbe interactions can affect host physiological and behavioral responses to ethanol, suggesting that microbial composition could play a role in human alcohol use disorders.

Introduction

The human microbiota, the community of microorganisms including bacteria and fungi that resides in and on our bodies, contributes to human metabolism, immunity, and defense against pathogens (Eloe-Fadrosh and Rasko 2013; Elson et al. 2005). Surprisingly, recent evidence suggests that the bacterial microbiota of the gut can also influence learning, memory, anxiety, depression, and autism-associated behaviors in some animals (Lee and Brey 2013; Gonzalez et al. 2011; Foster and McVey Neufeld 2013; Strati et al. 2017). The number of connections being made between symbiotic bacteria and host physiologies and behaviors is rapidly expanding, making it likely that more associations await discovery. Furthermore, we understand relatively little about the molecular mechanisms that mediate any of these host-microbe interactions.

Drosophila is emerging as an excellent model to dissect the role of the microbiota in animal physiology and behavior. Studies in *Drosophila* benefit from the ability to generate mutants and control genetic homogeneity, and quickly and inexpensively obtain large sample sizes that have significant statistical power. Links between the microbiota and host physiology and behavior are also present in *Drosophila*. The fly microbiota can modulate insulin, insulin-like growth factor, and TOR signaling thereby affecting systemic homeostasis in the fly (S C Shin et al. 2011; Storelli et al. 2011). Fly behaviors such as egg laying behavior, feeding behavior, male competitive behavior, and kin recognition all respond to changes in the microbiota (Fischer et al. 2017; Sharon et al. 2011; Lize, McKay, and Lewis 2014). Furthermore, host-pathogen studies in *Drosophila* have proven invaluable to unraveling the mechanisms of human innate immunity (Bonfini, Liu, and Buchon 2016; Bier and Guichard 2012).

Most large scale studies have probed the host transcriptome (Leulier 2014; Broderick, Buchon, and Lemaitre 2014; Elya et al. 2016; Erkosar et al. 2013). Proteome analysis provides valuable information about post-translational modifications (PTMs) and protein stability, for example, that is invisible at the transcript level (Vogel and Marcotte 2012). Furthermore, there can be remarkably little correlation between changes in mRNA expression and changes in protein abundance (Anderson and Seilhamer 1997; Greenbaum et al. 2003; Maier, Güell, and Serrano 2009; Munoz Descalzo et al. 2012; Gygi et al. 1999). Two-Dimensional Difference Gel Electrophoresis (2D-DIGE) is a powerful technique to reveal proteomic changes between two or three protein samples simultaneously run on the same gel (Gong et al. 2004; Filiou et al. 2011; C., M., and U. 2011). Combined with a high dynamic-range fluorescence imaging system, 2D-DIGE can detect protein over a million-fold concentration range, as low as 0.2 fmol (Minden 2012; Van, Bass, et al. 2014). Typically, difference proteins are then identified using liquid chromatography coupled to tandem mass spectrometry (LC-MS/MS).

Here we used 2D-DIGE to identify *Drosophila* proteins that are responsive to the microbiota. We focused on the *Drosophila* head proteome in order to bias our screen toward proteins that may have a role in neural function and behavior, as this aspect of host-microbe interactions is not well understood. Furthermore, adjacent to the brain lays a fat body, the main endocrine organ that can directly and indirectly communicate with the brain (Droujinine and Perrimon 2016). By comparing the head proteomes of male or female flies raised with a conventional microbiota (CV) to those raised in a sterile environment (axenic, AX), we identified 16 proteins that are either increasing or decreasing in abundance in the heads of AX flies. Interestingly, some of these differences are sex specific. We identified one of the male-specific difference proteins as Alcohol Dehydrogenase (ADH), a key enzyme in alcohol

metabolism in all animals, and showed that the difference was reversed by reintroducing the conventional microbiota to AX adult males. ADH is elevated in the heads of AX males, suggesting that they may have altered physiological and behavioral responses to alcohol. Indeed, we found that AX males exhibit significantly enhanced alcohol-induced hyperactivity, a response that we show is ADH dependent, male specific, and sensitive to host genetic background. Using different measures of ethanol preference, we found that when offered a choice, AX males prefer to consume food containing alcohol significantly more than their CV siblings. Taken together, our work demonstrates a novel connection between the microbiota and host physiological and behavioral responses to alcohol in Drosophila that may have implications for our understanding of the microbiota's role in alcohol use disorders (AUD).

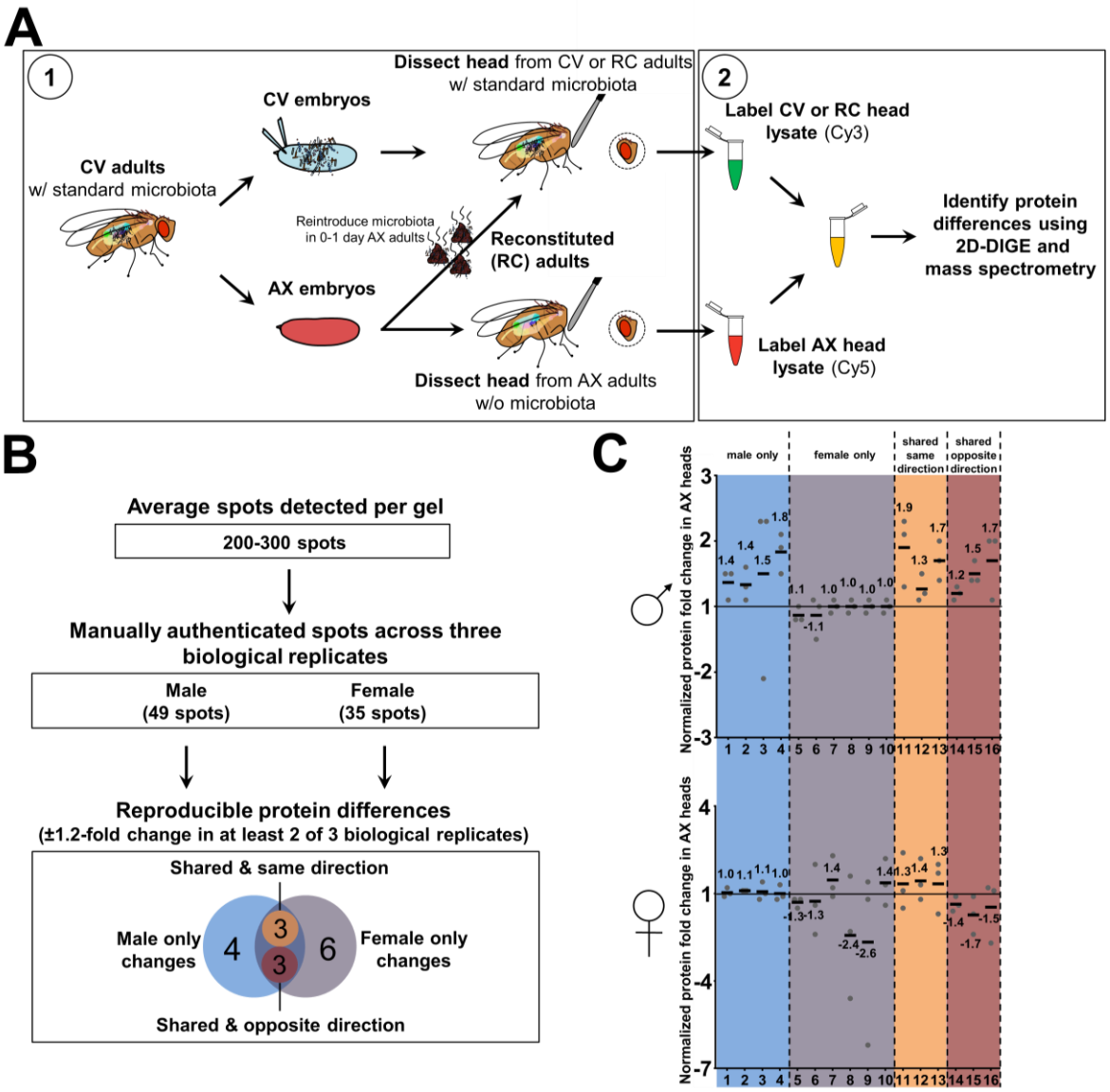

Figure 3.1. The AX head proteome is different from the CV head proteome.

(A) The 2D-DIGE screen experimental design. (1) CV, AX, and RC siblings were derived from cohorts of embryos with the same parents. CV embryos were transferred directly to sterile bottles, while AX embryos were first dechorinated (see methods). CV and AX adult flies were collected daily and aged in sterile vials for 5-6 days. For microbial reconstitution, 0-1 day old AX flies were transferred to vials conditioned with *Drosophila* feces and aged for 5-6 days. Protein lysates were prepared from dry dissected heads and (2) were covalently labeled with

either propyl-Cy3 or methyl-Cy5, combined, and co-electrophoresed on a 2DE gel. Difference proteins were identified by LC-MS/MS. **(B)** A summary of the reproducible protein differences in the AX head proteome. 200-300 protein spots per gel were detected using SourceExtractor (Bertin and Arnouts 1996), then manually validated and crossed referenced between three biological replicates. The Venn diagram shows a summary of the 16 reproducible protein differences across three biological replicates for male and female data sets. **(C)** Measured fold-change for each protein difference that was calculated using the Cy3 and Cy5 raw fluorescence intensities. Fold-change ratios <1 were converted to negative fold-change. The color code matches that of panel B.

Materials and methods

Creation of Top Banana Conventional (CV), Axenic (AX), and Reconstituted (RC) cultures

CV and AX cultures were derived from embryos obtained from the same parents. A 4 hour collection of embryos was transferred in standard embryo wash (120 mM NaCl and 0.04% Triton X-100) to a plastic petri dish. For CV cultures, approximately 150 embryos were transferred to a fresh culture bottle containing molasses fly food (7% molasses, 6% corn meal, 0.90% yeast, 0.70% agar, 0.20% proprionic acid, 0.23% methyl-parahydroxybenzoate, 0.23% ethanol). Autoclaved inactive yeast was added to the bottle cultures (0.2-0.3g per bottle). Embryos for AX cultures were prepared as previously described (Koyle et al. 2016; Tech et al. 2015) with a few adaptations. Embryos were transferred to a separate microcentrifuge tube and incubated in filtered sterilized 50% bleach for two minutes, then rinsed with filter sterilized 70% ethanol twice, and once with filter sterililized water to dechorionate the embryos and remove microbes that were associated with the chorion. Approximately 250 AX embryos were transferred to an autoclaved culture bottle containing autoclaved yeast granules as above. The difference in embryo seeding density for the two culture conditions was necessary to ensure consistent larval density and comparable nutritional environments. Adult flies were collected 0-1 day post-eclosion into food vials containing ~0.05g autoclaved inactive yeast granules. The flies remained in these collection vials for 5 days before being used for experiments. For RC flies, 0-1 day old AX adults were placed in food vials that had housed 10-12 day old males for 4 days, and then aged in those preconditioned vials for 5 days. All fly cultures were reared and adult progeny maintained at 22-23ºC/70% relative humidity/12-12hr light-dark cycle.

Verification of AX cultures

For culture-dependent characterization, ten 5-6 day old males (CV, AX, or RC) were surface sterilized with 10% bleach for one minute followed by one rinse each in 70% ethanol and filter sterilized water. The flies were homogenized in 125 µL filter sterilized 1X PBS containing 1mm zirconia beads in the bead beater for 30 seconds, until no obvious particulates could be seen. The samples were diluted 10^1, 10^2, 10^3, 10^4, 10^5 in 1X PBS and x µl of each dilution was plated on LB, MRS and/or Ace media. We incubated the plates at 30 °C (LB and Ace) or 37 °C (MRS) for ~48h then counted colonies on plates with 20-100 colonies.

For culture-independent characterization, two 0-1 day old males were homogenized manually in filter sterilized squishing buffer (10 mM Tris @ pH 8.0, 1 mM EDTA @ pH 8.0, and 25 mM NaCl) with a fitted pestle until no obvious particulates could be seen. The homogenates were incubated with Proteinase K for 1 hour and boiled for 5 minutes. 150 ng of total DNA was used as template for PCR amplification (see table for primer information). Amplified DNAs were Sanger sequenced by Genewiz (South Plainfield, NJ).

Two-dimensional fluorescence difference gel electrophoresis (2D-DIGE), imaging analysis and protein quantification

Five to six day old flies were dry dissected on a sterile CO_2 pad and the 40 heads were pooled in lysis buffer (7 M urea, 2 M thiourea, 4% CHAPS, 10 mM DTT and 10 mM Na-Hepes pH 8.0) spiked with 1% protease inhibitor (Sigma-Aldrich, St. Louis MO, USA). The heads were homogenized manually with a fitted pestle until no obvious particulates could be seen. Head lysates were adjusted to 2 mg/ml protein concentration with lysis buffer. Protein lysate solutions containing a total of 100 µg of protein were labeled with 2 µl of either 1mM propyl-Cy3-NHS or

0.83 mM methyl-Cy5-NHS (CyDye DIGE Fluors; GE Healthcare) as described previously (Unlu, Morgan, and Minden 1997), resulting in fewer than one dye molecule per protein to prevent changing protein migration in 2DE gels. Reciprocal labeling experiments were performed to control for dye-dependent changes and to have technical replicates of each sample. Two-dimensional electrophoresis (2DE) was performed as previously described (Van, Ganesan, et al. 2014).After second dimension electrophoresis, the gels were fixed in a solution of 40% methanol and 10% acetic acid overnight then imaged in a Structured Illumination Gel Imager (Van, Bass, et al. 2014). Protein differences were determined by quantifying grey scale images of each channel using Source Extractor as previously described (Bertin and Arnouts 1996; Van, Bass, et al. 2014). To determine the fold-difference between CV and AX expression of a protein, the intensity values of each channel were normalized to five "guide star" proteins, protein spots that reliably do not change within the proteome (determined from multiple biological replicates), and analyzed as previously described (Gong et al. 2004; Van, Bass, et al. 2014; Blundon et al. 2016).

Immuno-blotting of ADH protein

For standard western blots, CV brain and fat body lysates were prepared in 2X Laemmli sample buffer treated with 0.1% Protease Inhibitor Cocktail (Sigma-Aldrich, St. Louis MO, USA) and separated by SDS-PAGE. For 2D-Westerns, CV head lysate was labeled with Cy5 dye and run on a 2DE gel, as described above. Gels were equilibrated in a Tris buffer at pH7.5 with 20% glycerol for 30 minutes. Proteins were transferred to Protran nitrocellulose membranes (Whatman, Little Chalfont Buckinghamshire, UK) overnight in carbonate transfer buffer at pH 9.9 (100mM $NaHCO_3$ and 80uM Na_2HCO_3) at constant 25 V. Membranes were immuno-blotted

using a goat anti-Drosophila Alcohol Dehydrogenase antibody at 1:500 (Santa Cruz Biotechnologies, Dallas TX, USA). Donkey anti-goat HRP secondary antibody (Jackson Immunoresearch, West Grove PA, USA) was used at 1:2,000. Immuno-luminescence (Pierce ECL Western Blotting Substrate, Thermo Scientific) was detected using a ChemiDoc MP Imaging System (Bio-rad).

qRT-PCR analyses of *Adh* gene expression levels

Five to six day old CV and AX fly heads were dry dissected under CO_2 sedation. Heads were immediately bead beaten with approximately 50µl of 0.5 mm Zirconia/Silica beads in 500µl of Trizol (Invitrogen, Carlsbad CA, USA). The homogenates were immediately frozen at -20ºC until RNA extraction (stored no longer than 2 weeks).

RNA was extracted from Drosophila heads with Direct-zol RNA mini kit (Zymo, Irvine CA, USA). 500 ng of high quality RNA ($A_{260/280}$ ~1.8-2.0) was used as template for the synthesis of first strand of cDNA using SuperScript VILO synthesis kit (Invitrogen, Carlsbad CA, USA). After first strand cDNA synthesis, 100 ng of the cDNA product was directly used for qRT-PCR using PowerUp SYBR Green Master Mix in a 7300 Real Time PCR System (Applied Biosystems, Foster City CA, USA) using Sequence Detection Software (v1.4.0.25, Applied Biosystems, Foster City CA, USA).

Housekeeping genes, *rpl32* (*ribosomal protein L32*) and *ef1* (*elongation factor 1*), were used for normalization (Ponton et al. 2011). Data were analyzed with *rpl32* and data analysis was carried out using the Pfaffl-ΔΔCT method (Pfaffl 2001) in Fig. 2. We also determined the primer efficiencies for all primer sets used to calculate the fold-change between CV and AX flies. Fold

changes presented are the mean results from six biological replicates for males and four for females.

Assessing alcohol induced hyperactivity

Locomotor activity was analyzed with a Drosophila Activity Monitor 2 (Trikinetics, Waltham, MA, USA). Single 5-6 day old adults were placed under mild CO_2 sedation and transferred into monitoring plastic tubes (5 mm diameter) capped at one end with a rubber cap. Tubes were randomly loaded onto a Trikinetics exhaust manifold. Base line activity was established for the first hour followed by a two hour ethanol (PHARMCO-AAPER, Shelby KT, USA) exposure using a 10:1 ratio of air to ethanol vapor mixture (empirically determined for max hyperactivity difference) delivered by a homemade vaporizer. Activity data (crossings of an infrared beam) were collected by the Trikinetics computer software in bins every 30 seconds and later converted to 5 minute bins. A total of 8 flies from each condition were run in parallel for four trials. Data were pooled from 32 total individual flies for each condition to obtain average activity levels. Locomotor activity curves were generated and statistical analysis was performed by GraphPad Prism 7 tool. A Two-way ANOVA was used to compare the hyperactivity curves.

Assessing alcohol induced sedation

Alcohol sedation was performed as described Maples and Rothenfluh with minor adaptations. 0-1 day adult males were collected in batches of 8 under CO_2 and aged to 5-6 days. Fresh fly food vials were converted into ethanol chambers by creating a flat cotton bed at the bottom of the vial and sealing the chamber with a cotton ball soaked in 100% ethanol (Maples

and Rothenfluh 2011)(PHARMCO-AAPER, Shelby KT, USA). The chamber size was roughly 1.25" in height.

A typical alcohol sensitivity experiment contained 4-5 vials each of CV males and AX males. The flies were transferred to ethanol chambers, conditions randomized, and numbered. The vials were taped together in batches of 4-5 vials. An iPad (Apple Inc., Cupertino CA, USA) was used to record videos of each trial. Before recording, each dry ethanol chamber cotton ball was replaced with a cotton ball soaked in roughly 1.2 mL of red dyed ethanol. Time zero started after all dry cotton balls were replaced. During the experiment, the vials were tapped every minute and immobility was assessed after a 15 second recovery period until full sedation was reached. After the 15 second recovery period, the number of flies immobilized was recorded and the mobile fraction was calculated. The ethanol cotton ball was readjusted after every tap series to ensure the chamber was approximately 1.25" high throughout the experiment. The videos were analyzed by two observers who were blinded to the microbial conditions of the flies. Flies were deemed immobile if: (1) the fly traveled less than the radius of the vial (to account for postural struggle or spontaneous jumps after immobilized), (2) the fly lost postural control and flipped orientation, or (3) the fly was completely motionless or stationary with tremors while maintaining postural control. Statistical significance was determined by performing a Two-way ANOVA comparing the sedation curves and a One-way ANOVA with the ST50 values, using GraphPad Prism 7 tool.

Assessing alcohol food preference using the Two-choice Capillary Feeder (CAFÉ) assay

CV, AX, and RC male sibling flies were tested in the CAFÉ assay as previously described (Pohl et al. 2012). Each vial housed 8 flies and contained 4 capillaries. The capillaries

contained a liquid food comprised of 5% yeast extract and 5% sucrose with either no ethanol (2) or 10% ethanol (2). Measurements of food levels in the capillaries were taken daily by four observers. Death counts for each vial were also noted per day. The assay was carried out for 5 days and measurements were taken at the same time each day. Capillaries were replaced with fresh food solution each day.

BARCODE alcohol preference assay

Fifty 5-6 day old CV, AX, RC flies were tested in parallel in three separate BARCODE chambers (A. Park, Tran, and Atkinson 2017). Standard molasses based fly food with agar was used for preference assays. Fly food was liquified and additives were mixed in once the food was cooled to ~35° C. The food grid was filled in an alternating pattern with food containing 5% ethanol or non-ethanol food to which a matching volume of water was added. The food type specific oligomers were added to the corresponding food type at 3.5 ng/µl. After 2 days, the flies were collected from the chamber using CO_2 and frozen immediately for future DNA extraction (see below).

Positional alcohol preference analysis

Preference was tested behaviorally in the BARCODE assay by capturing images of the position of flies on the food pad in 5 minute intervals for 48 hrs. We used BTV Pro for Mac (Ben Software) for automatic capture and analyzed using a custom Perl script and ImageMagick (ImageMagick 7.0.5-0). Preference Index (PI) was measured by averaging number of flies on ethanol and non-ethanol food wells per day and calculated using the equation below; PI = (N Flies on Ethanol - N Flies on Non-Ethanol) / Total N Flies on Stage.

Consumptive alcohol preference analysis

Consumptive preference was measured following the conclusion of the behavioral assay. Flies were washed using the washing protocol by (A. Park, Tran, and Atkinson 2017) and homogenized in a squishing buffer containing previously described. For each biological replicate, we homogenized five flies per N. Homogenates were then incubated with Proteinase K NEB (Ipswich, MA, Product No. P8107S) and spun down for 2 minutes at 10,000 G. The supernatant was used for qPCR, with the ThermoFisher Power SYBR™ Green PCR Master Mix reagents (Waltham, MA, Catalog No. 4367659). Samples and mix were loaded into a 96-well real time PCR plate. We used a ThermoFisher Viia 7 Real-Time PCR System (Waltham, MA) with a T_m = 60° C and 40 cycles per run.

Measuring alcohol levels

Flies (20 males) were pretreated with 10% ethanol vapor for 30 minutes then frozen immediately. Flies were then homogenized with glass dounce homogenizers using 20 µL ddH_2O per fly. The homogenate was pipetted into 1.5 mL tubes and centrifuged at 10,0000 G for 3 minutes. 10 µL of the supernatant was taken and used for the sample. We used the Megazyme Ethanol Assay Kit (Bray, Co. Wicklow, Ireland, Product code: K-ETOH). Absorbance measurements were taken using a Nanodrop ND-1000 (Nano-drop Technologies, Inc., Wilmington, DE). We took our A_1 measurement 5 minutes following the addition of the ALDH enzyme and our A_2 measurement 15 minutes following the addition of the ADH. ALDH absorbance was background subtracted from ADH absorbance to calculate NADH produced.

Alcohol dehydrogenase enzymatic levels

We used the Alcohol Dehydrogenase activity assay kit from Sigma-Aldrich (product code: MAK053). Flies (20 males) were pretreated with 10% ethanol vapor for 30 minutes then immediately homogenized with a fitted plastic pestle in 200 µL of ice cold ADH assay buffer, in a 1.5 mL microcentrifudge tube, until no particulates were visible. The homogenates were centrifuged at 10,0000 G for 10 minutes. 10 µL of the supernatant was taken and used for the sample. Absorbance measurements were taken using a Tecan Safire 2 Plate Reader (Tecan Group Ltd., Männedorf, Zürich, Switzerland). An NADH standard curve was generated. We took our initial absorbance measurement 2 minutes following the addition of the proprietary enzyme mix (ADH assay buffer, developer, isopropanol substrate). Absorbance measurements were recorded every minute for a total of 25 minutes. A ΔAbsorbance (ΔA) value was calculated per sample by subtracting the initial absorbance from the final absorbance value. The ΔA was used to calculate the ADH activity using the following equation:

$$ADH\ activity = \frac{(\Delta A)\ x\ (sample\ dilution\ factor)}{(Reaction\ time) x\ (volume\ of\ reaction)}$$

Primers used in this study

Primer	Sequence	Purpose	Reference
Universal forward (8F)	5'-AGAGTTTGATCMTGGCTCAG-3'	Testing microbes in fly cultures	(Edwards et al. 1989)
Universal reverse (1492R)	5'-GGMTACCTTGTTACGACTT	Testing microbes in fly cultures	(Eden et al. 1991)
Acetobacter forward	5'-TAGTGGCGGACGGGTGAGTA-3'	Testing microbes in fly cultures	(Elgart et al. 2016)

Acetobacter reverse	5'-AATCAAACGCAGGCTCCTCC-3'	Testing microbes in fly cultures	
Lactobacillus forward	5'-AGGTAACGGCTCACCATGGC-3'	Testing microbes in fly cultures	
Lactobacillus reverse	5'-ATTCCCTACTGCTGCCTCCC-3'	Testing microbes in fly cultures	
DNA Oligomer 1	5'-ACCTACACGCTGCGCAACCGAGTCATGCCAATATAAGCAGATTAGCATTACTTTGAGCAACGTATCGGCGATCAGTTCGCCAGCAGTTGTAATGAGCCCC -3'	BARCODE assay	(A. Park, Tran, and Atkinson 2017)
DNA Oligomer 2	5'-GGGCAGCAGGATAACTCGAATGTCTTAGTGCTAGAGGCTTGGGGCGTGTAAGTGTATCGAAGAAGTTCGTGTTAAACGCTTTGGAATGACTGTAATGTAG-3'	BARCODE assay	
Forward qPCR Primer 1	5' -GCAACCGAGTCATGCCAATA -3'	BARCODE consumptive alcohol preference	
Reverse qPCR Primer 1	5' –TTACAACTGCTGGCG	BARCODE consumptiv	

	AACTG -3’	e alcohol preference	
Forward qPCR Primer 2	5’ – CAGCAGGATAACTCG AATGTCTTA – 3’	BARCODE consumptiv e alcohol preference	
Reverse qPCR Primer 2	5’– CAGTCATTCCAAAGC GTTTAACA – 3’	BARCODE consumptiv e alcohol preference	
cyp1 Forward qPCR primer	5’– ACCAACCACAACGGC ACTG – 3’	BARCODE consumptiv e alcohol preference	
cyp1 Reverse qPCR primer	3’– TGCTTCAGCTCGAAG TTCTCATC -5’	BARCODE consumptiv e alcohol preference	

Results

The *Drosophila* head proteome is responsive to microbial condition

To identify the *Drosophila* head proteome changes associated with the loss of the microbiota, we compared head lysates (Fig. 1A) of conventional (CV) and axenic (AX) *Top Banana* (a recently isolated wild strain from M. Dickinson, CalTech) siblings. We confirmed the cultures were AX using both culture-dependent and culture-independent approaches (SFig. 1). AX cultures were developmentally delayed compared to CV cultures, similar to previous reports (12.7 days and 11.4 days respectively; Appendix B, SFig. 3.1A) (Seung Chul Shin et al. 2011; Storelli et al. 2011; Whon et al. 2017). In addition, we isolated the two main taxa of the *Drosophila* microbiota, *Lactobacillus spps*. and *Acetobacter spps.* from surface sterilized whole fly CV homogenates and demonstrated that growth was absent from AX whole fly homogenates (SFig. 1B). Additionally, we confirmed the presence or absence of these taxa through PCR using universal, Wolbachia specific, *Lactobacillus* specific and *Acetobacter spps.* specific 16S rRNA primers followed by Sanger sequencing (SFig. 1C).

Lysates from CV and AX fly heads were independently labeled with either Cy3 or Cy5 dyes, combined, and then separated on the same 2DE gel (Fig. 1A). We detected and quantified the protein spots using an open-source astronomy software package called SourceExtractor, as previously described (see methods for full details) (Bertin and Arnouts 1996; Gong et al. 2004; Blundon et al. 2016). Across three biological replicates for male comparisons and for female comparisons, we detected and manually authenticated 49 and 35 consistently resolved protein spots, respectively (Fig. 1B). To confidently detect meaningful protein differences, we used a 20% (1.2-fold) cut off for a significant total abundance change; this is approximately three standard deviations above the technical noise in a standard 2D-DIGE experiment (see methods).

We measured 10 reproducible protein differences in males and 12 in females that were composed of moderately to highly abundant proteins (Fig. 1B&C, SFig. 2). Of these, we observed some protein differences that were shared and some that were unique between males and females. We identified four male specific protein differences (Fig. 1B&C, blue shaded region) and six female specific protein differences (Fig. 1B&C, grey shaded region). Among the shared proteins, we found three proteins that changed in abundance in the same direction in AX male and female flies (Fig. 1B&C, purple shaded region) and three proteins whose abundance changed in the opposite direction between males and females (Fig. 1B&C, orange shaded region). These data suggest that loss of the gut microbiota leads to significant and sexually dimorphic differences in *Drosophila* head proteomes.

Alcohol Dehydrogenase protein level is elevated in the head of AX male flies

Mass spectrometry identified spot #4 as the metabolic enzyme Alcohol Dehydrogenase (ADH). We confirmed the protein identity by immunoblotting for *Drosophila* ADH after 2DE separation of CV head lysate (Fig. 2B). Our 2D-DIGE analysis showed that the loss of microbiota leads to elevated ADH protein in the heads of AX males but not AX females (Fig. 1C and 2C). On average, ADH protein was elevated 1.8-fold, and the protein could be restored to CV levels when the microbiota was reintroduced in 0-1 day old adult males (Reconstituted, RC; Fig. 1A; Fig. 2C). One explanation for the elevation of ADH protein in the heads of AX males is an increase in gene expression, but we found no consistent elevation of *Adh* transcripts in either AX male or AX female heads (Fig. 2D). These data suggest that the microbiota plays a role in maintaining the proper level of ADH protein in the male head through a mechanism that

regulates ADH protein stability or translation efficiency. There does not appear to be any precedent for these types of ADH regulation.

AX male flies have altered physiological responses to alcohol

An animal's first line of defense against the toxic effects of rising levels of ethanol is to metabolize it. ADH is the first step in that process that catalyzes the oxidation of ethanol to acetaldehyde, and its activity influences several physiological responses to alcohol including hyperactivity (Fig. S3A) (Rodan and Rothenfluh 2010; Edenberg 2007; Wolf et al. 2002). Elevated ADH in AX male fly heads suggested that AX males may have altered physiological responses to alcohol. To test this hypothesis, we assessed two phases of alcohol-induced responses common to all animals and well described in Drosophila– alcohol-induced hyperactivity and sedation (Wolf and Heberlein 2003; Devineni and Heberlein 2013).

To assess alcohol-induced hyperactivity, we monitored locomotor activity in CV, AX, RC aged-matched males using the *Drosophila* activity monitor 2 (DAM2, Trikinetics, Waltham MA), an automated system that uses two infrared beams to quantify fly motility in the absence or presence of alcohol (Fig. 3A). After monitoring locomotion for 60 mins without alcohol to establish a baseline, we exposed the flies to a low concentration of ethanol vapor (10:1 air to ethanol vapor) and continued monitoring for 120 mins. Shortly after being exposed to alcohol vapor, CV males entered a period of hyperactivity peaking at an average of 3.4 laser passes/10 min (Fig. 3B, Table 1). At approximately the same time of onset, AX males entered the hyperactivity phase with a peak of 9.5 laser passes/10 min, which was restored to CV levels in reconstituted AX males (Fig. 3B, Table 1). Consistent with the lack of ADH elevation in AX

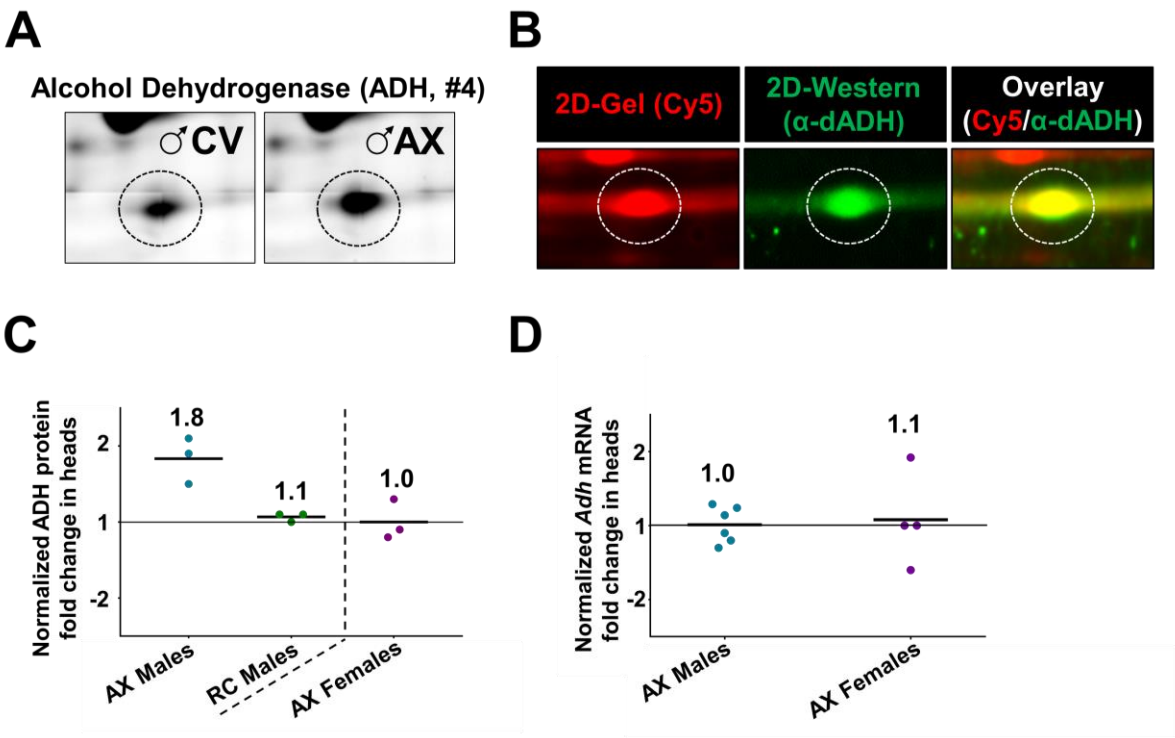

Figure 3.2. Alcohol Dehydrogenase (ADH) proteins levels are elevated in AX heads.

(A) Tiled array images of whole gels were cropped to produce the representing cut outs gels shown in SFigure 2. ADH protein (in dotted circles) was elevated in the AX head proteome. **(B)** 2D-Western of the ADH protein in the CV head proteome. Fluorescent images of Conventional head lysates that were separately labeled with Cy5 DIGE dye, resolved on different 2DE gels and transferred to nitrocellulose. Immuno-blot images of proteins stained with anti-DmADH antibody. Superimposed images of total, Cy5-labeled protein (red) and the ADH 2D-immuno-blot (green) confirm protein identification by LC-MS/MS. **(C)** Measured fold-change for ADH protein difference calculated in AX male and female flies using the Cy3 and Cy5 raw fluorescence intensities. **(D)** Relative *Adh* transcript in AX heads compared to CV heads (Normalized to *rpl32*).

female heads, there was no difference in alcohol-induced hyperactivity between CV and AX females (Fig. 3C, Table 1).

Because host genetic background is important for alcohol induced physiological changes and host genetic background influences the microbiota and its downstream effects (M A Schuckit 1994; Rodan and Rothenfluh 2010; A. Park et al. 2017; Chaston et al. 2016; Ericsson et al. 2015; Early et al. 2017), we asked whether the genetic background influences the microbiota-dependent alcohol induced hyperactivity by examining two additional wild type lab strains, Canton S (CS) and Oregon R (OR). Interestingly, we did not observe a difference in alcohol-induced hyperactivity between CS CV and AX males (SFig. 3B, Table 1). We did observe a lesser, but significant, increase in alcohol-induced hyperactivity between OR CV and AX males (SFig. 3C, Table 1). These data support the idea that the host genetic background interacts with the microbiota to influence alcohol-induced hyperactivity in male flies. Alternatively, these wild-type fly populations could harbor different strains of *Lactobacillus* and *Acetobacter* that do not mediate microbiota-dependent alcohol physiologies.

Next we asked whether the microbiota influences alcohol-induced sedation, a physiological response that is largely independent of ADH activity and ethanol metabolism (Singh and Heberlein 2000; Scholz et al. 2000; Kaun, Devineni, and Heberlein 2012). To test this, we exposed groups of CV, AX, and RC males to alcohol vapor in fly vials and assessed the time to immobilization for the entire fly population in a vial (Fig. 3D, (Maples and Rothenfluh 2011)). Although the time to complete sedation did not vary significantly by microbial condition (Fig. 3E), the rate of sedation, assessed by comparing the ST50 (time at which 50% of the population was immobilized) differed significantly between CV and AX males (Fig. 3F). On average, AX males took longer to immobilize (ST50=15.9 min) compared to CV males

(ST50=11.7 min), and this was restored to CV levels in RC males (ST50=13.2 min). Overall, these data demonstrate that AX male flies have microbiota-dependent changes to alcohol-induced physiological responses some of which may be the result of elevated ADH protein.

ADH protein activity is required for the microbiota-dependent alcohol induced hyperactivity

To begin to understand the connection between elevated ADH protein and the changes in physiological response that we saw, we first asked whether the microbiota-dependent increase in hyperactivity in AX males requires ADH activity by treating CV and AX males with an ADH inhibitor (4-Methylpyrazole, 4MP; Cadieu et al. 1999). If the elevated alcohol-induced hyperactivity in AX males requires ADH enzymatic activity, inhibiting that activity should reduce hyperactivity to lower CV-like levels. Indeed, AX males aged in the presence of the inhibitor for five days exhibited reduced hyperactivity compared to control untreated AX males (Fig. 4A). Interestingly, the same inhibitor treatment of CV males did not significantly decrease their alcohol-induced hyperactivity suggesting that the inhibitor treatment did not completely abolish ADH activity (Fig. 4A).

Next we asked if the higher level of ADH protein in AX males results in increased ADH activity and increased ethanol metabolism by quantifying ADH enzymatic activity and ethanol levels in CV, AX, and RC males after exposing them to ethanol vapor. Because ADH-dependent ethanol metabolism occurs primarily in the fat body of *Drosophila* (Geer, Dybas, and Shanner 1989), and the fat body is located both in the head and abdomen, we decided to first characterize whole fly ethanol metabolism. After a 30 minute vapor exposure, whole fly lysates were immediately prepared from cohorts of pre- and post-exposed flies. We did not observe any

significant difference in ADH enzymatic activity or ethanol levels depending on the microbial composition of the fly (Fig. 4B,C). This does not rule out the possibility of tissue or cell type specific increases in ADH activity and ethanol metabolism, but does suggest that there is no significant systemic change.

To begin to address the question of tissue specificity, we asked whether ADH is expressed in the brain itself, or in other cell types in the head. We separately lysed fly brains and the remaining head capsule and detected ADH by immunoblot. Consistent with previous reports that ADH is not significantly expressed in fly brain (N., J., and M.C. 1992), we only detected ADH in the head capsule (Fig. 4D). Because high levels of ADH are expressed in the abdominal fat body (N., J., and M.C. 1992), the most likely site of ADH expression in the head is in the fat body that lies immediately anterior to the brain.

AX males flies have altered alcohol food preference

Human studies have shown that differences in ethanol sensitivity between individuals is one predictor of future alcohol addiction, as individuals who are less sensitive to alcohol have an increased risk of addiction (Marc A. Schuckit 1994). *Drosophila* has been a great model for understanding the genetics underlying alcohol consumption, preference, and addiction (Kaun, Devineni, and Heberlein 2012; Devineni and Heberlein 2009). To ask whether the microbiota affects alcohol consumption and preference, we asked if AX males have an altered preference for alcohol. We first assessed alcohol feeding preference using the Two-choice Capillary Feeder (CAFE) assay for five days where flies choose to consume either normal liquid yeast meal or ethanol-spiked (10%) liquid yeast meal (Fig. 5A) (Ja et al. 2007; Devineni and Heberlein 2009; Deshpande et al. 2014). We calculated a food preference index (PI) by taking the difference in

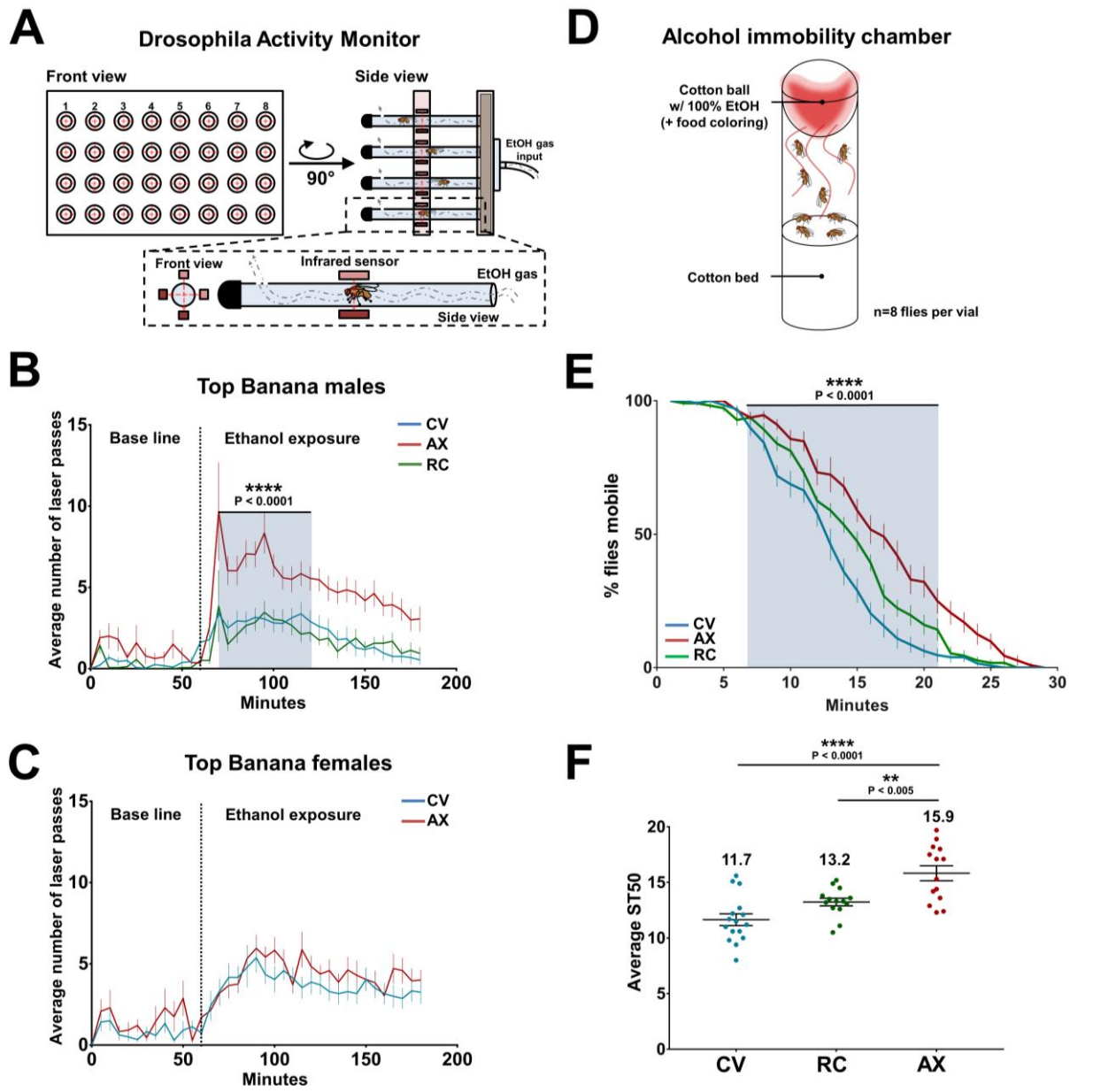

Figure 3.3. AX male flies are less sensitive to alcohol vapor exposure.

(A) A schematic of the *Drosophila* Activity Monitor 2 (Trikinetics, Inc.) to test alcohol induced hyperactivity. An individual fly is a biological replicate. **(B)** CV, AX, and RC male flies were assessed for alcohol induced hyperactivity. The n tested is 32 flies in 4 trials. Bars indicate standard error of the mean. Flow rate: H2O:EtOH (10:1). Statistical significance between CV and AX male flies (blue shaded region) was assigned by a Two-way ANOVA (Tukey's multiple comparisons post hoc test). Dotted line indicates start of ethanol exposure. **(C)** CV, AX, and RC

Top Banana female flies were assessed for alcohol induced hyperactivity. The n tested is 32 flies in 4 trials. Bars indicate standard error of the mean. Flow rate: H2O:EtOH (10:1). **(D)** A schematic of the alcohol immobility chamber to test alcohol induced sedation. Each vial housed up to eight flies. An individual vial is a biological replicate. **(E)** CV, AX, and RC male flies were assessed for alcohol induced sedation. The n tested for CV, AX, and RC is 128, 112, and 112 flies, respectively, in 4 trials. Bars indicate standard error of the mean. Statistical significance (blue shaded region) was assigned by a Two-way ANOVA (Dunnett's multiple comparisons post hoc test). **(F)** The time it takes for 50% of the population to sedate, ST50, from the alcohol induce sedation curves from male flies in panel E. Each dot represents the ST50 produced from a single vial of that respective condition. Bars indicate standard error of the mean. The n tested for CV, AX, RC is 16, 14, and 14 vials, respectively. Statistical significance was assigned by a One-way ANOVA (Tukey's multiple comparisons post hoc test).

normal food from ethanol-laced food consumed, normalized to the total amount of food consumed. ADH activity is required for ethanol odorant preference in adult flies (Ogueta et al. 2010), but olfactory preference does not predict ethanol consumption preference (Peru et al. 2014; Sekhon et al. 2016). Thus, elevated ADH alone does not predict significantly altered ethanol consumption preference. While males of some wild type strains have an increased PI over time (Devineni and Heberlein 2009), on average Top Banana CV males had no alcohol food preference for the duration of the assay (PI = -0.01; Fig. 5B). In contrast, AX males had a slight, but significant, preference for food with alcohol (PI = 0.08) that increased over time (Fig. 5B & Fig. S5A). Reconstituting the microbiota in AX males had a very surprising effect; instead of reducing preference to CV levels as expected, RC males had a dramatic increase in alcohol food preference compared to AX (PI = 0.29; Fig. 5B). The pattern of total food consumption over the 5 days also varied significantly between the different microbial conditions (Fig. 5C). For CV males, total consumption/day did not vary significantly, while AX flies consumption started low and increased with time, and RC flies consumption started high, decreased, and then rebounded (Fig. 5C). Together these results suggest that the microbiota can alter alcohol food preference in males, but the surprising behavior of the RC flies and the differences in total food consumption raise the possibility that there may be an uncontrolled variable affecting feeding patterns and alcohol preference. Although the CAFE assay is well-established in the field, some evidence suggests that flies are starving (Devineni and Heberlein 2009; Peru et al. 2014; Pohl et al. 2012). Consistent with a stressful environment in the CAFÉ, approximately 15% of the flies in each condition died by the end of day 5 (data not shown).

BARCODE is a new alcohol preference paradigm not associated with lethality that allows the flies to have at will access to large quantities of food, and a more natural feeding

Table 3.1: Summary of flies tested for ethanol induced hyperactivity. Below are the peak average hyperactivity of each genotype and sex tested.

Genotype	Condition	Sex	Average hyperactivity peak during alcohol exposure (average laser passes)	ST ERR
TB	CV	M	3.4	0.94
TB	AX	M	9.5	3.04
TB	CV	F	4.2	0.78
TB	AX	F	5	0.71
CS	CV	M	3.7	0.52
CS	AX	M	3.2	0.89
OR	CV	M	3.5	0.78
OR	AX	M	4.9	0.58

behavior of roaming and sampling, by using a sectioned stage with alternating squares of solid fly food with and without ethanol in a large chamber (A. Park, Tran, and Atkinson 2017; Fig. 5D). In this assay, we measured two aspects of alcohol preference –positional preference and food consumption preference. To determine positional preference, a picture of the stage was captured every five minutes for two days and an alcohol preference index was calculated by the difference in the number of flies on non-ethanol squares from flies on ethanol squares, normalized to the total number of flies on the stage. CV males have a slight aversion to the ethanol squares (average PI = -0.10) that decreased toward neutral by the second day (Fig. 5E & Fig. S5B). The positional preference of RC males was indistinguishable from that of CV males (Fig. 5E & Fig. S4B). In contrast, AX males exhibited a significant increase in positional preference for ethanol (average PI = +0.10) that did not change significantly over the two days of the assay (Fig. 5E & Fig. S5B).

To quantify alcohol food consumption preference, the ethanol squares and the non-ethanol squares were spiked with two different oligonucleotide tags. Following the two days of the assay, the relative quantity of these sequences was detected in surface-washed fly lysates with qPCR, and these values were used to calculate the alcohol consumption preference index (Fig. 5F). Although CV males spent slightly less time on the ethanol squares (Fig. 5E), they consumed slightly more ethanol food than non-ethanol food (PI = 0.12; Fig. 5F). RC males exhibited a similar pattern (Fig. 5F). Consistent with the increase in positional preference, AX males consumed significantly more ethanol food than CV or RC males (PI = 0.40; Fig. 5F). Together, the CAFE assay and the BARCODE assay indicate that AX males have a significantly stronger preference for food containing ethanol than their CV siblings. RC males exhibited significantly different behavior in the two assays; in the more physiologically-relevant

BARCODE assay, alcohol preference for the RC males was indistinguishable from CV, consistent with a restoration of CV alcohol responses when microbes were reintroduced to adult AX males. The unexpected spike in alcohol preference and total food consumption in AX males in the CAFE assay (Fig. 5B,C) suggests that CV males and RC males may have some metabolic differences that influence their response to nutrient deprivation. Alternatively, differences in microbiota abundance or composition could account for response differences to nutrient deprivation. Indeed we did observe a slight increase in *Lactobacillus* species in RC flies (Fig. S1D), supporting this possibility.

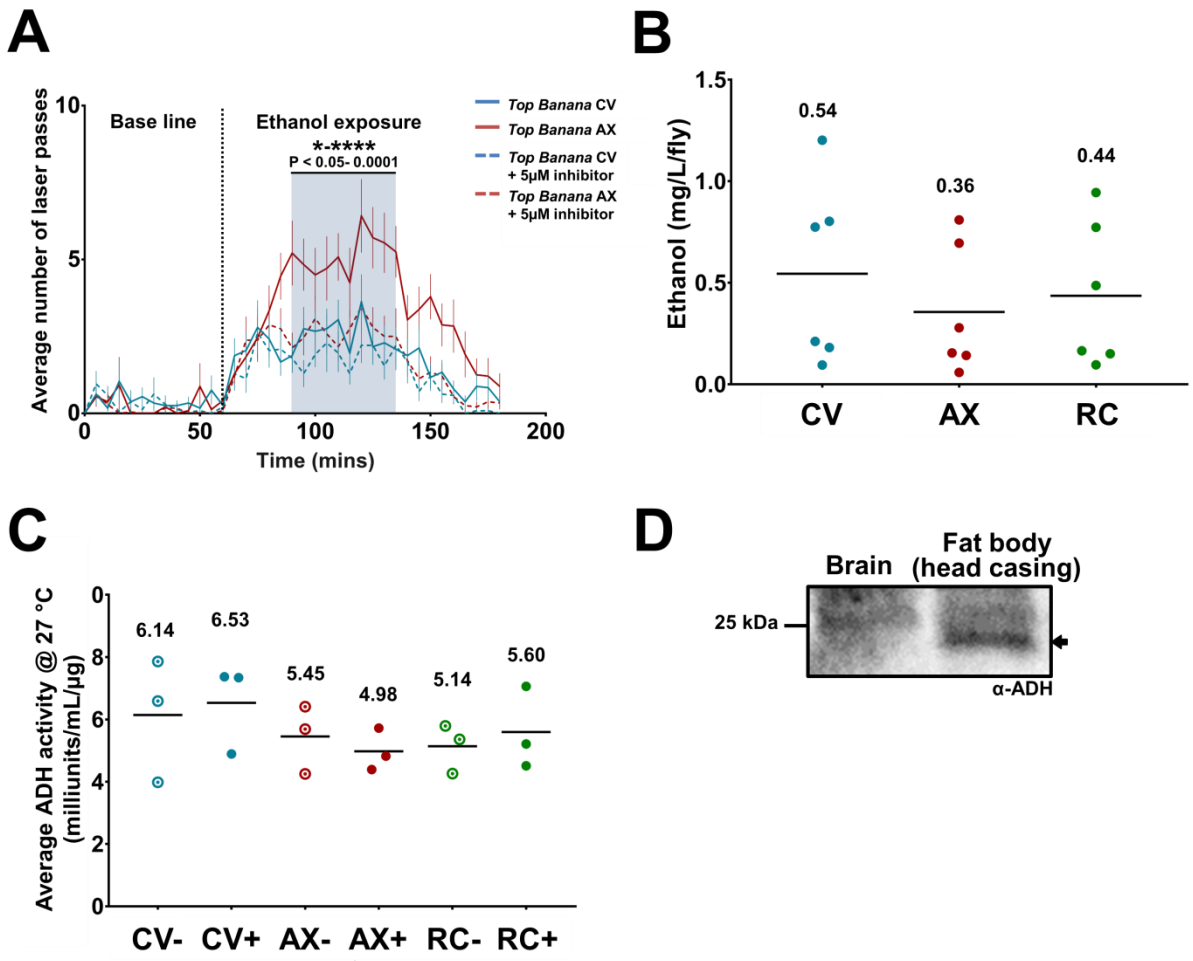

Figure 3.4. The microbiota-dependent hyperactivity requires ADH enzymatic activity but not ethanol metabolism.

(A) CV and AX male flies with and without 5μM 4-Methylpyrazole (4MP) were assessed for alcohol induced hyperactivity. The n tested is 24 flies in 3 trials. Bars indicate standard error of the mean. Flow rate: H2O:EtOH (10:1). Statistical significance between CV and AX controls (blue shaded region) was assigned by a Two-way ANOVA (Dunett's multiple comparisons post hoc test). **(B)** Endogenous ethanol levels of CV, AX, and RC male flies after exposed to 10% ethanol for thirty minutes. Each dot represents a biological replicate containing twenty whole flies. Solid black bar indicates the mean. **(C)** Endogenous ADH enzymatic activity levels of CV, AX, and RC male flies after exposed to 10% ethanol for thirty minutes. Each dot represents a

biological replicate containing ten whole flies. Solid black bar indicates the mean. **(D)** Anti-ADH immunoblot of isolated CV male brain and head casing (containing the fat body).

Discussion

The microbiota's ability to profoundly influence host physiology and behavior has huge implications for understanding both normal biology and disease states. Using a gel-based proteomic screen, we identified both general and sex-specific microbiota-dependent proteome changes in the *Drosophila* head. A growing number of studies are demonstrating that the composition of the gut microbiota and microbiota-dependent effects on some aspects of host physiology are significantly influenced by host sex. In humans, mice, and flies, the composition of the microbiota is different in males and females (Org et al. 2016; Haro et al. 2016; Han et al. 2017), and in mice this difference has been shown to be mediated by sex hormones, sex-specific differences in bile acids, and sex-specific differences in immunity (Yurkovetskiy et al. 2013; Xie et al. 2017; Fransen et al. 2017). Furthermore, connections between sex and the gut microbiota appear to be contributing to sex-specific differences in Type 1 diabetes (Yurkovetskiy et al. 2013) and liver carcinogenesis (Xie et al. 2017). While these connections are being made, the precise molecular mechanisms are largely unknown. We found that the fly head proteome also exhibits sex-specific microbiota-dependent changes. In addition to individual proteins, like ADH, that exhibit sex-specific changes, we are particularly intrigued by those proteins that exhibit microbiota-dependent elevation in males and a decrease in females. We anticipate that future identification of those proteins will yield important insight into the underlying molecular mechanism connecting sex, the microbiota, and host biology.

Alcohol abuse disorders (AUD) have a complex genetic basis. Multiple phenotypes contribute to the risk of alcoholism including disinhibition/impulsivity, patterns of alcohol metabolism, and a low level of response to alcohol (M. a Schuckit, Smith, and Kalmijn 2004). Among these, low level of responsiveness to alcohol is the most well studied risk factor; it

strongly predicts future alcoholism, and its heritability is as high as 60%. Many challenges contribute to the identification of genes involved in these AUD risk phenotypes because multiple genes contribute to each, and because environmental influences on genotype substantially affect risk (M. a Schuckit, Smith, and Kalmijn 2004). Our demonstration that AX males have an increased responsiveness to alcohol as reflected in elevated hyperactivity suggests that there are components of the microbiota that influence alcohol responsiveness (Fig. 3). The fact that this is only true for male *Drosophila* is an interesting parallel to what has been found in human studies; while decreased alcohol responsiveness is strongly associated with an increased risk of alcohol abuse in men, the same does not appear to be true in women (Heath et al. 1999).

Increased alcohol preference can lead to increased consumption triggering a positive feedback loop that can promote addiction phenotypes (Peru et al. 2014; Koob and Volkow 2010; Barson, Morganstern, and Leibowitz 2011). If CV males with a lower responsiveness to alcohol are at greater risk for alcohol dependency, one might predict that they would exhibit a greater consumption preference for alcohol, but this is not the case (Fig. 5); AX males had a higher consumption preference for alcohol than their CV siblings. Studies of alcohol responses in mice have identified a number of molecular systems in the brain that affect alcohol responses including dopamine (Crabbe et al. 2006), which is necessary for conditioned alcohol preference in *Drosophila* (Kaun, Devineni, and Heberlein 2012). Interestingly, disruptions in dopamine neurotransmission have been reported in germ-free mice (Parashar and Udayabanu 2017), suggesting a possible mechanism by which the microbiota could influence alcohol preference in *Drosophila*.

In addition to a role in responsiveness and preference that we have demonstrated here, emerging evidence suggests that alcohol consumption can cause the dysbiosis of the gut

microbiota observed in a subset of alcoholic patients (Canesso et al. 2014; Mutlu et al. 2012); this dysbiosis appears to contribute to the neuro-inflammatory withdrawal response (Gorky and Schwaber 2016), and to the emotional effects of alcohol abuse (Leclercq et al. 2014). Our results suggest that differences in the microbiota could also contribute to the initial risk of addiction. Furthermore, genetic heterogeneity may contribute to the significant interpersonal variability observed in response to therapies (Litten et al. 2015). Because there is significant variation in the microbiota between people (Benson et al. 2010), the composition of the gut microbiota could also play a role in therapeutic success.

We showed that the increased responsiveness of AX males to alcohol requires the activity of ADH, suggesting that alcohol metabolism does play a role in at least some of the microbiota-mediated effects. The fact that we are not able to detect any systemic difference in ADH activity or ethanol metabolism between CV and AX flies (Fig. 4) suggests that this activity may be tissue or cell type specific. Our preliminary analysis of ADH expression in the *Drosophila* head is consistent with a model that the change in ADH does not occur in the brain itself (Fig. 4D), but is more likely to be in the fat body that lies anterior to the brain in the head capsule. This is consistent with the model that alcohol metabolism in the brain is primarily driven by catalase (Zimatkin and Lindros 1996; Cederbaum 2013; Reddy, Boyadjieva, and Sarkar 1995). The *Drosophila* fat body is a major endocrine organ that regulates aspects of brain and immune physiology and the brain can communicate to the fat body (Droujinine and Perrimon 2016; Y. Zhang and Xi 2014; Q. Liu and Jin 2017). This raises the possibility that elevated ADH protein in the fat body of AX males could influence neural activity, or that the elevation in ADH is in response to upstream microbiota-dependent changes in brain function. Because the level of *Adh* transcript is unchanged in response to microbial differences, we propose that ADH is elevated as

the result of increased translation initiation or protein stability. ADH can be modified post-translationally (Lange III et al. 1975; Hans Jörnvall et al. 1977; H Jörnvall et al. 1980) and such modifications can alter protein stability, but we did not observe any change in ADH's p*I* or molecular weight in our 2D-DIGE analysis indicative of a difference in post-translational modification. Alternatively, ADH may interact with a microbiota-responsive binding partner that stabilizes it. More work is required to distinguish the possibilities.

Regardless of the precise molecular mechanism, the elevation in ADH could be a direct response to the loss of the microbiota because the microbiota plays a direct and adaptive role in regulating alcohol responses in *Drosophila*. Because *Drosophila* in the wild feed on fermenting fruit with a typical alcohol content of 5%, it is reasonable to propose a model in which microbial symbionts modulate alcohol responses that promote successful foraging. Alternatively, the elevation in ADH could be a byproduct of other microbiota-dependent changes. For example, ADH increase in AX males could be a mechanism to compensate for a decrease in microbial-derived short-chain fatty acids (scFA) that normally promote host metabolic activities such as glycolysis, lipogenesis, and insulin signaling (Tremaroli and Bäckhed 2012), and also affect other aspects of host development, physiology, and behavior (Macfabe MD 2012; MacFabe 2015; Meyer et al. 2009; Sekirov et al. 2010; Bourassa et al. 2016; Marchesi et al. 2015). Ethanol metabolism, is driven in part by ADH activity, can promote lipid synthesis directly by converting ethanol to acetate, an scFA building block (Chakir et al. 1993). Consistent with the hypothesis that elevated ADH could be a response to defects in lipogenesis, AX adult flies have abnormally high triglycerides indicative of a defect in lipid metabolism (Newell and Douglas 2014; Wong, Dobson, and Douglas 2014) that appears to be influenced by both sex and diet content. Interestingly, germ-free mice do not accumulate lipids after ethanol consumption like CV mice

(Canesso et al. 2014). Dissecting the connection between the microbiota and ADH and lipid metabolism in the host is a high priority for the future.

Because we know that many genes and cellular processes independent of alcohol metabolism contribute to alcohol induced physiology and behavior (Rodan and Rothenfluh 2010; M A Schuckit 1994; A. Park et al. 2017), increased ADH in AX males is unlikely to be the single explanation for the microbial-dependent changes in the alcohol responses we observed. For example, *Drosophila* responds to ethanol by modulating neurotransmitter and neuropeptide activity, transcription factors and histones for gene expression, as well as alterations to the cytoskeleton and cell adhesion (Rodan and Rothenfluh 2010; A. Park et al. 2017). Future work will seek to uncover the scope of microbial-dependent mechanisms affecting host alcohol responses. Identification of the specific bacterial strains necessary to restore CV responses will be an important next step.

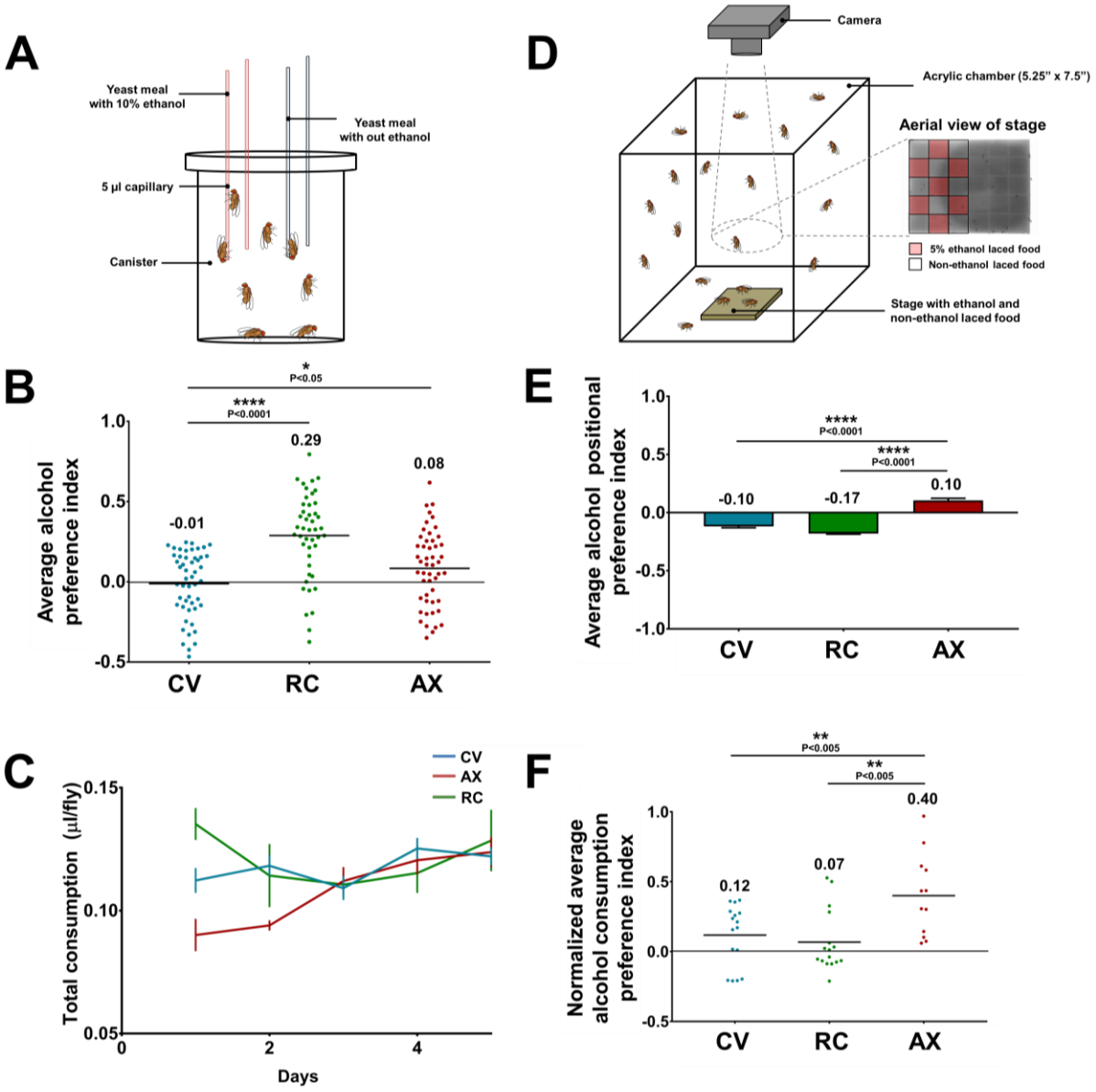

Figure 3.5. AX male flies prefer alcohol more than their CV male siblings.

(A) A schematic of the Two-choice capillary feeder assay to test alcohol preference. Each chamber housed up to eight flies. An individual chamber is a biological replicate. **(B)** CV, AX, and RC male flies were assessed for daily alcohol consumption preference for five days with 0% EtOH vs. 10% EtOH. An alcohol preference index was calculated by taking the difference in consumed normal food from ethanol laced food, normalized to the total amount of food consumed. The n tested for CV, AX, and RC is 71, 77, and 63 flies (10, 10, and 9 chambers),

respectively. Bars indicate standard error of the mean. Statistical significance was assigned by a Two-way ANOVA (Dunnett's multiple comparisons post hoc test). **(C)** Total average alcohol preference index of CV, AX, and RC male flies from data set in panel B. Each dot represents a PI produced from a chamber of that respective condition, over the five days. Solid black bar indicates the mean. Statistical significance was assigned by a One-way ANOVA (Dunnett's multiple comparisons post hoc test). **(D)** A schematic of the BARCODE assay to test alcohol preference. Each chamber housed up to fifty flies. An individual fly is a biological replicate. **(E)** CV, AX, and RC male flies were assessed for daily alcohol position preference for two days with 0% EtOH vs. 5% EtOH. An alcohol preference index was calculated by the difference in the number of flies on non-ethanol squares from ethanol squares, normalized to the total number of flies on the stage. The n tested for each condition is 50 flies. Colored bars indicate standard error of the mean. Statistical significance was assigned by a Kruskal-Wallis test (Dunn's multiple comparisons post hoc test). **(F)** Total average alcohol consumption preference index of CV, AX, and RC male flies from data set in panel E. Each dot represents a PI produced from RNA extracted from five male flies of that respective condition after the two days. Relative quantities of food were calculated from ΔCT and alcohol preference index was calculated from the difference in non-ethanol food from ethanol food, normalized over the total amount of food. Solid black bar indicates the mean. Relative Ethanol oligo transcript compared to non-ethanol oligo in whole flies (Normalized to cyclophilin). Statistical significance was assigned by a One-way ANOVA (Holm-Sidak's multiple comparisons post hoc test).

Future directions

We have identified microbial-dependent changes in *Drosophila's* alcohol responses but we do not yet fully understand the mechanism(s) by which this occurs. A lot of important objectives still remain in order to fully understand fully how the microbiota modulates alcohol response in the fly. We are interested in pursuing both ADH-dependent and independent mechanisms by which the microbiota influences alcohol responses. Below are the first proposed experiments necessary to move forward with this investigation.

Identify specific bacterial strains necessary to restore CV responses to alcohol

We predict that underlying microbial-dependent alcohol responses, such as the regulation of ADH protein abundance, are specific bacterial taxa residing in the gut and that are communicating with the host, possibly through bacterial metabolites such as scFAs (MacFabe 2015; Macfabe MD 2012). Identification of those bacterial taxa is an essential step to understanding the mechanism(s) by which microbes are regulating alcohol related host physiology and behavior. To this date, Scott Keith in the lab has isolated different bacterial species from our flies in the *Lactobacillus* and *Acetobacter* genera, and has successfully reintroduced them individually and as mixed populations to create gnotobiotic flies – flies with a known, defined microbiota. We will test these gnotobiotic strains for elevated ADH and increased responsiveness to alcohol to identify the relevant bacteria. From there several different approaches can be taken to identify the bacterial gene products and pathways that are required to properly regulate ADH-dependent and -independent alcohol responses.

Identify host brain regions and genes required for the microbial-dependent alcohol food preference

We have demonstrated the microbiota influences alcohol preference in AX male flies. The preference for alcohol in *Drosophila* requires a host of neurodevelopmental gene products (Morozova et al. 2015; I. F. G. King et al. 2014) and requires dopaminergic and αβ neurons of the mushroom body (Kaun et al. 2011; I. King et al. 2011; Yamagata et al. 2015). We predict that the microbiota is altering the flies' preference for alcohol through the regulation of specific genes, cell types, and brain regions. To begin to understand the microbial-dependent mechanisms that regulate alcohol preference in *Drosophila*, we can use the wealth of genetic tools available to reduce the activity of selected brain regions, cell types, and gene products in AX male flies, and ask which are required for the increase in preference for ethanol in AX male flies. Additionally, transcriptome analysis between AX male brain tissue before and after ethanol consumption could provide deeper insight.

Dissecting the connection between the microbiota, host fat body, and ADH-dependent lipid metabolism

We have provided evidence that the microbiota is necessary for modulating male flies' responsiveness to alcohol (Fig. 3.3). This effect in part requires ADH protein activity. However, there are no detectable differences in overall alcohol metabolism between CV and AX male flies. These observations pose an alternative hypothesis for elevated ADH protein abundance in AX male flies – 1. The increase activity of ADH protein is tissue or cell specific, and 2. elevated ADH could be a byproduct of other microbiota-dependent changes, such as changes in metabolism. One such metabolic outlet, lipogensis, is affected by both the microbiota and ADH

activity. Because lipogenesis occurs in the fat body, we will first test whether ADH activity in the fat body is required for mediating the microbiota-dependent hyperactivity (or responsiveness). We predict that knocking down ADH function in part, or all of the fat body should have significant consequences on the alcohol induced hyperactivity in AX male flies. Additionally, we will investigate whether lipid dysregulation is occuring in our flies by first characterizing the triglyceride levels and fat content of our AX males.

APPENDIX A: APC PROJECT SUPPLEMENT MATERIAL

Table 1: Source Extractor protein counts of the *APC2* null proteome changes in Fig. 2.2.

Region	Channel	Spot	Flux	Corrected Flux	Relative abundance (to unchanged spot D)	spot Fold change (Cy3/Cy5)	Total protein counts (per channel)	Total protein abundance difference (% of Cy3:Cy5)	Notes
1	WT - Cy3								
		Left	2,039,266.00	2,444,475.42	3.77E-01	-1.55	2,810,035.30	-0.54%	
		Left	304,962.70	365,559.88					
	APC2 - Cy5								
		Left	1,575,496.00	--	--	3.29	2,779,942.00	--	
		Left	1,204,446.00	--					
2	WT - Cy3								
		Left	5,187.59	6,218.38	9.50E-04	-2.78	7,837.11	-11.40%	
		Right	1,350.40	1,618.73					
	APC2 - Cy5								
		Left	2,236.82	--	--	2.03	6,232.86	--	
		Right	3,996.03	--					
3	WT - Cy3								
		Left	204,076.90	244,627.71	2.94E-01	7.11	2,173,310.57	0.15%	
		Right	1,608,974.00	1,928,682.87					
	APC2 - Cy5								
		Left	1,740,304.00	--	--	-4.39	2,180,025.40	--	
		Right	439,721.40	--					
4	WT - Cy3								
		Left	1,745,245.00	2,092,031.40	4.02E-01	-1.40	2,846,390.42	4.34%	
		Right	629,312.40	754,359.02					
	APC2 - Cy5								
		Left	1,496,724.00	--	--	2.13	3,104,835.00	--	
		Right	1,608,111.00	--					
5	WT - Cy3								
		Left	1,954,976.00	2,343,436.70	2.75E-01	-4.78	2,660,584.29	-2.66%	
		Middle	7,862,011.20						
		Right	162,602.40	194,912.08					
	APC2 – Cy5								
		Left	490,718.90		--	5.38	2,522,743.30	--	
		Middle	982,751.40						
		Right	1,049,273.00						
	WT- Cy3								
		Left	1,173,663.00	1,406,874.02	1.32E-01	-5.26	1,585,601.68	-62.67%	

		Right	149,100.80	178,727.66					
	APC2- Cy5								
		Left	186,283.00	--	--	-1.01	363,884.60	--	
		Right	177,601.60	--					

6	WT - Cy3								
		Left	297,192.40	356,245.59	3.13E-01	2.72	2,335,856.58	-0.80%	
		Right	1,651,460.0	1,979,610.99					
	APC2 - Cy5								
		Left	970,214.00	--	--	-1.49	2,298,552.00	--	
		Right	1,328,338.0	--					
7	WT - Cy3								
		Left	971,623.20	1,164,688.19	8.06E-01	2.03	6,358,922.46	-6.54%	
		Right	4,333,210.0	5,194,234.27					
	APC2 - Cy5								
		Left	2,361,440.0	--	--	-1.61	5,578,528.00	--	
		Right	3,217,088.0	--					
8	WT - Cy3								
		Left	3,764,766.0	4,512,838.42	8.85E-01	-2.21	7,551,192.34	-15.16%	
		Right	2,534,700.0	3,038,353.92					
	APC2 - Cy5								
		Left	2,043,906.0	--	--	1.16	5,563,248.00	--	
		Right	3,519,342.0	--					
9	WT - Cy3								
		Left	2,832,386.0	3,395,191.19	7.21E-01	1.15	5,247,188.20	1.69%	
		Right	1,545,000.0	1,851,997.00					
	APC2 - Cy5								
		Left	3,907,155.0	--	--	-1.22	5,427,372.00	--	
		Right	1,520,217.0	--					
10	WT - Cy3								
		Left	996,161.20	1,194,101.98	1.95E-01	-9.39	1,487,130.34	-3.06%	
		Right	244,454.40	293,028.36					
	APC2 - Cy5								
		Left	127,126.00	--	--	4.34	1,398,736.00	--	
		Right	1,271,610.0	--					
11	WT - Cy3								
		Left	636,839.50	763,381.78	8.34E-02	-3.79	777,556.84	-25.86%	
		Right	11,825.33	14,175.07					
	APC2 - Cy5								
		Left	201,168.30	--	--	18.12	458,047.90	--	
		Right	256,879.60	--					
12	WT - Cy3								
		Left	1,130,829.0	1,355,528.75	4.98E-01	-3.02	4,633,840.35	-25.64%	
		Right	2,734,881.0	3,278,311.60					
	APC2 - Cy5								

		Left	449,431.0	--	--	-1.43	2,742,599.00	--	
		Right	2,293,168.0	--					
13	WT - Cy3								
		Left	216,354.0	259,344.31	1.79E-01	3.92	1,578,693.79	-19.28%	
		Right	1,100,647.0	1,319,349.48					
	APC2 - Cy5								
		Left	1,017,788.0	--	--	-26.13	1,068,275.31	--	
		Right	50,487.31	--					
14	WT - Cy3								
		Left	1,832,385.0	2,196,486.43	7.28E-01	1.46	5,453,102.69	-1.20%	
		Right	2,716,782.0	3,256,616.26					
	APC2 - Cy5								
		Left	3,197,809.0	--	--	-1.53	5,324,205.00	--	
		Right	2,126,396.0	--					
15	WT - Cy3								
		Left	677,725.40	812,391.85	6.81E-01	3.40	5,454,522.44	-8.09%	
		Right	3,872,626.0	4,642,130.58					
	APC2 - Cy5								
		Left	2,759,017.0	--	--	-2.47	4,637,823.00	--	
		Right	1,878,806.0	--					
16	WT - Cy3								
		Left	205,669.60	246,536.88	3.66E-01	4.45	3,819,215.31	-41.03%	
		Right	2,980,452.0	3,572,678.43					
	APC2 - Cy5								
		Left	1,095,903.0	--	--	-7.13	1,597,054.90	--	
		Right	501,151.90	--					

Table 2: Identified proteins in *APC2* null 2D-DIGE gels.

Region	Gene	Protein name	Peptide # (1st run)	Peptide # (2nd run)	Molecular weight (kDa)	Calculated pI	Molecular Function	Biological processes
1	*CG2918*	N/A	12	16	106	5.1	Chaperone protein	N/A
2	*ade2*	Phosphoribsylformylglycinamidine synthase	23	16	148	6.6	Metabolic protein	Purine biosynthesis
3	*Irp-1B*	Iron binding protein 1 B	3	3	99	5.7	RNA-binding	Protein translation initiation
4	*Dp1*	Dodeca-satellite-binding protein 1	5	14	144	5.9	DNA-binding	Heterochromatin organization
5	*CG1516*	Pyruvate carboxylase	8	11	133	6.2	Metabolic protein	Cellular respiration
6	*CG14476*	N/A	5	--	106	6.1	Metabolic protein	Carbohydrate processing
7	GlyP	Phosphorylase	7	--	97	6.1	RNA-binding	Amino acid synthesis
8	*Aats-gly*	Glycyl-tRNA synthetase	4	9	76	6.0	Metabolic protein	Protein translation
	ND75	NADH-ubiquinone reductase	2	--	75	6.4	Metabolic protein	Cellular respiration
9	*ApepP*	Aminopeptidase P	4	9	63	5.6	Protease	Proteolysis
	CG8963	N/A	3	--	69	5.8	RNA-binding	N/A
10	*CaBP1*	Calcium binding protein 1	10	3	47	5.5	Signaling	Stress signaling
11	*mRpS30*	Mitochondrial ribosomal protein S30	4	9	65	8.5	RNA-binding	Protein translation
12	*Cbs*	Cystathionine beta-synthase	8	7	57	6.6	Metabolic protein	Amino acid synthesis
	CG8231	TCP-1zeta	6	6	58	6.2	N/A	Protein chaperone
13	*La*	La autoantigen-like	4	3	45	7.7	RNA-binding	RNA processing
	vig2	Vig2	2	--	45	9.4	DNA-binding	Heterochromatin organization

14	*blw*	Bellwether, ATP synthase subunit	13	7	59	9.1	Metabolic protein	Cellular respiration
	AdSL	Adenylosuccinate lyase	4	3	54	7.2	Metabolic protein	Purine biosynthesis
15	*Uch*	Ubiquitin carboxy-terminal hydrolase, isoform B	7	7	26	5.3	Protease	Protein deubiquitination
16	*CG1633*	Jafrac 1	13	4	22	5.5	Metabolic protein	Redox homeostasis
	CG2216	Ferritin 1 heavy chain homologue	5	1	23	5.6	Metabolic protein	Iron ion transport

Table 3A: Wild-type variability 2D-DIGE experiments.

Region	Protein ID	WT^{Mc} vs. WT^{D}	WT^{Mc} vs. WT^{P}
1	CG2918	-	-
2	Phosphoribosylformylglycinamidine synthase	-	+
3	Iron binding protein 1B	+	+
4	Dodeca-satellite-binding protein 1	-	-
5	Pyruvate carboxylase	+	+
6	CG14476	-	+
7	Glycogen phosphorylase	-	-
8	Glycyl-tRNA synthetase	+	+
9	Aminopeptidase P	-	-
10	Calcium binding protein 1	-	+
11	Mitochondrial ribosomal protein S30	-	-
12-1	Cystathionine beta-synthase	-	-
12-2	TCP-1zeta	-	-
13	La autoantigen-like protein	-	+
14	Bellwether, ATP synthase subunit	-	+
15	Ubiquitin carboxy-terminal hydrolase	-	+
16	Jafrac1	-	-

+ = difference-protein isoform present; - = difference-protein isoforms not present

Table 3B: *APC2* compensation 2D-DIGE experiments.

Region	Protein ID	***FL-GFP-APC2;*** ***APC^{g10}*** **vs. WT**	***FL-GFP-APC2;*** ***APC^{g10}*** **vs.** ***APC^{g10}***
1	CG2918	-	+
2	Phosphoribosylformylglycinamidine synthase	+	-
3	Iron binding protein 1B	+	-
4	Dodeca-satellite-binding protein 1	-	+
5	Pyruvate carboxylase	-	+
6	CG14476	+	+
7	Glycogen phosphorylase	-	-
8	Glycyl-tRNA synthetase	-	-
9	Aminopeptidase P	-	+
10	Calcium binding protein 1	-	+
11	Mitochondrial ribosomal protein S30	+	-
12-1	Cystathionine beta-synthase	-	-
12-2	TCP-1zeta	-	-
13	La autoantigen-like protein	-	+
14	Bellwether, ATP synthase subunit	+	-
15	Ubiquitin carboxy-terminal hydrolase	-	+
16	Jafrac1	+	-

+ = difference-protein isoform present; - = difference-protein isoforms not present

Table 3C: Various *APC* mutant 2D-DIGE experiments.

Region	Protein ID	*APC1*^{Q8} vs. WT	*APC2*^{g10}*APC1*^{Q8} vs. WT	*MTD>UAS-APC2 dsRNA vs.* WT
1	CG2918	+	+	-
2	Phosphoribosylformylglycinamidine synthase	-	+	+
3	Iron binding protein 1B	-	+	+
4	Dodeca-satellite-binding protein 1	+	-	+
5	Pyruvate carboxylase	+	+	+
6	CG14476	+	-	+
7	Glycogen phosphorylase	+	-	+
8	Glycyl-tRNA synthetase	+	-	+
9	Aminopeptidase P	+	+	+
10	Calcium binding protein 1	+	+	+
11	Mitochondrial ribosomal protein S30	-	+	+
12-1	Cystathionine beta-synthase	-	-	-
12-2	TCP-1zeta	-	-	-
13	La autoantigen-like protein	+	-	+
14	Bellwether, ATP synthase subunit	+	-	-
15	Ubiquitin carboxy-terminal hydrolase	+	+	+
16	Jafrac1	-	-	-

+ = difference-protein isoform present; - = difference-protein isoforms not present

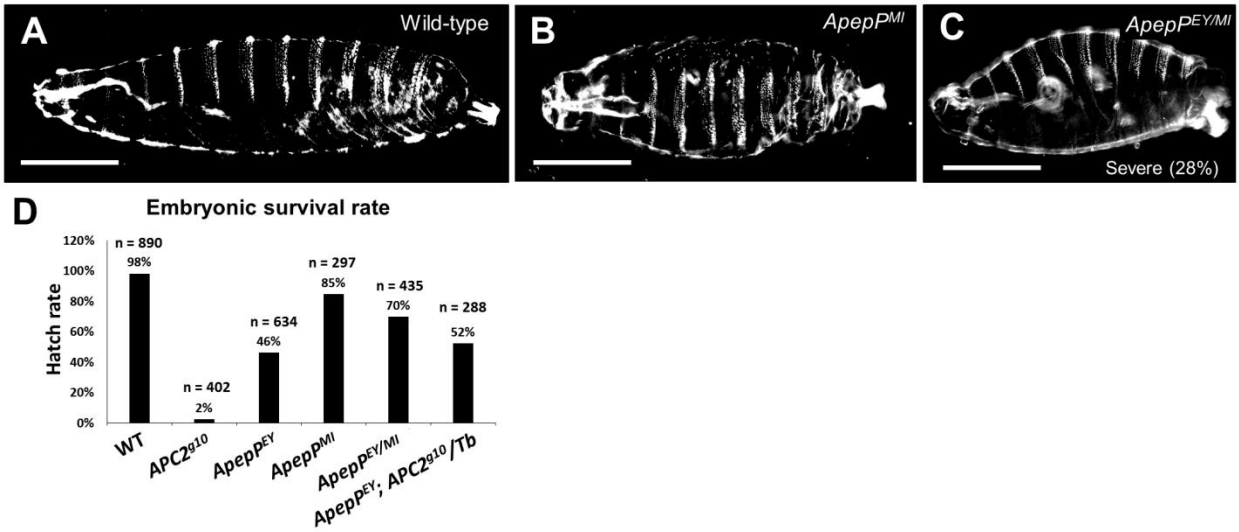

SFig. 1. *ApepP*^{MI} embryos and *ApepP*$^{EY/MI}$ embryos display Wnt activation phenotypes similar to *ApepP*^{EY} mutant embryos.

Cuticle analysis of: **(A)** Wild-type, **(B)** *ApepP*^{MI}, and **(C)** *ApepP*$^{EY/MI}$. **(D)** Embryonic survival rate for wild-type, *APC2*^{g10}, and various *ApepP* mutant embryos.

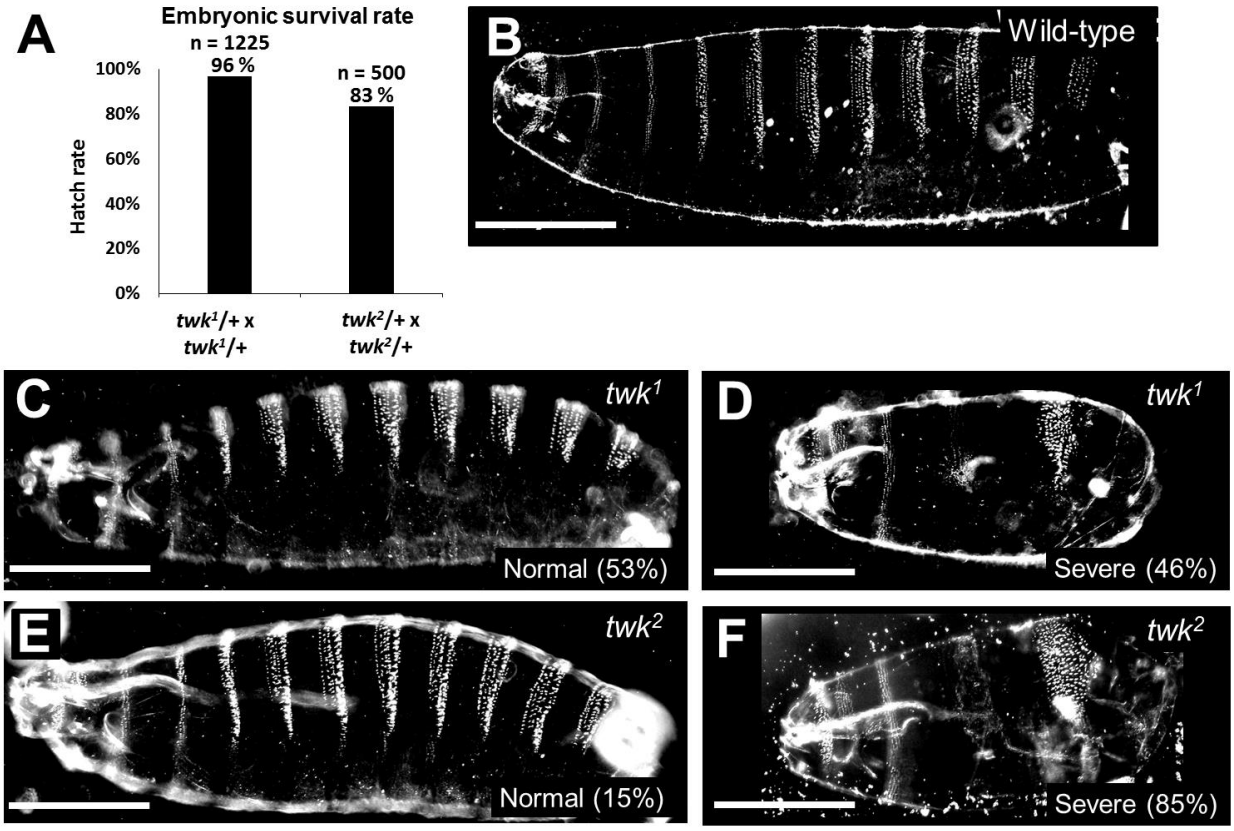

SFig 2. *twk*^{1} and *twk*^{2} embryos do not display Wnt activation phenotypes similar to *ApepP*^{EY} mutant embryos.

(A) Embryonic survival rate for embryos from *twk*^{1}/+ mothers crossed to *twk*^{1}/+ fathers. The same was performed on *twk*^{2} mutants. Cuticle analysis of: **(B)** A representative wild-type larva. Dead embryos, presumably *twk*/*twk*, have a range of embryonic phenotypes. For *twk*^{1}/*twk*^{1} dead embryos, half had normal cuticles **(C)**, while half exhibited a *nanos*-like cuticle phenotype **(D)**. The majority of *twk*^{2}/*tw2*^{1} dead embryos displayed the *nanos*-like phenotype **(F)**, while the remainder appeared normal **(E)**.

APPENDIX B: ADH-MICROBIOTA PROJECT SUPPLEMENT MATERIAL

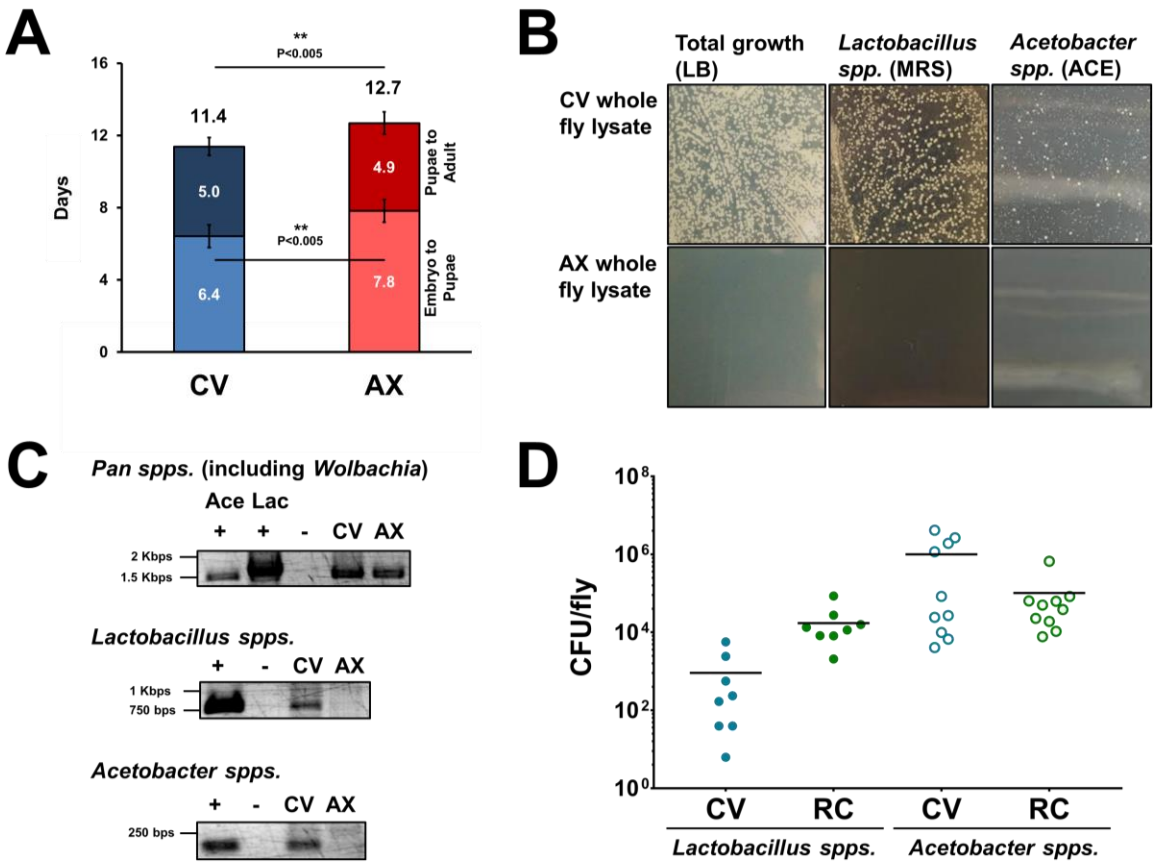

Supplement Figure 3.1. Verification of AX cultures.

(A) CV and AX culture were monitored for time to adulthood from embryos. Two phases of development were monitored, Embryo to pupae (bottom lighter color of bar) and pupae to adult (top darker color of bar). The n tested is 69 bottles and 59 bottles for CV and AX, respectively. Bars indicate standard error of the mean. Statistical significance was assigned by a Mann-Whitney test. **(B)** Cropped pictures from media plate of ten surface sterilized whole flies homogenates from CV and AX cultures. **(C)** PCR using pan-bacterial, *Lactobacillus*, and

Acetobacter specific primers on isolated CV and AX male homogenates. **(D)** The total number of bacterial colony-forming units (CFU) from whole fly CV and RC homogenates. Homogenates contained ten surfaced-sterilized 5-6 day old male flies. *Lactobacillus* species were counted on MRS plates, while *Acetobacter* species were counted on Ace plates. Error bars indicate SEM. A single dot represents a biological replicate, containing ten male flies. Missing dots indicates no bacterial growth observed for that biological replicate.

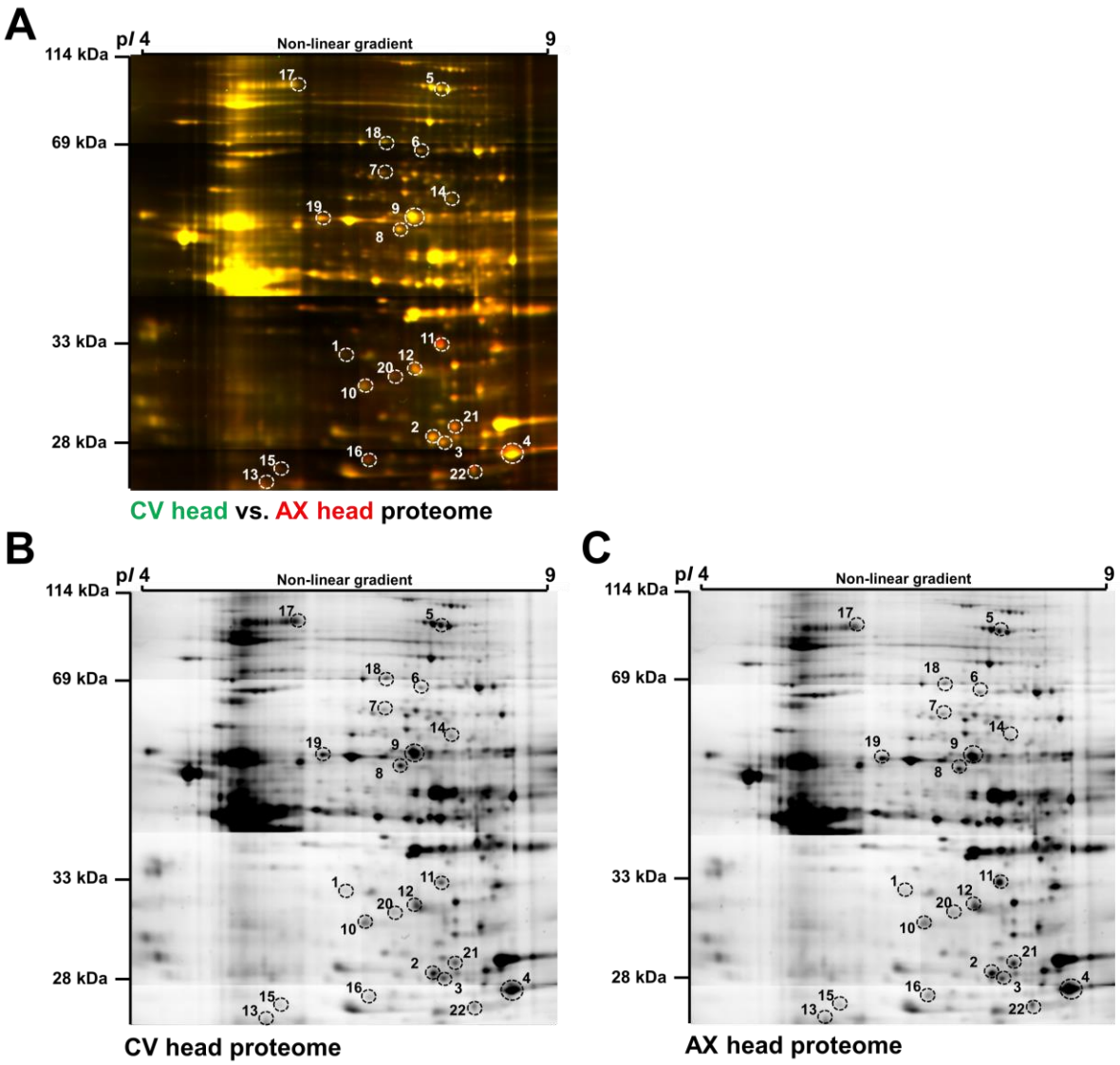

Supplement Figure 3.2. 2D-DIGE of CV versus AX *Drosophila* heads.

(A) A tiled array of a whole gel comparing CV heads (shown in green) and AX heads (shown in red). The 22 microbiota-dependent protein differences (between both male and females) are demarcated with white dotted circles. Contrasting and brightness was manipulated on the whole gel images using ImageJ. Full details of image analysis can be found in the supplementary materials. **(B)** Gray scale image of the CV head proteome with the same demarcation as in panel A. **(C)** Gray scale image of the AX head proteome with the same demarcation as in panel A.

SFIGURE 3

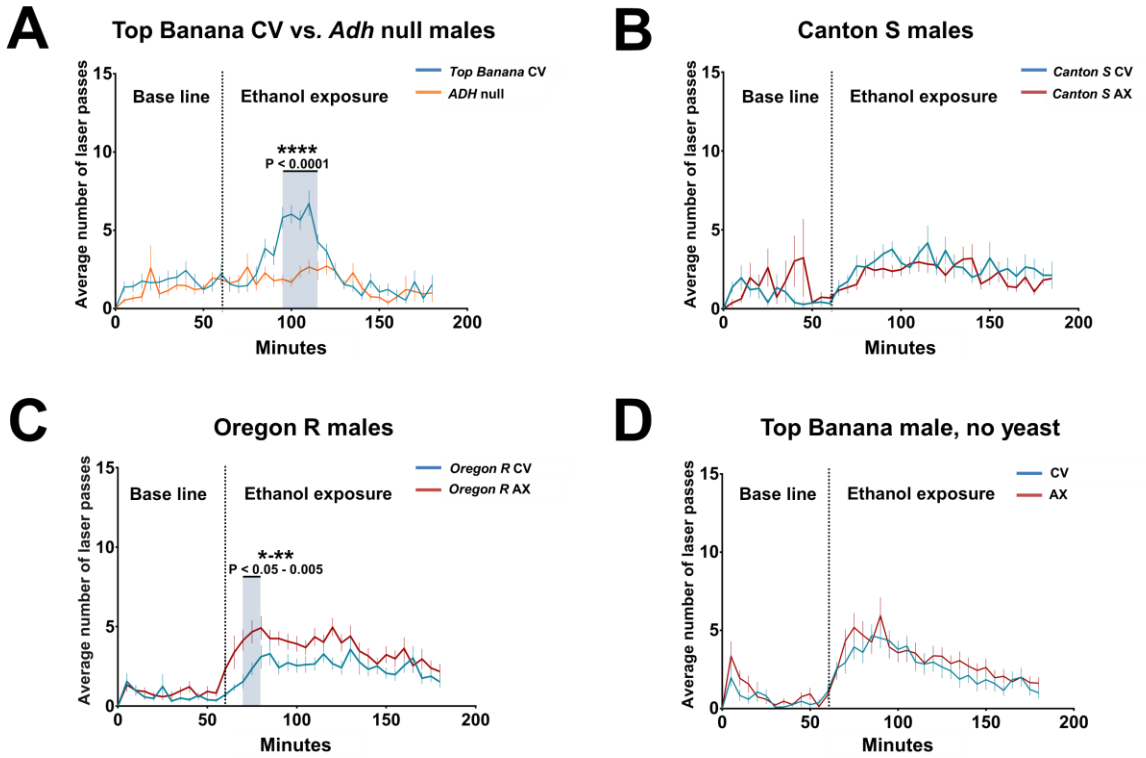

Supplement Figure 3.3. The microbiota-dependent hyperactivity is influence by high protein diet and host genetic background.

(A) *Top Banana* CV and ADH null male flies were assessed for alcohol induced hyperactivity. The n tested is 32 flies in 4 trials. Bars indicate standard error of the mean. Flow rate: H2O:EtOH (10:1). Statistical significance between CV and ADH null male flies (blue shaded region) was assigned by a Two-way ANOVA (Sidak's multiple comparisons post hoc test). **(B)** *Canton S* CV and AX male flies were assessed for alcohol induced hyperactivity. The n tested is 48 flies in 6 trials. Bars indicate standard error of the mean. Flow rate: H2O:EtOH (10:1). **(C)** *Oregon R* CV and ADH null male flies were assessed for alcohol induced hyperactivity. The n tested is 48 flies in 6 trials. Bars indicate standard error of the mean. Flow rate: H2O:EtOH (10:1). Statistical significance between *Oregon R* CV and AX male flies (blue shaded region) was assigned by a

Two-way ANOVA (Sidak's multiple comparisons post hoc test). **(D)** *Top Banana* CV and AX male flies were raised in the absence of autoclave yeast granules and assessed for alcohol induced hyperactivity. The n tested is 32 flies in 4 trials. Bars indicate standard error of the mean. Flow rate: H2O:EtOH (10:1).

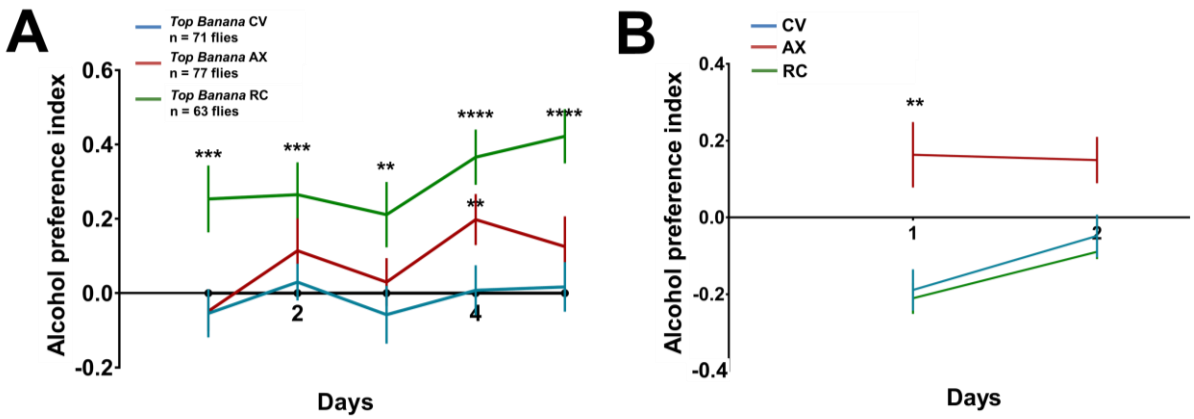

Supplement Figure 3.4. AX males have altered feeding consumption for alcohol

(A) Total daily consumption (ethanol and non-ethanol food) of CV, AX, and RC male flies in the CAFÉ assay in Fig. 4, A-C. **(B)** CV, AX, and RC male flies were assessed for daily alcohol positional preference for two days with 0% EtOH vs. 10% EtOH. This is the same data set used in Fig. 4, D-F. An alcohol preference index was calculated by taking the difference in flies on normal food from flies on ethanol laced food, normalized to the total number of flies on the stage. The n tested for CV, AX, and RC 50 flies for each condition. Bars indicate standard error of the mean. Statistical significance was assigned by a Two-way ANOVA (Turkey's multiple comparisons post hoc test). On day one, AX male flies were significantly different from CV and RC flies (**, P=0.0092 and P=0.0032, respectively). No significant difference was observed on day two.

BIBLIOGRAPHY

Ahmed, Yashi, Shigemi Hayashi, Arnold Levine, and Eric Wieschaus. 1998. "Regulation of Armadillo by a Drosophila APC Inhibits Neuronal Apoptotis during Retinal Development." *Cell* 93 (7): 1171–82. doi:10.1016/S0092-8674(00)81461-0.

Akong, Kathryn, Elizabeth E Grevengoed, Meredith H Price, Brooke M McCartney, Melissa A Hayden, Jan C DeNofrio, and Mark Peifer. 2002. "Drosophila APC2 and APC1 Play Overlapping Roles in Wingless Signaling in the Embryo and Imaginal Discs." *Developmental Biology* 250 (1): 91–100. doi:10.1006/dbio.2002.0776.

Al-Ruwaili, Jamal A, Samantha E T Larkin, Bashar A Zeidan, Matthew G Taylor, Chaker N Adra, Claire L Aukim-Hastie, and Paul A Townsend. 2010. "Discovery of Serum Protein Biomarkers for Prostate Cancer Progression by Proteomic Analysis." *Cancer Genomics & Proteomics* 7 (2): 93–103.

Altelaar, A. F. Maarten, Javier Munoz, and Albert J. R. Heck. 2012. "Next-Generation Proteomics: Towards an Integrative View of Proteome Dynamics." *Nature Reviews Genetics* 14 (1): 35–48. doi:10.1038/nrg3356.

Anderson, Leigh, and Jeff Seilhamer. 1997. "A Comparison of Selected mRNA and Protein Abundances in Human Liver." In *Electrophoresis*, 18:533–37. doi:10.1002/elps.1150180333.

Arentz, Georgia, Florian Weiland, Martin K. Oehler, and Peter Hoffmann. 2015. "State of the Art of 2D DIGE." *Proteomics - Clinical Applications*. doi:10.1002/prca.201400119.

Bantscheff, Marcus, Markus Schirle, Gavain Sweetman, Jens Rick, and Bernhard Kuster. 2007. "Quantitative Mass Spectrometry in Proteomics: A Critical Review." *Analytical and Bioanalytical Chemistry* 389 (4). Springer-Verlag: 1017–31. doi:10.1007/s00216-007-1486-6.

Barson, Jessica R, Irene Morganstern, and Sarah F Leibowitz. 2011. "Similarities in Hypothalamic and Mesocorticolimbic Circuits Regulating the Overconsumption of Food and Alcohol." *Physiology & Behavior* 104 (1). NIH Public Access: 128–37. doi:10.1016/j.physbeh.2011.04.054.

Barth, A I, K A Siemers, and W J Nelson. 2002. "Dissecting Interactions between EB1, Microtubules and APC in Cortical Clusters at the Plasma Membrane." *J Cell Sci* 115 (Pt 8): 1583–90. http://www.ncbi.nlm.nih.gov/pubmed/11950877.

Barua, D, and W S Hlavacek. 2013. "Modeling the Effect of APC Truncation on Destruction Complex Function in Colorectal Cancer Cells." *PLoS Comput Biol* 9 (9): e1003217. doi:10.1371/journal.pcbi.1003217.

Bejsovec, Amy. 2013. "Wingless/Wnt Signaling in Drosophila: The Pattern and the Pathway." *Molecular Reproduction and Development*. doi:10.1002/mrd.22228.

Belkowski, S M, D Polkovitch, and M R D'Andrea. 2005. "Synergistic Approaches to Clinical Oncology Biomarker Discovery." *Curr Top Med Chem* 5 (11): 1047–51.

http://www.ncbi.nlm.nih.gov/pubmed/16181130.

Ben-Tabou de-Leon, Smadar, and Eric H Davidson. 2007. "Gene Regulation: Gene Control Network in Development." *Annual Review of Biophysics and Biomolecular Structure* 36: 191. doi:10.1146/annurev.biophys.35.040405.102002.

Benson, Andrew K, Scott A Kelly, Ryan Legge, Fangrui Ma, Soo Jen Low, Jaehyoung Kim, Min Zhang, et al. 2010. "Individuality in Gut Microbiota Composition Is a Complex Polygenic Trait Shaped by Multiple Environmental and Host Genetic Factors." *Proceedings of the National Academy of Sciences of the United States of America* 107 (44). National Academy of Sciences: 18933–38. doi:10.1073/pnas.1007028107.

Bertin, E., and S. Arnouts. 1996. "SExtractor: Software for Source Extraction." *Astronomy and Astrophysics Supplement Series* 117 (2): 393–404. doi:10.1051/aas:1996164.

Bhatt, Anant Narayan, Rohit Mathur, Abdullah Farooque, Amit Verma, and B S Dwarakanath. 2010. "Cancer Biomarkers - Current Perspectives." *The Indian Journal of Medical Research* 132 (August): 129–49.

Bier, E, and A Guichard. 2012. "Deconstructing Host-Pathogen Interactions in Drosophila." *Dis Model Mech* 5 (1): 48–61. doi:10.1242/dmm.000406.

Blennow, Kaj. 2010. *Biomarkers in Alzheimer's Disease Drug Development. Nature Medicine*. Vol. 16. doi:10.1038/nm.2221.

Blennow, Kaj, Harald Hampel, Michael Weiner, and Henrik Zetterberg. 2010. "Cerebrospinal Fluid and Plasma Biomarkers in Alzheimer Disease." *Nature Reviews Neurology* 6 (3): 131–44. doi:10.1038/nrneurol.2010.4.

Blundon, Malachi A., Danielle R. Schlesinger, Amritha Parthasarathy, Samantha L. Smith, Hannah M. Kolev, David A. Vinson, Ezgi Kunttas-Tatli, Brooke M. McCartney, and Jonathan S. Minden. 2016. "Proteomic Analysis Reveals APC-Dependent Post Translational Modifications and Identifies a Novel Regulator of β-Catenin." *Development*, dev.130567. doi:10.1242/dev.130567.

Bonfini, Alessandro, Xi Liu, and Nicolas Buchon. 2016. "From Pathogens to Microbiota: How Drosophila Intestinal Stem Cells React to Gut Microbes." *Developmental and Comparative Immunology* 64: 22–38. doi:10.1016/j.dci.2016.02.008.

Bourassa, Megan W., Ishraq Alim, Scott J. Bultman, and Rajiv R. Ratan. 2016. "Butyrate, Neuroepigenetics and the Gut Microbiome: Can a High Fiber Diet Improve Brain Health?" *Neuroscience Letters*. doi:10.1016/j.neulet.2016.02.009.

Broderick, Nichole a. NA, Nicolas Buchon, and Bruno Lemaitre. 2014. "Microbiota-Induced Changes in Drosophila Melanogaster Host Gene Expression and Gut Morphology." *mBio* 5 (3): 1–13. doi:10.1128/mBio.01117-14.Editor.

Burrell, Rebecca A., Nicholas McGranahan, Jiri Bartek, and Charles Swanton. 2013. "The Causes and Consequences of Genetic Heterogeneity in Cancer Evolution." *Nature* 501 (7467): 338–45. doi:10.1038/nature12625.

Byrne, J C, M R Downes, N O'Donoghue, C O'Keane, A O'Neill, Y Fan, J M Fitzpatrick, M Dunn, and R W Watson. 2009. "2D-DIGE as a Strategy to Identify Serum Markers for the Progression of Prostate Cancer." *J Proteome Res* 8 (2): 942–57. doi:10.1021/pr800570s.

C., Kumsta, Thamsen M., and Jakob U. 2011. "Effects of Oxidative Stress on Behavior, Physiology, and the Redox Thiol Proteome of Caenorhabditis Elegans." *Antioxidants and Redox Signaling* 14 (6): 1023–37. doi:10.1089/ars.2010.3203.

Cadieu, N., J. C. Cadieu, L. El Ghadraoui, A. Grimal, and Y. Lambœuf. 1999. "Conditioning to Ethanol in the Fruit Fly - A Study Using an Inhibitor of ADH." *Journal of Insect Physiology* 45 (6): 579–86. doi:10.1016/S0022-1910(99)00041-4.

Cadigan, K M, and M Peifer. 2009. "Wnt Signaling from Development to Disease: Insights from Model Systems." *Cold Spring Harb Perspect Biol* 1 (2): a002881. doi:10.1101/cshperspect.a002881.

Canesso, M. C. C., N. L. Lacerda, C. M. Ferreira, J. L. Gonçalves, D. Almeida, C. Gamba, G. Cassali, et al. 2014. "Comparing the Effects of Acute Alcohol Consumption in Germ-Free and Conventional Mice: The Role of the Gut Microbiota." *BMC Microbiology* 14 (1): 240. doi:10.1186/s12866-014-0240-4.

Cederbaum, Arthur I. 2013. "Alcohol Metabolism." *Clin Liver Dis* 16 (4): 667–85. doi:10.1016/j.cld.2012.08.002.ALCOHOL.

Chafey, P, L Finzi, R Boisgard, M Cauzac, G Clary, C Broussard, J P Pegorier, et al. 2009. "Proteomic Analysis of Beta-Catenin Activation in Mouse Liver by DIGE Analysis Identifies Glucose Metabolism as a New Target of the Wnt Pathway." *Proteomics* 9 (15): 3889–3900. doi:10.1002/pmic.200800609.

Chakir, M, O Peridy, P Capy, E Pla, and J R David. 1993. "Adaptation to Alcoholic Fermentation in Drosophila: A Parallel Selection Imposed by Environmental Ethanol and Acetic Acid." *Proceedings of the National Academy of Sciences of the United States of America* 90 (8): 3621–25. doi:10.1073/pnas.90.8.3621.

Chaston, John M., Adam J. Dobson, Peter D. Newell, and Angela E. Douglas. 2016. "Host Genetic Control of the Microbiota Mediates the Drosophila Nutritional Phenotype." *Applied and Environmental Microbiology* 82 (2): 671–79. doi:10.1128/AEM.03301-15.

Chong, Poh Kuan, Huiyin Lee, Marie Chiew Shia Loh, Lee Yee Choong, Qingsong Lin, Jimmy Bok Yan So, Khong Hee Lim, et al. 2010. "Upregulation of Plasma C9 Protein in Gastric Cancer Patients." *Proteomics* 10 (18): 3210–21. doi:10.1002/pmic.201000127.

Chou, T B, and N Perrimon. 1996. "The Autosomal FLP-DFS Technique for Generating Germline Mosaics in Drosophila Melanogaster." *Genetics* 144 (4): 1673–79. http://www.ncbi.nlm.nih.gov/pubmed/8978054.

Clevers, Hans, and Roel Nusse. 2012. "Wnt/??-Catenin Signaling and Disease." *Cell*. doi:10.1016/j.cell.2012.05.012.

Crabbe, John C., Tamara J. Phillips, R. Adron Harris, Michael A. Arends, and George F. Koob.

2006. “Alcohol-Related Genes: Contributions from Studies with Genetically Engineered Mice.” *Addiction Biology*. doi:10.1111/j.1369-1600.2006.00038.x.

Davidson, Eric H. 2010. “Emerging Properties of Animal Gene Regulatory Networks.” *Nature* 468 (7326): 911–20. doi:10.1038/nature09645.

Deshpande, Sonali A, Gil B Carvalho, Ariadna Amador, Angela M Phillips, Sany Hoxha, Keith J Lizotte, and William W Ja. 2014. “Quantifying Drosophila Food Intake: Comparative Analysis of Current Methodology.” *Nat Methods* 11 (5): 535–40. doi:10.1038/nmeth.2899.

Devineni, Anita V., and Ulrike Heberlein. 2009. “Preferential Ethanol Consumption in Drosophila Models Features of Addiction.” *Current Biology* 19 (24). Elsevier Ltd: 2126–32. doi:10.1016/j.cub.2009.10.070.

Devineni, Anita V, and Ulrike Heberlein. 2013. “The Evolution of Drosophila Melanogaster as a Model for Alcohol Research.” *Annual Review of Neuroscience* 36: 121–38. doi:10.1146/annurev-neuro-062012-170256.

Diez, Roberto, Michael Herbstreith, Cristina Osorio, and Oscar Alzate. 2010. “2-D Fluorescence Difference Gel Electrophoresis (DIGE) in Neuroproteomics.” *Neuroproteomics*, no. 7: 1–14. http://www.ncbi.nlm.nih.gov/pubmed/21882449.

Dowsey, Andrew W., Jane A. English, Frederique Lisacek, Jeffrey S. Morris, Guang Zhong Yang, and Michael J. Dunn. 2010. “Image Analysis Tools and Emerging Algorithms for Expression Proteomics.” *Proteomics*. doi:10.1002/pmic.200900635.

Droujinine, Ilia A, and Norbert Perrimon. 2016. “Interorgan Communication Pathways in Physiology: Focus on Drosophila.” *Annual Review of Genetics* 50: 539–70. doi:10.1146/annurev-genet-121415-122024.

Early, Angela M., Niroshan Shanmugarajah, Nicolas Buchon, and Andrew G. Clark. 2017. “Drosophila Genotype Influences Commensal Bacterial Levels.” *Plos One* 12 (1): e0170332. doi:10.1371/journal.pone.0170332.

Eden, P a, T M Schmidt, R P Blakemore, and N R Pace. 1991. “Phylogenetic Analysis of Aquaspirillum Magnetotacticum Using Polymerase Chain Reaction-Amplified 16S rRNA-Specific DNA.” *International Journal of Systematic Bacteriology* 41 (2): 324–25. doi:10.1099/00207713-41-2-324.

Edenberg, Howard J. 2007. “The Genetics of Alcohol Metabolism: Role of Alcohol Dehydrogenase and Aldehyde Dehydrogenase Variants.” *Alcohol Research & Health : The Journal of the National Institute on Alcohol Abuse and Alcoholism* 30 (1): 5–13. doi:10.3168/jds.2010-3914.

Edwards, Ulrike, Till Rogall, Helmut Blöcker, Monica Emde, and Erik C. Böttger. 1989. “Isolation and Direct Complete Nucleotide Determination of Entire Genes. Characterization of a Gene Coding for 16S Ribosomal RNA.” *Nucleic Acids Research* 17 (19): 7843–53. doi:10.1093/nar/17.19.7843.

Elgart, M, S Stern, O Salton, Y Gnainsky, Y Heifetz, and Y Soen. 2016. “Impact of Gut

Microbiots on the Fly's Germ Line." *Nature Communications*.

Eloe-Fadrosh, E A, and D A Rasko. 2013. "The Human Microbiome: From Symbiosis to Pathogenesis." *Annu Rev Med* 64: 145–63. doi:10.1146/annurev-med-010312-133513.

Elson, C O, Y Cong, V J McCracken, R A Dimmitt, R G Lorenz, and C T Weaver. 2005. "Experimental Models of Inflammatory Bowel Disease Reveal Innate, Adaptive, and Regulatory Mechanisms of Host Dialogue with the Microbiota." *Immunol Rev* 206: 260–76. doi:10.1111/j.0105-2896.2005.00291.x.

Elya, Carolyn, Vivian Zhang, William B. Ludington, and Michael B. Eisen. 2016. "Stable Host Gene Expression in the Gut of Adult Drosophila Melanogaster with Different Bacterial Mono-Associations." *PLoS ONE* 11 (11). doi:10.1371/journal.pone.0167357.

Ericsson, Aaron C., J. Wade Davis, William Spollen, Nathan Bivens, Scott Givan, Catherine E. Hagan, Mark McIntosh, and Craig L. Franklin. 2015. "Effects of Vendor and Genetic Background on the Composition of the Fecal Microbiota of Inbred Mice." *PLoS ONE* 10 (2). doi:10.1371/journal.pone.0116704.

Erkosar, Berra, Gilles Storelli, Arnaud Defaye, and François Leulier. 2013. "Host-Intestinal Microbiota Mutualism: 'Learning on the Fly.'" *Cell Host & Microbe* 13 (1): 8–14. doi:10.1016/j.chom.2012.12.004.

Ersahin, C, A M Szpaderska, A T Orawski, and W H Simmons. 2005. "Aminopeptidase P Isozyme Expression in Human Tissues and Peripheral Blood Mononuclear Cell Fractions." *Arch Biochem Biophys* 435 (2): 303–10. doi:10.1016/j.abb.2004.12.023.

Ersahin, C, A M Szpaderska, and W H Simmons. 2003. "Rat and Mouse Membrane Aminopeptidase P: Structure Analysis and Tissue Distribution." *Arch Biochem Biophys* 417 (2): 131–40. http://www.ncbi.nlm.nih.gov/pubmed/12941294.

Esteller, Manel. 2011. "Non-Coding RNAs in Human Disease." *Nature Reviews Genetics* 12 (12): 861–74. doi:10.1038/nrg3074.

Filiou, Michaela D., Yaoyang Zhang, Larysa Teplytska, Stefan Reckow, Philipp Gormanns, Giuseppina MacCarrone, Elisabeth Frank, et al. 2011. "Proteomics and Metabolomics Analysis of a Trait Anxiety Mouse Model Reveals Divergent Mitochondrial Pathways." *Biological Psychiatry* 70 (11): 1074–82. doi:10.1016/j.biopsych.2011.06.009.

Fischer, Caleb, Eric P Trautman, Jason M Crawford, Eric V Stabb, Jo Handelsman, and Nichole A Broderick. 2017. "Metabolite Exchange between Microbiome Members Produces Compounds That Influence *Drosophila* Behavior." *eLife* 6: 1–25. doi:10.7554/eLife.18855.

Foster, Jane a., and Karen Anne McVey Neufeld. 2013. "Gut-Brain Axis: How the Microbiome Influences Anxiety and Depression." *Trends in Neurosciences* 36 (5). Elsevier Ltd: 305–12. doi:10.1016/j.tins.2013.01.005.

Frank, Richard, and Richard Hargreaves. 2003. "Clinical Biomarkers in Drug Discovery and Development." *Nature Reviews. Drug Discovery* 2 (7): 566–80. doi:10.1038/nrd1130.

Fransen, Floris, Adriaan A. van Beek, Theo Borghuis, Ben Meijer, Floor Hugenholtz, Christa van der Gaast-de Jongh, Huub F. Savelkoul, et al. 2017. "The Impact of Gut Microbiota on Gender-Specific Differences in Immunity." *Frontiers in Immunology* 8 (June): 754. doi:10.3389/fimmu.2017.00754.

Friedman, David B, and Kathryn S Lilley. 2008. "Optimizing the Difference Gel Electrophoresis (DIGE) Technology." *Methods in Molecular Biology (Clifton, N.J.)* 428: 93–124. doi:10.1007/978-1-59745-117-8_6.

Geer, B W, L K Dybas, and L J Shanner. 1989. "Alcohol Dehydrogenase and Ethanol Tolerance at the Cellular Level in *Drosophila Melanogaster*." *The Journal of Experimental Zoology* 250 (1): 22–39. doi:10.1002/jez.1402500105.

Geisler, Sarah, and Jeff Coller. 2013. "RNA in Unexpected Places: Long Non-Coding RNA Functions in Diverse Cellular Contexts." *Nature Reviews Molecular Cell Biology* 14 (11): 699–712. doi:10.1038/nrm3679.

Gemoll, Timo, Uwe Johannes Roblick, Gert Auer, Hans Jörnvall, and Jens Karsten Habermann. 2010. "SELDI-TOF Serum Proteomics and Colorectal Cancer: A Current Overview." *Archives of Physiology and Biochemistry* 116 (4–5): 188–96. doi:10.3109/13813455.2010.495130.

Giancotti, Filippo G. 2014. "Deregulation of Cell Signaling in Cancer." *FEBS Letters*. doi:10.1016/j.febslet.2014.02.005.

Gong, Lei, Mamta Puri, Mustafa Unlü, Margaret Young, Katherine Robertson, Surya Viswanathan, Arun Krishnaswamy, Susan R Dowd, and Jonathan S Minden. 2004. "Drosophila Ventral Furrow Morphogenesis: A Proteomic Analysis." *Development (Cambridge, England)* 131 (3): 643–56. doi:10.1242/dev.00955.

Gonzalez, A, J Stombaugh, C Lozupone, P J Turnbaugh, J I Gordon, and R Knight. 2011. "The Mind-Body-Microbial Continuum." *Dialogues Clin Neurosci* 13 (1): 55–62. http://www.ncbi.nlm.nih.gov/pubmed/21485746.

Görg, A, W Postel, and S Günther. 1988. "The Current State of Two-Dimensional Electrophoresis with Immobilized pH Gradients." *Electrophoresis* 9 (9): 531–46. doi:10.1002/elps.1150090913.

Gorky, Jonathan, and James Schwaber. 2016. "The Role of the Gut – Brain Axis in Alcohol Use Disorders." *Progress in Neuro-Psychopharmacology & Biological Psychiatry* 65: 234–41.

Greenbaum, Dov, Christopher Colangelo, Kenneth Williams, and Mark Gerstein. 2003. "Comparing Protein Abundance and mRNA Expression Levels on a Genomic Scale." *Genome Biology* 4 (9): 117. doi:10.1186/gb-2003-4-9-117.

Gygi, Steven P, Yvan Rochon, B Robert Franza, and Ruedi Aebersold. 1999. "Correlation between Protein and mRNA Abundance in Yeast Correlation between Protein and mRNA Abundance in Yeast." *Molecular and Cellular Biology* 19 (3): 1720–30. doi:10.1128/MCB.19.3.1720.

Hamdan, Mahmoud, and Pier Giorgio Righetti. 2005. *Proteomics Today: Protein Assessment and Biomarkers Using Mass Spectrometry, 2D Electrophoresis, and Microarray Technology*. *Proteomics Today: Protein Assessment and Biomarkers Using Mass Spectrometry, 2D Electrophoresis, and Microarray Technology*. doi:10.1002/0471709158.

Han, Gangsik, Hyo Jung Lee, Sang Eun Jeong, Che Ok Jeon, and Seogang Hyun. 2017. "Comparative Analysis of Drosophila Melanogaster Gut Microbiota with Respect to Host Strain, Sex, and Age." *Microbial Ecology*. Microbial Ecology. doi:10.1007/s00248-016-0925-3.

Haro, Carmen, Oriol A Rangel-zú, Juan F Alcalá-díaz, Francisco Gómez-Delgado, Pablo Pérez-Martínez, Javier Delgado-Lista, Gracia M Quintana-Navarro, et al. 2016. "Intestinal Microbiota Is Influenced by Gender and Body Mass Index." *PLoS ONE*, no. May: 1–16. doi:10.5061/dryad.j0q5m.Funding.

Hawkins, R. David, Gary C. Hon, and Bing Ren. 2011. "Next-Generation Genomics: An Integrative Approach." *Nature Reviews Genetics*. doi:10.1038/nrg2795.

He, Qing-Yu, George K K Lau, Yuan Zhou, Siu-Tsan Yuen, Marie C Lin, Hsiang-Fu Kung, and Jen-Fu Chiu. 2003. "Serum Biomarkers of Hepatitis B Virus Infected Liver Inflammation: A Proteomic Study." *PROTEOMICS* 3 (5): 666–74. doi:10.1002/pmic.200300394.

Heath, A C, P A F Madden, K K Bucholz, S H Dinwiddie, W S Slutske, L J Bierut, J W Rohrbaugh, et al. 1999. "Genetic Differences in Alcohol Sensitivity and the Inheritance of Alcoholism Risk." *Psychological Medicine* 29: 1069–81. doi:10.1017/S0033291799008909.

Hernandez-Valladares, Maria, Marc Vaudel, Frode Selheim, Frode Berven, and Øystein Bruserud. 2017. "Proteogenomics Approaches for Studying Cancer Biology and Their Potential in the Identification of Acute Myeloid Leukemia Biomarkers." *Expert Review of Proteomics* 14 (8): 649–63. doi:10.1080/14789450.2017.1352474.

Hettich, Robert L., Chongle Pan, Karuna Chourey, and Richard J. Giannone. 2013. "Metaproteomics: Harnessing the Power of High Performance Mass Spectrometry to Identify the Suite of Proteins That Control Metabolic Activities in Microbial Communities." *Analytical Chemistry* 85 (9): 4203–14. doi:10.1021/ac303053e.

Holland, Jane D., Alexandra Klaus, Alistair N. Garratt, and Walter Birchmeier. 2013. "Wnt Signaling in Stem and Cancer Stem Cells." *Current Opinion in Cell Biology*. doi:10.1016/j.ceb.2013.01.004.

Ja, William W, Gil B Carvalho, Elizabeth M Mak, Noelle N de la Rosa, Annie Y Fang, Jonathan C Liong, Ted Brummel, and Seymour Benzer. 2007. "Prandiology of Drosophila and the CAFE Assay." *Proc Natl Acad Sci U S A* 104 (20): 8253–56. doi:0702726104 [pii]\r10.1073/pnas.0702726104.

Jaiswal, R, V Stepanik, A Rankova, O Molinar, B L Goode, and B M McCartney. 2013. "Drosophila Homologues of Adenomatous Polyposis Coli (APC) and the Formin Diaphanous Collaborate by a Conserved Mechanism to Stimulate Actin Filament Assembly." *J Biol Chem* 288 (19): 13897–905. doi:10.1074/jbc.M113.462051.

Jaiswal, Richa, Vince Stepanik, Aneliya Rankova, Olivia Molinar, Bruce L. Goode, and Brooke M. McCartney. 2013. "Drosophila Homologues of Adenomatous Polyposis Coli (APC) and the Formin Diaphanous Collaborate by a Conserved Mechanism to Stimulate Actin Filament Assembly." *Journal of Biological Chemistry* 288 (22): 2385. doi:10.1074/jbc.M113.462051.

Jörnvall, H, T Fairwell, P Kratofil, and C Wills. 1980. "Differences in Alpha-Amino Acetylation of Isozymes of Yeast Alcohol Dehydrogenase." *FEBS Letters* 111 (1): 214–18. http://www.ncbi.nlm.nih.gov/pubmed/6987085.

Jörnvall, Hans, Louis G. Lange, James F. Riordan, and Bert L. Vallee. 1977. "Identification of a Reactive Arginyl Residue in Horse Liver Alcohol Dehydrogenase." *Biochemical and Biophysical Research Communications* 77 (1): 73–78. doi:10.1016/S0006-291X(77)80166-6.

Kanazawa, Hidetoshi, Masato Nagino, Satoshi Kamiya, Shunichiro Komatsu, Toshihiko Mayumi, Kenji Takagi, Takashi Asahara, Koji Nomoto, Ryuichiro Tanaka, and Yuji Nimura. 2005. "Synbiotics Reduce Postoperative Infectious Complications: A Randomized Controlled Trial in Biliary Cancer Patients Undergoing Hepatectomy." *Langenbeck's Archives of Surgery* 390 (2): 104–13. doi:10.1007/s00423-004-0536-1.

Kaun, Karla R., Anita V. Devineni, and Ulrike Heberlein. 2012. "Drosophila Melanogaster as a Model to Study Drug Addiction." *Human Genetics* 131 (6): 959–75. doi:10.1007/s00439-012-1146-6.

Kaun, Karla R, Reza Azanchi, Zaw Maung, Jay Hirsh, and Ulrike Heberlein. 2011. "A Drosophila Model for Alcohol Reward." *Nature Neuroscience* 14 (5). Nature Publishing Group: 612–19. doi:10.1038/nn.2805.

Kawasaki, Y, R Sato, and T Akiyama. 2003. "Mutated APC and Asef Are Involved in the Migration of Colorectal Tumour Cells." *Nat Cell Biol* 5 (3): 211–15. http://www.ncbi.nlm.nih.gov/entrez/query.fcgi?cmd=Retrieve&db=PubMed&dopt=Citation&list_uids=12598901.

Kawasaki, Y, T Senda, T Ishidate, R Koyama, T Morishita, Y Iwayama, O Higuchi, and T Akiyama. 2000. "Asef, a Link between the Tumor Suppressor APC and G-Protein Signaling." *Science (New York, N.Y.)* 289 (5482): 1194–97. http://www.ncbi.nlm.nih.gov/pubmed/10947987.

Kawasaki, Y, S Tsuji, K Muroya, S Furukawa, Y Shibata, M Okuno, S Ohwada, and T Akiyama. 2009. "The Adenomatous Polyposis Coli-Associated Exchange Factors Asef and Asef2 Are Required for Adenoma Formation in Apc(Min/+)mice." *EMBO Rep* 10 (12): 1355–62. http://www.ncbi.nlm.nih.gov/entrez/query.fcgi?cmd=Retrieve&db=PubMed&dopt=Citation&list_uids=19893577.

Khoury, G A, R C Baliban, and C A Floudas. 2011. "Proteome-Wide Post-Translational Modification Statistics: Frequency Analysis and Curation of the Swiss-Prot Database." *Sci Rep* 1. doi:10.1038/srep00090.

Kiernan, Urban A., Dobrin Nedelkov, and Randall W. Nelson. 2006. "Multiplexed Mass Spectrometric Immunoassay in Biomarker Research: A Novel Approach to the Determination of a Myocardial Infarct." *Journal of Proteome Research* 5 (11): 2928–34. doi:10.1021/pr060062+.

Kim, K S, S Kumar, W H Simmons, and N J Brown. 2000. "Inhibition of Aminopeptidase P Potentiates Wheal Response to Bradykinin in Angiotensin-Converting Enzyme Inhibitor-Treated Humans." *J Pharmacol Exp Ther* 292 (1): 295–98. http://www.ncbi.nlm.nih.gov/pubmed/10604961.

King, Ian F G, Mark Eddison, Karla R. Kaun, and Ulrike Heberlein. 2014. "EGFR and FGFR Pathways Have Distinct Roles in Drosophila Mushroom Body Development and Ethanol-Induced Behavior." *PLoS ONE* 9 (1): 1–9. doi:10.1371/journal.pone.0087714.

King, I, L T Tsai, R Pflanz, A Voigt, S Lee, H Jackle, B Lu, and U Heberlein. 2011. "Drosophila Tao Controls Mushroom Body Development and Ethanol-Stimulated Behavior through Par-1." *J Neurosci* 31 (3): 1139–48. doi:10.1523/JNEUROSCI.4416-10.2011.

Klose, J. 1975. "Protein Mapping by Combined Isoelectric Focusing and Electrophoresis of Mouse Tissues. A Novel Approach to Testing for Induced Point Mutations in Mammals." *Humangenetik* 26 (3): 231–43. doi:10.1007/BF00281458.

Kolmeder, Carolin A., and Willem M. de Vos. 2014. "Metaproteomics of Our Microbiome - Developing Insight in Function and Activity in Man and Model Systems." *Journal of Proteomics*. doi:10.1016/j.jprot.2013.05.018.

Kolmeder, Carolin A., Jarmo Ritari, Froukje J. Verdam, Thilo Muth, Salla Keskitalo, Markku Varjosalo, Susana Fuentes, et al. 2015. "Colonic Metaproteomic Signatures of Active Bacteria and the Host in Obesity." *PROTEOMICS* 15 (20): 3544–52. doi:10.1002/pmic.201500049.

Kondo, Tadashi, Masahiro Seike, Yasuharu Mori, Kazuyasu Fujii, Tesshi Yamada, and Setsuo Hirohashi. 2003. "Application of Sensitive Fluorescent Dyes in Linkage of Laser Microdissection and Two-Dimensional Gel Electrophoresis as a Cancer Proteomic Study Tool." In *Proteomics*, 3:1758–66. doi:10.1002/pmic.200300531.

Koob, George F, and Nora D Volkow. 2010. "Neurocircuitry of Addiction." *Neuropsychopharmacology : Official Publication of the American College of Neuropsychopharmacology* 35 (1). Nature Publishing Group: 217–38. doi:10.1038/npp.2009.110.

Koyle, Melinda L., Madeline Veloz, Alec M. Judd, Adam C.-N. Wong, Peter D. Newell, Angela E. Douglas, and John M. Chaston. 2016. "Rearing the Fruit Fly Drosophila Melanogaster Under Axenic and Gnotobiotic Conditions." *Journal of Visualized Experiments*, no. 113: 1–8. doi:10.3791/54219.

Kozinski, K, and A Dobrzyn. 2013. "[Wnt Signaling Pathway--Its Role in Regulation of Cell Metabolism]." *Postepy Hig Med Dosw (Online)* 67: 1098–1108. http://www.ncbi.nlm.nih.gov/pubmed/24379251.

Kulkarni, G V, and D D Deobagkar. 2002. “A Cytosolic Form of Aminopeptidase P from Drosophila Melanogaster: Molecular Cloning and Characterization.” *J Biochem* 131 (3): 445–52. http://www.ncbi.nlm.nih.gov/pubmed/11872174.

Kunttas-Tatli, E., R. A. Von Kleeck, B. D. Greaves, D. Vinson, D. M. Roberts, and B. M. McCartney. 2015. “The Two SAMP Repeats and Their Phosphorylation State in Drosophila Adenomatous Polyposis Coli-2 Play Mechanistically Distinct Roles to Negatively Regulate Wnt Signaling.” *Molecular Biology of the Cell* 26 (1): 1–5. doi:10.1091/mbc.E15-07-0515.

Kunttas-Tatli, Ezgi, David M Roberts, and Brooke M McCartney. 2014. “Self-Association of the APC Tumor Suppressor Is Required for the Assembly, Stability, and Activity of the Wnt Signaling Destruction Complex.” *Molecular Biology of the Cell* 25 (21): 3424–36. doi:10.1091/mbc.E14-04-0885.

Kunttas-Tatli, Ezgi, Meng Ning Zhou, Sandra Zimmerman, Olivia Molinar, Fangyuan Zhouzheng, Krista Carter, Megha Kapur, Alys Cheatle, Richard Decal, and Brooke M. McCartney. 2012. “Destruction Complex Function in the Wnt Signaling Pathway of Drosophila Requires Multiple Interactions between Adenomatous Polyposis Coli 2 and Armadillo.” *Genetics* 190 (3): 1059–75. doi:10.1534/genetics.111.133280.

Lange III, L G, J F Riordan, B L Vallee, and C I Branden. 1975. “The Role of Arginyl Residues in Directing Carboxymethylation of Horse Liver Alcohol Dehydrogenase.” *Biochemistry* 14 (15): 3497–3502.

Leclercq, S, S Matamoros, P D Cani, A M Neyrinck, F Jamar, P Starkel, K Windey, et al. 2014. “Intestinal Permeability, Gut-Bacterial Dysbiosis, and Behavioral Markers of Alcohol-Dependence Severity.” *Proc Natl Acad Sci U S A* 111 (42): E4485-93. doi:10.1073/pnas.1415174111.

Lee, W J, and P T Brey. 2013. “How Microbiomes Influence Metazoan Development: Insights from History and Drosophila Modeling of Gut-Microbe Interactions.” *Annu Rev Cell Dev Biol* 29: 571–92. doi:10.1146/annurev-cellbio-101512-122333.

Leulier, Fran??ois. 2014. “Drosophila Microbiota Modulates Host Metabolic Gene Expression via IMD/NF-??B Signaling.” *PloS One* 9 (4): e94729. doi:10.1371/journal.pone.0094729.

Lévy, Laurence, Yu Wei, Charlotte Labalette, Yuanfei Wu, Claire-Angélique Renard, Marie Annick Buendia, and Christine Neuveut. 2004. “Acetylation of β-Catenin by p300 Regulates β-Catenin-Tcf4 Interaction.” *Molecular and Cellular Biology* 24 (8): 3404–14. doi:10.1128/MCB.24.8.3404.

Lilley, K S, and D B Friedman. 2004. “All about DIGE: Quantification Technology for Differential-Display 2D-Gel Proteomics.” *Expert Rev Proteomics* 1 (4): 401–9. doi:10.1586/14789450.1.4.401.

Lippolis, Rosa, and Maria De Angelis. 2016. “Proteomics and Human Diseases.” *Journal of Proteomics & Bioinformatics* 9 (3): 63–74. doi:10.4172/jpb.1000391.

Litten, Raye Z., Megan L. Ryan, Daniel E. Falk, Matthew Reilly, Joanne B. Fertig, and George

F. Koob. 2015. “Heterogeneity of Alcohol Use Disorder: Understanding Mechanisms to Advance Personalized Treatment.” *Alcoholism: Clinical and Experimental Research* 39 (4): 579–84. doi:10.1111/acer.12669.

Liu, Qiang, and Li Hua Jin. 2017. “Organ-to-Organ Communication: A Drosophila Gastrointestinal Tract Perspective.” *Frontiers in Cell and Developmental Biology* 5 (April): 29. doi:10.3389/fcell.2017.00029.

Liu, Xiaojun, Qiping Feng, Yong Chen, Jin Zuo, Nishith Gupta, Yongsheng Chang, and Fude Fang. 2009. “Proteomics-Based Identification of Differentially-Expressed Proteins Including Galectin-1 in the Blood Plasma of Type 2 Diabetic Patients.” *Journal of Proteome Research* 8 (3): 1255–62. doi:10.1021/pr800850a.

Lize, A, R McKay, and Z Lewis. 2014. “Kin Recognition in Drosophila: The Importance of Ecology and Gut Microbiota.” *ISME J* 8 (2): 469–77. doi:10.1038/ismej.2013.157.

Logan, Catriona Y, and Roel Nusse. 2004. “THE WNT SIGNALING PATHWAY IN DEVELOPMENT AND DISEASE.” *Annu. Rev. Cell Dev. Biol* 20: 781–810. doi:10.1146/annurev.cellbio.20.010403.113126.

MacFabe, Derrick F. 2015. “Enteric Short-Chain Fatty Acids: Microbial Messengers of Metabolism, Mitochondria, and Mind: Implications in Autism Spectrum Disorders.” *Microbial Ecology in Health and Disease* 26: 28177. doi:10.3402/mehd.v26.28177.

Macfabe MD, Derrick F. 2012. “Short-Chain Fatty Acid Fermentation Products of the Gut Microbiome: Implications in Autism Spectrum Disorders.” *Microbial Ecology in Health and Disease* 23: 1–24.

Maier, Tobias, Marc Güell, and Luis Serrano. 2009. “Correlation of mRNA and Protein in Complex Biological Samples.” *FEBS Letters*. doi:10.1016/j.febslet.2009.10.036.

Maples, Thomas, and Adrian Rothenfluh. 2011. “A Simple Way to Measure Ethanol Sensitivity in Flies.” *Journal of Visualized Experiments : JoVE*, no. 48: 48–50. doi:10.3791/2541.

Marchesi, Julian R, David H Adams, Francesca Fava, Gerben D a Hermes, Gideon M Hirschfield, Georgina Hold, Mohammed Nabil Quraishi, et al. 2015. “The Gut Microbiota and Host Health: A New Clinical Frontier.” *Gut* , 1–10. doi:10.1136/gutjnl-2015-309990.

Marouga, R, S David, and E Hawkins. 2005. “The Development of the DIGE System: 2D Fluorescence Difference Gel Analysis Technology.” *Anal Bioanal Chem* 382 (3): 669–78. doi:10.1007/s00216-005-3126-3.

Martinez, Kristina B., Vanessa Leone, and Eugene B. Chang. 2017. “Microbial Metabolites in Health and Disease: Navigating the Unknown in Search of Function.” *Journal of Biological Chemistry* 292 (21): 8553–59. doi:10.1074/jbc.R116.752899.

Martyniuk, Christopher J., Sophie Alvarez, and Nancy D. Denslow. 2012. “DIGE and iTRAQ as Biomarker Discovery Tools in Aquatic Toxicology.” *Ecotoxicology and Environmental Safety* 76 (1): 3–10. doi:10.1016/j.ecoenv.2011.09.020.

Mayers, Michael D., Clara Moon, Gregory S. Stupp, Andrew I. Su, and Dennis W. Wolan. 2017. "Quantitative Metaproteomics and Activity-Based Probe Enrichment Reveals Significant Alterations in Protein Expression from a Mouse Model of Inflammatory Bowel Disease." *Journal of Proteome Research* 16 (2): 1014–26. doi:10.1021/acs.jproteome.6b00938.

McCartney, B M, H A Dierick, C Kirkpatrick, M M Moline, A Baas, M Peifer, and A Bejsovec. 1999. "Drosophila APC2 Is a Cytoskeletally-Associated Protein That Regulates Wingless Signaling in the Embryonic Epidermis." *J Cell Biol* 146 (6): 1303–18. http://www.ncbi.nlm.nih.gov/entrez/query.fcgi?cmd=Retrieve&db=PubMed&dopt=Citation&list_uids=10491393.

McCartney, B M, D G McEwen, E Grevengoed, P Maddox, a Bejsovec, and M Peifer. 2001. "Drosophila APC2 and Armadillo Participate in Tethering Mitotic Spindles to Cortical Actin." *Nature Cell Biology* 3 (10): 933–38. doi:10.1038/ncb1001-933.

McCartney, Brooke M., and Inke S. Näthke. 2008. "Cell Regulation by the Apc Protein. Apc as Master Regulator of Epithelia." *Current Opinion in Cell Biology* 20 (2): 186–93. doi:10.1016/j.ceb.2008.02.001.

McCartney, Brooke M, Meredith H Price, Rebecca L Webb, Melissa a Hayden, Lesley M Holot, Mengning Zhou, Amy Bejsovec, and Mark Peifer. 2006. "Testing Hypotheses for the Functions of APC Family Proteins Using Null and Truncation Alleles in Drosophila." *Development (Cambridge, England)* 133 (12): 2407–18. doi:10.1242/dev.02398.

McClellan, Jon, and Mary-Claire King. 2010. "Genetic Heterogeneity in Human Disease." *Cell* 141 (2): 210–17. doi:10.1016/j.cell.2010.03.032.

McGettigan, Paul A. 2013. "Transcriptomics in the RNA-Seq Era." *Current Opinion in Chemical Biology*. doi:10.1016/j.cbpa.2012.12.008.

Medeiros, M S, and A J Turner. 1994. "Post-Secretory Processing of Regulatory Peptides: The Pancreatic Polypeptide Family as a Model Example." *Biochimie* 76 (3–4): 283–87. http://www.ncbi.nlm.nih.gov/pubmed/7819336.

Mercer, Tim R., Marcel E. Dinger, and John S. Mattick. 2009. "Long Non-Coding RNAs: Insights into Functions." *Nature Reviews Genetics* 10 (3): 155–59. doi:10.1038/nrg2521.

Mertins, Philipp, D. R. Mani, Kelly V. Ruggles, Michael A. Gillette, Karl R. Clauser, Pei Wang, Xianlong Wang, et al. 2016. "Proteogenomics Connects Somatic Mutations to Signalling in Breast Cancer." *Nature* 534 (7605): 55–62. doi:10.1038/nature18003.

Mesri, Mehdi, and Mehdi. 2014. "Advances in Proteomic Technologies and Its Contribution to the Field of Cancer." *Advances in Medicine* 2014: 1–25. doi:10.1155/2014/238045.

Meyer, C, E Kowarz, J Hofmann, A Renneville, J Zuna, J Trka, R Ben Abdelali, et al. 2009. "New Insights to the MLL Recombinome of Acute Leukemias." *Leukemia* 23 (8): 1490–99. doi:10.1038/leu.2009.33.

Miller, M. J., P. K. Vo, C. Nielsen, E. P. Geiduschek, and N. H. Xuong. 1982. "Computer Analysis of Two-Dimensional Gels: Semi-Automatic Matching." *Clinical Chemistry* 28 (4

II): 867–75.

Minami, Sho, Yuichi Sato, Toshihide Matsumoto, Taihei Kageyama, Yusuke Kawashima, Kodera Yoshio, Jun Ichiro Ishii, Kazumasa Matsumoto, Ryo Nagashio, and Isao Okayasu. 2010. "Proteomic Study of Sera from Patients with Bladder Cancer: Usefulness of S100A8 and S100A9 Proteins." *Cancer Genomics and Proteomics* 7 (4): 181–90. doi:7/4/181 [pii].

Minden, J S. 2012. "Two-Dimensional Difference Gel Electrophoresis." *Methods Mol Biol* 869: 287–304. doi:10.1007/978-1-61779-821-4_24.

Moradian, Annie, Anastasia Kalli, Michael J. Sweredoski, and Sonja Hess. 2014. "The Top-Down, Middle-Down, and Bottom-up Mass Spectrometry Approaches for Characterization of Histone Variants and Their Post-Translational Modifications." *Proteomics*. doi:10.1002/pmic.201300256.

Morozova, T V, W Huang, V A Pray, T Whitham, R R Anholt, and T F Mackay. 2015. "Polymorphisms in Early Neurodevelopmental Genes Affect Natural Variation in Alcohol Sensitivity in Adult Drosophila." *BMC Genomics* 16 (1): 865. doi:10.1186/s12864-015-2064-5.

Munoz Descalzo, S, P Rue, J Garcia-Ojalvo, and A Martinez Arias. 2012. "Correlations between the Levels of Oct4 and Nanog as a Signature for Naive Pluripotency in Mouse Embryonic Stem Cells." *Stem Cells* 30 (12): 2683–91. doi:10.1002/stem.1230.

Mutlu, Ece a, Patrick M Gillevet, Huzefa Rangwala, Masoumeh Sikaroodi, Ammar Naqvi, Phillip a Engen, Mary Kwasny, Cynthia K Lau, and Ali Keshavarzian. 2012. "Colonic Microbiome Is Altered in Alcoholism." *American Journal of Physiology. Gastrointestinal and Liver Physiology* 302 (9): G966-78. doi:10.1152/ajpgi.00380.2011.

N., Visa, Fibla J., and Santa-Cruz M.C. 1992. "Developmental Profile and Tissue Distribution of Drosophila Alcohol Dehydrogenase: An Immunochemical Analysis with Monoclonal Antibodies." *Journal of Histochemistry and Cytochemistry* 40 (1): 39–49. http://ovidsp.ovid.com/ovidweb.cgi?T=JS&PAGE=reference&D=emed2&NEWS=N&AN=1992021195.

Nakagawa, H, K Koyama, Y Murata, M Morito, T Akiyama, and Y Nakamura. 2000. "EB3, a Novel Member of the EB1 Family Preferentially Expressed in the Central Nervous System, Binds to a CNS-Specific APC Homologue." *Oncogene* 19 (2): 210–16. doi:10.1038/sj.onc.1203308.

Nathke, I. 2006. "Cytoskeleton out of the Cupboard: Colon Cancer and Cytoskeletal Changes Induced by Loss of APC." *Nat Rev Cancer* 6 (12): 967–74. doi:10.1038/nrc2010.

Nathke, I S. 2004. "The Adenomatous Polyposis Coli Protein: The Achilles Heel of the Gut Epithelium." *Annu Rev Cell Dev Biol* 20: 337–66. doi:10.1146/annurev.cellbio.20.012103.094541.

Newell, Peter D., and Angela E. Douglas. 2014. "Interspecies Interactions Determine the Impact of the Gut Microbiota on Nutrient Allocation in Drosophila Melanogaster." *Applied and*

Environmental Microbiology 80 (2): 788–96. doi:10.1128/AEM.02742-13.

Nieuwenhuis, M H, and H F Vasen. 2007. "Correlations between Mutation Site in APC and Phenotype of Familial Adenomatous Polyposis (FAP): A Review of the Literature." *Crit Rev Oncol Hematol* 61 (2): 153–61. doi:10.1016/j.critrevonc.2006.07.004.

O'Farrell, P H. 1975. "High Resolution Two-Dimensional Electrophoresis of Proteins." *The Journal of Biological Chemistry* 250 (10): 4007–21. doi:10.1016/j.bbi.2008.05.010.

Ogueta, Maite, Osman Cibik, Rouven Eltrop, Andrea Schneider, and Henrike Scholz. 2010. "The Influence of Adh Function on Ethanol Preference and Tolerance in Adult Dsrosophila Melanogaster." *Chemical Senses* 35 (9): 813–22. doi:10.1093/chemse/bjq084.

Okada, Ryo, Kaz Nagaosa, Takayuki Kuraishi, Hiroshi Nakayama, Naoko Yamamoto, Yukiko Nakagawa, Naoshi Dohmae, Akiko Shiratsuchi, and Yoshinobu Nakanishi. 2012. "Apoptosis-Dependent Externalization and Involvement in Apoptotic Cell Clearance of DmCaBP1, an Endoplasmic Reticulum Protein of Drosophila." *Journal of Biological Chemistry* 287 (5): 3138–46. doi:10.1074/jbc.M111.277921.

Okano, Tetsuya, Tadashi Kondo, Tatsuhiko Kakisaka, Kiyonaga Fujii, Masayo Yamada, Harubumi Kato, Toshihide Nishimura, Akihiko Gemma, Shoji Kudoh, and Setsuo Hirohashi. 2006. "Plasma Proteomics of Lung Cancer by a Linkage of Multi-Dimensional Liquid Chromatography and Two-Dimensional Difference Gel Electrophoresis." *Proteomics* 6 (13): 3938–48. doi:10.1002/pmic.200500883.

Org, Elin, Margarete Mehrabian, Brian W. Parks, Petia Shipkova, Xiaoqin Liu, Thomas A. Drake, and Aldons J. Lusis. 2016. "Sex Differences and Hormonal Effects on Gut Microbiota Composition in Mice." *Gut Microbes* 7 (4). Taylor & Francis: 313–22. doi:10.1080/19490976.2016.1203502.

Oshima, H, M Oshima, M Kobayashi, M Tsutsumi, and M M Taketo. 1997. "Morphological and Molecular Processes of Polyp Formation in Apc(delta716) Knockout Mice." *Cancer Res* 57 (9): 1644–49. http://www.ncbi.nlm.nih.gov/pubmed/9135000.

Oshima, M, H Oshima, K Kitagawa, M Kobayashi, C Itakura, and M Taketo. 1995. "Loss of Apc Heterozygosity and Abnormal Tissue Building in Nascent Intestinal Polyps in Mice Carrying a Truncated Apc Gene." *Proc Natl Acad Sci U S A* 92 (10): 4482–86. http://www.ncbi.nlm.nih.gov/pubmed/7753829.

Pai, L M, S Orsulic, A Bejsovec, and M Peifer. 1997. "Negative Regulation of Armadillo, a Wingless Effector in Drosophila." *Development* 124 (11): 2255–66. http://www.ncbi.nlm.nih.gov/pubmed/9187151.

Parashar, Arun, and Malairaman Udayabanu. 2017. "Gut Microbiota: Implications in Parkinson's Disease." *Parkinsonism & Related Disorders* 38: 1–7. doi:10.1016/j.parkreldis.2017.02.002.

Park, Annie, Alfredo Ghezzi, Thilini P. Wijesekera, and Nigel S. Atkinson. 2017. "Genetics and Genomics of Alcohol Responses in Drosophila." *Neuropharmacology*.

doi:10.1016/j.neuropharm.2017.01.032.

Park, Annie, Tracy Tran, and Nigel S. Atkinson. 2017. "BARCODE: Monitoring Consumption in Drosophila by Oligonucleotide Tagging." *Unpublished*.

Park, Jong Min, Na Young Han, Young Min Han, Mi Kyung Chung, Hoo Keun Lee, Kwang Hyun Ko, Eun Hee Kim, and Ki Baik Hahm. 2014. "Predictive Proteomic Biomarkers for Inflammatory Bowel Disease-Associated Cancer: Where Are We Now in the Era of the next Generation Proteomics?" *World Journal of Gastroenterology* 20 (37): 13466–76. doi:10.3748/wjg.v20.i37.13466.

Parker, D S, J Jemison, and K M Cadigan. 2002. "Pygopus, a Nuclear PHD-Finger Protein Required for Wingless Signaling in Drosophila." *Development* 129 (11): 2565–76. http://www.ncbi.nlm.nih.gov/pubmed/12015286.

Peru, Raniero L., Shamsideen A. Ojelade, Pranav S. Penninti, Rachel J. Dove, Matthew J. Nye, Summer F. Acevedo, Antonio Lopez, Aylin R. Rodan, and Adrian Rothenfluh. 2014. "Long-Lasting, Experience-Dependent Alcohol Preference in Drosophila." *Addiction Biology* 19 (3): 392–401. doi:10.1111/adb.12105.

Pfaffl, M W. 2001. "A New Mathematical Model for Relative Quantification in Real-Time RT-PCR." *Nucleic Acids Research* 29 (9): e45. doi:10.1093/nar/29.9.e45.

Pierrakos, Charalampos, and Jean-Louis Vincent. 2010. "Sepsis Biomarkers: A Review." *Critical Care* 14 (1): R15. doi:10.1186/cc8872.

Pohl, Jascha B., Brett A. Baldwin, Boingoc L. Dinh, Pinkey Rahman, Dustin Smerek, Francisco J. Prado, Nyssa Sherazee, and Nigel S. Atkinson. 2012. "Ethanol Preference in Drosophila Melanogaster Is Driven by Its Caloric Value." *Alcoholism: Clinical and Experimental Research* 36 (11): 1903–12. doi:10.1111/j.1530-0277.2012.01817.x.

Polakis, P. 2012. "Drugging Wnt Signalling in Cancer." *EMBO J* 31 (12): 2737–46. doi:10.1038/emboj.2012.126.

Ponton, Fleur, Marie Pierre Chapuis, Mathieu Pernice, Gregory A. Sword, and Stephen J. Simpson. 2011. "Evaluation of Potential Reference Genes for Reverse Transcription-qPCR Studies of Physiological Responses in Drosophila Melanogaster." *Journal of Insect Physiology* 57 (6). Elsevier Ltd: 840–50. doi:10.1016/j.jinsphys.2011.03.014.

Port, Fillip, Hui-min Chen, Tzumin Lee, and Simon L Bullock. 2014. "Optimized CRISPR / Cas Tools for Efficient Germline and Somatic Genome Engineering in Drosophila." doi:10.1073/pnas.1405500111.

Pradet-Balade, Bérengère, Florence Boulmé, Hartmut Beug, Ernst W. Müllner, and Jose A. Garcia-Sanz. 2001. "Translation Control: Bridging the Gap between Genomics and Proteomics?" *Trends in Biochemical Sciences*. doi:10.1016/S0968-0004(00)01776-X.

Preitner, Nicolas, Jie Quan, Dan W. Nowakowski, Melissa L. Hancock, Jianhua Shi, Joseph Tcherkezian, Tracy L. Young-Pearse, and John G. Flanagan. 2014. "APC Is an RNA-Binding Protein, and Its Interactome Provides a Link to Neural Development and

Microtubule Assembly." *Cell* 158 (2). Elsevier Inc.: 368–82. doi:10.1016/j.cell.2014.05.042.

Qin, X, S Ahn, T P Speed, and G M Rubin. 2007. "Global Analyses of mRNA Translational Control during Early Drosophila Embryogenesis." *Genome Biol* 8 (4): R63. doi:10.1186/gb-2007-8-4-r63.

Ransohoff, David F., Christopher Martin, Wesley S. Wiggins, Ben A. Hitt, Temitope O. Keku, Joseph A. Galanko, and Robert S. Sandler. 2008. "Assessment of Serum Proteomics to Detect Large Colon Adenomas." *Cancer Epidemiology Biomarkers and Prevention* 17 (8): 2188–93. doi:10.1158/1055-9965.EPI-07-2767.

Rao, Tata Purushothama, and Michael Kühl. 2010. "An Updated Overview on Wnt Signaling Pathways: A Prelude for More." *Circulation Research* 106 (12): 1798–1806. doi:10.1161/CIRCRESAHA.110.219840.

Reddy, B V, N Boyadjieva, and D K Sarkar. 1995. "Effect of Ethanol, Propanol, Butanol, and Catalase Enzyme Blockers on Beta-Endorphin Secretion from Primary Cultures of Hypothalamic Neurons: Evidence for a Mediatory Role of Acetaldehyde in Ethanol Stimulation of Beta-Endorphin Release." *Alcoholism, Clinical and Experimental Research* 19 (2): 339–44. http://www.ncbi.nlm.nih.gov/pubmed/7625566.

Riaz, Samreen, Saadia Shahzad Alam, Surjit Kaila Srai, Vernon Skinner, Aasma Riaz, and M Waheed Akhtar. 2010. "Proteomic Identification of Human Urinary Biomarkers in Diabetes Mellitus Type 2." *Diabetes Technology & Therapeutics* 12 (12): 979–88. doi:10.1089/dia.2010.0078.

Ring, A, Y M Kim, and M Kahn. 2014. "Wnt/catenin Signaling in Adult Stem Cell Physiology and Disease." *Stem Cell Rev* 10 (4): 512–25. doi:10.1007/s12015-014-9515-2.

Rodan, Aylin R., and Adrian Rothenfluh. 2010. "The Genetics of Behavioral Alcohol Responses in Drosophila." *International Review of Neurobiology* 91 (C): 25–51. doi:10.1016/S0074-7742(10)91002-7.

Rolland, Delphine C. M., Venkatesha Basrur, Yoon-Kyung Jeon, Carla McNeil-Schwalm, Damian Fermin, Kevin P. Conlon, Yeqiao Zhou, et al. 2017. "Functional Proteogenomics Reveals Biomarkers and Therapeutic Targets in Lymphomas." *Proceedings of the National Academy of Sciences* 114 (25): 6581–86. doi:10.1073/pnas.1701263114.

Sauka-Spengler, Tatjana, and Marianne Bronner-Fraser. 2008. "A Gene Regulatory Network Orchestrates Neural Crest Formation." *Nature Reviews Molecular Cell Biology* 9 (7): 557–68. doi:10.1038/nrm2428.

Scheele, George A. 1975. "Two-Dimensional Gel Analysis of Soluble Proteins. Charaterization of Guinea Pig Exocrine Pancreatic Proteins." *The Journal of Biological Chemistry* 250 (14): 5375–85.

Schneikert, J, A Grohmann, and J Behrens. 2007. "Truncated APC Regulates the Transcriptional Activity of Beta-Catenin in a Cell Cycle Dependent Manner." *Hum Mol Genet* 16 (2): 199–

209. doi:10.1093/hmg/ddl464.

Schneikert, Jean, Shree Harsha Vijaya Chandra, Jan Gustav Ruppert, Suparna Ray, Eva Maria Wenzel, and Jürgen Behrens. 2013. "Functional Comparison of Human Adenomatous Polyposis Coli (APC) and APC-Like in Targeting Beta-Catenin for Degradation." *PLoS ONE* 8 (7). doi:10.1371/journal.pone.0068072.

Scholz, Henrike, Jennifer Ramond, Carol M. Singh, and Ulrike Heberlein. 2000. "Functional Ethanol Tolerance in Drosophila." *Neuron* 28 (1): 261–71. doi:10.1016/S0896-6273(00)00101-X.

Schuckit, M A. 1994. "A Clinical Model of Genetic Influences in Alcohol Dependence." *J Stud Alcohol* 55 (1): 5–17. http://www.ncbi.nlm.nih.gov/pubmed/8189726.

Schuckit, Marc A. 1994. "Low Level of Response to Alcohol as a Predictor of Future Alcoholism." *American Journal of Psychiatry* 151 (2): 184–89. doi:10.1176/ajp.151.2.184.

Schuckit, Marc a, Tom L Smith, and Jelger Kalmijn. 2004. "The Search for Genes Contributing to the Low Level of Response to Alcohol: Patterns of Findings across Studies." *Alcoholism, Clinical and Experimental Research* 28 (10): 1449–58. doi:10.1097/01.ALC.0000141637.01925.F6.

Seifert, Jana, Martin Taubert, Nico Jehmlich, Frank Schmidt, Uwe Völker, Carsten Vogt, Hans Hermann Richnow, and Martin Von Bergen. 2012. "Protein-Based Stable Isotope Probing (Protein-SIP) in Functional Metaproteomics." *Mass Spectrometry Reviews*. doi:10.1002/mas.21346.

Sekhon, Morgan L., Omoteniola Lamina, Kerry E. Hogan, and Christopher L. Kliethermes. 2016. "Common Genes Regulate Food and Ethanol Intake in Drosophila." *Alcohol* 53. Elsevier Inc: 27–34. doi:10.1016/j.alcohol.2016.04.001.

Sekirov, I., S. L. Russell, L. C. M. Antunes, and B. B. Finlay. 2010. "Gut Microbiota in Health and Disease." *Physiological Reviews* 90 (3): 859–904. doi:10.1152/physrev.00045.2009.

Sharon, G, D Segal, I Zilber-Rosenberg, and E Rosenberg. 2011. "Symbiotic Bacteria Are Responsible for Diet-Induced Mating Preference in Drosophila Melanogaster, Providing Support for the Hologenome Concept of Evolution." *Gut Microbes* 2 (3): 190–92. http://www.ncbi.nlm.nih.gov/pubmed/21804354.

Shaw, Joanne, Rachel Rowlinson, Janice Nickson, Tim Stone, Alison Sweet, Karen Williams, and Robert Tonge. 2003. "Evaluation of Saturation Labelling Two-Dimensional Difference Gel Electrophoresis Fluorescent Dyes." In *Proteomics*, 3:1181–95. doi:10.1002/pmic.200300439.

Shaw, Margaret M., and Beat M. Riederer. 2003. "Sample Preparation for Two-Dimensional Gel Electrophoresis." In *Proteomics*, 3:1408–17. doi:10.1002/pmic.200300471.

Shin, S C, S H Kim, H You, B Kim, A C Kim, K A Lee, J H Yoon, J H Ryu, and W J Lee. 2011. "Drosophila Microbiome Modulates Host Developmental and Metabolic Homeostasis via Insulin Signaling." *Science* 334 (6056): 670–74. doi:10.1126/science.1212782.

Shin, Seung Chul, Sung-Hee Kim, Hyejin You, Boram Kim, Aeri C Kim, Kyung-Ah Lee, Joo-Heon Yoon, Ji-Hwan Ryu, and Won-Jae Lee. 2011. "Drosophila Microbiome Modulates Host Developmental and Metabolic Homeostasis via Insulin Signaling." *Science (New York, N.Y.)* 334 (6056): 670–74. doi:10.1126/science.1212782.

Sim, Sarah C., and Magnus Ingelman-Sundberg. 2011. "Pharmacogenomic Biomarkers: New Tools in Current and Future Drug Therapy." *Trends in Pharmacological Sciences*. doi:10.1016/j.tips.2010.11.008.

Simmons, W. H., and A. T. Orawski. 1992. "Membrane-Bound Aminopeptidase P from Bovine Lung. Its Purification, Properties, and Degradation of Bradykinin." *Journal of Biological Chemistry* 267 (7): 4897–4903.

Singh, Carol, and Ulrike Heberlein. 2000. "Genetic Control of Acute Ethanol-Induced Behaviors in Drosophila." *Alcoholism: Clinical and Experimental Research* 24 (8): 1127–36.

Sitek, Barbara, Sebastian Potthoff, Thomas Schulenborg, Johannes Stegbauer, Tobias Vinke, Lars Christian Rump, Helmut E. Meyer, Oliver Vonend, and Kai Stühler. 2006. "Novel Approaches to Analyse Glomerular Proteins from Smallest Scale Murine and Human Samples Using DIGE Saturation Labelling." *Proteomics* 6 (15): 4337–45. doi:10.1002/pmic.200500739.

Speicher, K D, O Kolbas, S Harper, and D W Speicher. 2000. "Systematic Analysis of Peptide Recoveries from in-Gel Digestions for Protein Identifications in Proteome Studies." *J Biomol Tech* 11 (2): 74–86. http://www.ncbi.nlm.nih.gov/pubmed/19499040.

Storelli, Gilles, Arnaud Defaye, Berra Erkosar, Pascal Hols, and Julien Royet. 2011. "Lactobacillus Plantarum Promotes Drosophila Systemic Growth by Modulating Hormonal Signals through TOR-Dependent Nutrient Sensing." *Cell Metabolism* 14: 403–14. doi:10.1016/j.cmet.2011.07.012.

Strati, Francesco, Duccio Cavalieri, Davide Albanese, Claudio De Felice, Claudio Donati, Joussef Hayek, Olivier Jousson, et al. 2017. "New Evidences on the Altered Gut Microbiota in Autism Spectrum Disorders." *Microbiome* 5 (1): 24. doi:10.1186/s40168-017-0242-1.

Swarup, S, and E M Verheyen. 2012. "Wnt/Wingless Signaling in Drosophila." *Cold Spring Harb Perspect Biol* 4 (6). doi:10.1101/cshperspect.a007930.

Tadros, W, and H D Lipshitz. 2009. "The Maternal-to-Zygotic Transition: A Play in Two Acts." *Development* 136 (18): 3033–42. doi:10.1242/dev.033183.

Takacs, C M, J R Baird, E G Hughes, S S Kent, H Benchabane, R Paik, and Y Ahmed. 2008. "Dual Positive and Negative Regulation of Wingless Signaling by Adenomatous Polyposis Coli." *Science* 319 (5861): 333–36. doi:10.1126/science.1151232.

Tavakoli, Hamid R, Michael Hull, and Lt Michael Okasinski. 2011. "Review of Current Clinical Biomarkers for the Detection of Alcohol Dependence." *Innovations in Clinical Neuroscience* 8: 26–33.

Tech, Adv, Biol Med, Debabrat Sabat, Eldin M Johnson, Arra Abhinay, Rasu Jayabalan, and

Monalisa Mishra. 2015. “A Protocol to Generate Germ Free Drosophila for Microbial Interaction Studies.” *Advanced Techniques in Biology & Medicine* S1: 1–6. doi:10.4172/2379-1764.S1-001.

Tirnauer, Jennifer S. 2004. “A New Cytoskeletal Connection for APC: Linked to Actin through IQGAP.” *Developmental Cell*. doi:10.1016/j.devcel.2004.11.012.

Toby, Timothy K., Luca Fornelli, and Neil L. Kelleher. 2016. “Progress in Top-Down Proteomics and the Analysis of Proteoforms.” *Annual Review of Analytical Chemistry* 9 (1): 499–519. doi:10.1146/annurev-anchem-071015-041550.

Tremaroli, Valentina, and Fredrik Bäckhed. 2012. “Functional Interactions between the Gut Microbiota and Host Metabolism.” *Nature* 489 (7415): 242–49. doi:10.1038/nature11552.

Unlu, M, M E Morgan, and J S Minden. 1997. “Difference Gel Electrophoresis: A Single Gel Method for Detecting Changes in Protein Extracts.” *Electrophoresis* 18 (11): 2071–77. doi:10.1002/elps.1150181133.

Van, Phu T., Victor Bass, Dan Shiwarski, Frederick Lanni, and Jonathan Minden. 2014. “High Dynamic Range Proteome Imaging with the Structured Illumination Gel Imager.” *Electrophoresis* 35 (18): 2642–55. doi:10.1002/elps.201400126.

Van, Phu T., Vinitha Ganesan, Victor Bass, Amritha Parthasarathy, Danielle Schlesinger, and Jonathan S. Minden. 2014. “In-Gel Equilibration for Improved Protein Retention in 2DE-Based Proteomic Workflows.” *Electrophoresis* 35 (20): 3012–17. doi:10.1002/elps.201400256.

van Dijk, Karin D., Charlotte E. Teunissen, Benjamin Drukarch, Connie R. Jimenez, Henk J. Groenewegen, Henk W. Berendse, and Wilma D J van de Berg. 2010. “Diagnostic Cerebrospinal Fluid Biomarkers for Parkinson’s Disease: A Pathogenetically Based Approach.” *Neurobiology of Disease*. doi:10.1016/j.nbd.2010.04.020.

Venter, J C, M D Adams, E W Myers, P W Li, R J Mural, G G Sutton, H O Smith, et al. 2001. “The Sequence of the Human Genome.” *Science* 291 (5507): 1304–51. doi:10.1126/science.1058040.

VerBerkmoes, Nathan C., Vincent J. Denef, Robert L. Hettich, and Jillian F. Banfield. 2009. “Systems Biology: Functional Analysis of Natural Microbial Consortia Using Community Proteomics.” *Nature Reviews Microbiology* 7 (3): 196–205. doi:10.1038/nrmicro2080.

Verstreken, P, T Ohyama, C Haueter, R L Habets, Y Q Lin, L E Swan, C V Ly, K J Venken, P De Camilli, and H J Bellen. 2009. “Tweek, an Evolutionarily Conserved Protein, Is Required for Synaptic Vesicle Recycling.” *Neuron* 63 (2): 203–15. doi:10.1016/j.neuron.2009.06.017.

Viswanathan, S, M Unlu, and J S Minden. 2006. “Two-Dimensional Difference Gel Electrophoresis.” *Nat Protoc* 1 (3): 1351–58. doi:10.1038/nprot.2006.234.

Vogel, Christine, and Edward M Marcotte. 2012. “Insights into the Regulation of Protein Abundance from Proteomic and Transcriptomic Analyses.” *Nature Reviews. Genetics* 13

(4): 227–32. doi:10.1038/nrg3185.

Wang, Hong, Shawn G Clouthier, Vladimir Galchev, David E Misek, Ulrich Duffner, Chang-Ki Min, Rong Zhao, et al. 2005. "Intact-Protein-Based High-Resolution Three-Dimensional Quantitative Analysis System for Proteome Profiling of Biological Fluids." *Molecular & Cellular Proteomics : MCP* 4 (5): 618–25. doi:10.1074/mcp.M400126-MCP200.

Wang, S H, N Li, Y Wei, Q R Li, and Z P Yu. 2014. "Beta-Catenin Deacetylation Is Essential for WNT-Induced Proliferation of Breast Cancer Cells." *Mol Med Rep* 9 (3): 973–78. doi:10.3892/mmr.2014.1889.

Webb, Rebecca L., Meng-Ning Zhou, and Brooke M. McCartney. 2009. "A Novel Role for an APC2-Diaphanous Complex in Regulating Actin Organization in Drosophila." *Development* 136 (8): 1283–93. doi:10.1242/dev.026963.

Wehr, T. 2006. "Top-Down Versus Bottom-Up Approaches in\rProteomics." *LCGC North America* 24 (9): 1004–10.

Welters, Hannah J., and Rohit N. Kulkarni. 2008. "Wnt Signaling: Relevance to β-Cell Biology and Diabetes." *Trends in Endocrinology and Metabolism*. doi:10.1016/j.tem.2008.08.004.

Wen, Ying, Christina H. Eng, Jan Schmoranzer, Noemi Cabrera-Poch, Edward J. S. Morris, Michael Chen, Bradley J. Wallar, Arthur S. Alberts, and Gregg G. Gundersen. 2004. "EB1 and APC Bind to mDia to Stabilize Microtubules Downstream of Rho and Promote Cell Migration." *Nature Cell Biology* 6 (9): 820–30. doi:10.1038/ncb1160.

Whon, Tae Woong, Na-Ri Shin, Mi-Ja Jung, Dong-Wook Hyun, Hyun Sik Kim, Pil Soo Kim, and Jin-Woo Bae. 2017. "Conditionally Pathogenic Gut Microbes Promote Larval Growth by Increasing Redox-Dependent Fat Storage in High Sugar Diet-Fed Drosophila." *Antioxidants & Redox Signaling* 0 (0): ars.2016.6790. doi:10.1089/ars.2016.6790.

Williams, Jonathan, Joachim Pleil, Joachim D Pleil, Michelle M Angrish, Michael C Madden, Jonathan D Beauchamp, Wolfram Miekisch, Matthew A Stiegel, and Kenneth W Fent. 2017. "High-Resolution Mass Spectrometry: Basic Principles for Using Exact Mass and Mass Defect for Discovery Analysis of Organic Molecules in Blood, Breath, Urine and Environmental Media." *J. Breath Res* 10. Accessed August 30. http://iopscience.iop.org/1752-7163/10/1/012001.

Wolf, Fred W, and Ulrike Heberlein. 2003. "Invertebrate Models of Drug Abuse." *Journal of Neurobiology* 54 (1): 161–78. doi:10.1002/neu.10166.

Wolf, Fred W, Aylin R Rodan, Linus T-Y Tsai, and Ulrike Heberlein. 2002. "High-Resolution Analysis of Ethanol-Induced Locomotor Stimulation in Drosophila." *The Journal of Neuroscience : The Official Journal of the Society for Neuroscience* 22 (24): 11035–44. doi:22/24/11035 [pii].

Wong, A C, A J Dobson, and A E Douglas. 2014. "Gut Microbiota Dictates the Metabolic Response of Drosophila to Diet." *J Exp Biol* 217 (Pt 11): 1894–1901. doi:10.1242/jeb.101725.

Woo, Sunghee, Seong Won Cha, Stefano Bonissone, Seungjin Na, David L. Tabb, Pavel A. Pevzner, and Vineet Bafna. 2015. "Advanced Proteogenomic Analysis Reveals Multiple Peptide Mutations and Complex Immunoglobulin Peptides in Colon Cancer." *Journal of Proteome Research* 14 (9): 3555–67. doi:10.1021/acs.jproteome.5b00264.

Wright, P. C., J. Noirel, S. Y. Ow, and A. Fazeli. 2012. "A Review of Current Proteomics Technologies with a Survey on Their Widespread Use in Reproductive Biology Investigations." *Theriogenology*. doi:10.1016/j.theriogenology.2011.11.012.

Wu, Y, X Wang, F Wu, R Huang, F Xue, G Liang, M Tao, P Cai, and Y Huang. 2012. "Transcriptome Profiling of the Cancer, Adjacent Non-Tumor and Distant Normal Tissues from a Colorectal Cancer Patient by Deep Sequencing." *PLoS One* 7 (8): e41001. doi:10.1371/journal.pone.0041001.

Xian, Feng, Christopher L. Hendrickson, and Alan G. Marshall. 2012. "High Resolution Mass Spectrometry." *Analytical Chemistry* 84 (2). American Chemical Society: 708–19. doi:10.1021/ac203191t.

Xie, Guoxiang, Xiaoning Wang, Aihua Zhao, Jingyu Yan, Wenlian Chen, Runqiu Jiang, Junfang Ji, et al. 2017. "Sex-Dependent Effects on Gut Microbiota Regulate Hepatic Carcinogenic Outcomes." *Scientific Reports* 7 (December 2016): 45232. doi:10.1038/srep45232.

Yamagata, N, T Ichinose, Y Aso, P Y Placais, A B Friedrich, R J Sima, T Preat, G M Rubin, and H Tanimoto. 2015. "Distinct Dopamine Neurons Mediate Reward Signals for Short- and Long-Term Memories." *Proc Natl Acad Sci U S A* 112 (2): 578–83. doi:10.1073/pnas.1421930112.

Yaron, A. 1987. "The Role of Proline in the Proteolytic Regulation of Biologically Active Peptides." *Biopolymers* 26 Suppl: S215-22. doi:10.1002/bip.360260019.

Yaron, A, and F Naider. 1993. "Proline-Dependent Structural and Biological Properties of Peptides and Proteins." *Crit Rev Biochem Mol Biol* 28 (1): 31–81. doi:10.3109/10409239309082572.

Yoshimoto, T, A T Orawski, and W H Simmons. 1994. "Substrate Specificity of Aminopeptidase P from Escherichia Coli: Comparison with Membrane-Bound Forms from Rat and Bovine Lung." *Arch Biochem Biophys* 311 (1): 28–34. doi:10.1006/abbi.1994.1204.

Yurkovetskiy, Leonid, Michael Burrows, Aly A. Khan, Laura Graham, Pavel Volchkov, Lev Becker, Dionysios Antonopoulos, Yoshinori Umesaki, and Alexander V. Chervonsky. 2013. "Gender Bias in Autoimmunity Is Influenced by Microbiota." *Immunity* 39 (2): 400–412. doi:10.1016/j.immuni.2013.08.013.

Zhang, Xu, Wendong Chen, Zhibin Ning, Janice Mayne, David Mack, Alain Stintzi, Ruijun Tian, and Daniel Figeys. 2017. "Deep Metaproteomics Approach for the Study of Human Microbiomes." *Analytical Chemistry*, August, acs.analchem.7b02224. doi:10.1021/acs.analchem.7b02224.

Zhang, Yafei, and Yongmei Xi. 2014. "Fat Body Development and Its Function in Energy

Storage and Nutrient Sensing in Drosophila Melanogaster." *Tissue Science & Engineering* 6 (1): 1–8. doi:10.4172/2157-7552.1000141.

Zhang, Z, S M Roe, M Diogon, E Kong, H El Alaoui, and D Barford. 2010. "Molecular Structure of the N-Terminal Domain of the APC/C Subunit Cdc27 Reveals a Homo-Dimeric Tetratricopeptide Repeat Architecture." *J Mol Biol* 397 (5): 1316–28. doi:10.1016/j.jmb.2010.02.045.

Zhou, Meng-Ning, Ezgi Kunttas-Tatli, Sandra Zimmerman, Fangyuan Zhouzheng, and Brooke M McCartney. 2011. "Cortical Localization of APC2 Plays a Role in Actin Organization but Not in Wnt Signaling in Drosophila." *Journal of Cell Science* 124 (Pt 9): 1589–1600. doi:10.1242/jcs.073916.

Zimatkin, S M, and K O Lindros. 1996. "Distribution of Catalase in Rat Brain: Aminergic Neurons as Possible Targets for Ethanol Effects." *Alcohol and Alcoholism (Oxford, Oxfordshire)* 31 (2): 167–74. doi:10.1093/oxfordjournals.alcalc.a008128.

Zwittink, Romy D., Diny van Zoeren-Grobben, Rocio Martin, Richard A. van Lingen, Liesbeth J. Groot Jebbink, Sjef Boeren, Ingrid B. Renes, Ruurd M. van Elburg, Clara Belzer, and Jan Knol. 2017. "Metaproteomics Reveals Functional Differences in Intestinal Microbiota Development of Preterm Infants." *Molecular & Cellular Proteomics* 16 (9): 1610–20. doi:10.1074/mcp.RA117.000102.